

# **A Study on Singularly Perturbed Problems under Adaptive Finite Element Framework**

A THESIS

SUBMITTED IN FULFILMENT OF THE

REQUIREMENT FOR THE AWARD OF THE DEGREE OF

**DOCTOR OF PHILOSOPHY**

IN

**MATHEMATICS**

*By*

**Brehmit Kaur**

**(Registration No.: 951211005)**

to the



**SCHOOL OF MATHEMATICS**

**THAPAR INSTITUTE OF ENGINEERING AND  
TECHNOLOGY, PATIALA-147004 (PUNJAB), INDIA**

**February, 2021**

---

# Certificate

---



This is to certify that the work contained in the thesis entitled “**A Study on Singularly Perturbed Problems under Adaptive Finite Element Framework**”, submitted by Ms. **Brehmit Kaur** (Roll No: 951211005) in the fulfilment of the requirements for the award of the degree of Doctoral of Philosophy in the School of Mathematics, Thapar Institute of Engineering and Technology, Patiala, is a record of the candidate's own work and has been carried out under my supervision and guidance. The matter presented in this thesis has not been submitted in part or full for the award of any degree in any other University or Institute.

**Attestation by supervisor**

**Dr. Vivek Sangwan**

Assistant Professor

School of Mathematics

T.I.E.T., Patiala-147004, INDIA

---

# Declaration

---

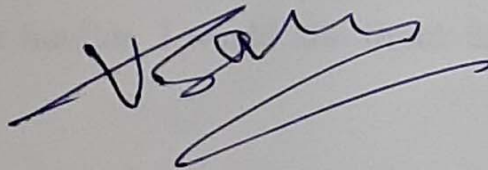
It is certified that the thesis is entirely my own work and that the ideas and references cited herein have been duly acknowledged.

*Brehmit Kaur*

Brehmit Kaur

(Regn. No. 951211005)

Attestation by supervisor



Dr. Vivek Sangwan

Assistant Professor

School of Mathematics

T.I.E.T., Patiala-147004, INDIA

---

# Acknowledgement

---

*People prefer to follow those who help them,  
not those who intimidate them.*

— C. Gene Wilkes

I am pleased to take this opportunity to express my heartily gratitude and thankfulness towards **Prof. Vivek Sangwan**, for introducing me to the concept of singularly perturbed problems, finite element method and adaptivity. This thesis would not have been possible without his support and continuous guidance. I would like to express my deep sense of gratitude for his constant encouragement during the progress of this work and his help to cross the hurdles. I would also thank him to let me evolve as a better human being.

I owe my sincere gratitude to Dr. Rafat Siddique, (Dean, Research and Sponsored Projects), Dr. S.S. Bhatia (Dean, Academic Affairs), Dr. Satish Kumar Sharma, (Head of the Department) and Dr. Kulvir Singh for rendering me a very good environment to work. I also extend my sincere thanks to all the faculty members of the School of Mathematics, Thapar Institute of Engineering and Technology, Patiala especially Prof. A.K. Lal, Prof. Avinash Chandra, Prof. Kavita, Prof. Paramjeet Singh and Prof. Harish Garg.

I express my heartiest thanks to all my close friends Bikramjeet Kaur, Tanupreet

Kaur and Jagbir Kaur. Thank you all for making my stay pleasant at campus and for all the lively discussions and support.

At last, but by no means the least, I express my deepest gratitude: To my dear parents who tolerated the onslaughts of time to bring me up to this position and for their blessings, continuous encouragement and moral support; To my family: *husband, in-laws, sister, jija-ji*, to my nephew *Gurnoor* and niece *Haraziz*; A very special thanks to my dear *Sukhmehar* for being so loving, caring and encouraging and giving me full emotional support during the preparation of the thesis.

Finally, I thank the Almighty for his gracious presence throughout my life and giving me a chance to learn.

Patiala

February, 2021

**(Brehmit Kaur)**

---

# Abstract

---

In this thesis work, robust and efficient adaptive finite element techniques have been proposed for approximating the solutions of singularly perturbed PDEs arising during the analysis of biological systems, heat transfer process, mass transfer process, etc.

The research work started with the following three objectives:

1. To propose robust and efficient numerical adaptive finite element technique for linear and non-linear one dimensional singularly perturbed problems.
2. To extend the proposed adaptive techniques (Objective 1) to higher dimensional singularly perturbed problems.
3. To solve some realistic problems arising in various branches of science and engineering. One of the model problems to be considered is Burger Huxley problem.

Keeping these objectives in view, the research work has been carried out. These objectives have been achieved via the work which has been categorized into five different Chapters, the details of which are given below:

## **Chapter 1: Introduction**

In the first Chapter, some definitions and basic concepts involved in the thesis have been discussed. A detailed survey on various adaptive finite element techniques has been carried out. In the survey, the main focus has been given on a posteriori error estimates, their efficiency, reliability and adaptive strategies designed to achieve the numerical solution with desired accuracy. Based on the survey, some gaps in the

literature have been pointed out and objectives have been set up.

## **Chapter 2: Adaptive finite element scheme for one-dimensional singularly perturbed parabolic problems**

The second Chapter deals with an adaptive finite element technique for numerical approximation of solutions of one-dimensional singularly perturbed linear and non-linear parabolic differential equations. The considered time dependent singularly perturbed linear partial differential equation is given by

$$\frac{\partial w}{\partial t} - \epsilon \frac{\partial^2 w}{\partial x^2} + a(x, t)w_x + b(x, t)w = f(x, t), \quad (x, t) \in D,$$

with boundary conditions

$$w(0, t) = f_1(t), \quad t \geq 0,$$

$$w(1, t) = f_2(t), \quad t \geq 0,$$

and initial condition defined by

$$w(x, 0) = w_0(x), \quad 0 \leq x \leq 1,$$

where  $D = \Omega \times (0, 1)$ ,  $\Omega = (0, 1)$  and  $\epsilon$  is singular perturbation parameter ( $0 < \epsilon \ll 1$ ). It has been assumed that  $a(x, t)$ ,  $b(x, t)$  and  $f(x, t)$  are smooth functions satisfying  $a(x, t) > \alpha > 0$  and  $b(x, t) \geq \beta \geq 0$ . Temporal semi-discretization has been carried out using implicit Euler scheme. Spatial discretization has been performed using finite element technique and Streamline upwind/Petrov-Galerkin (SUPG) method. Piecewise uniform Shishkin mesh has been considered for domain discretization. Exponentially fitted splines have been used as test functions. At the end, numerical tests have been carried out and it has been shown that the proposed schemes works very well on adaptive Shishkin grids. It has been shown that the proposed adaptive

schemes are very efficient in capturing sharp boundary layers as  $\epsilon$  becomes small. For non-linear time-dependent SPP, the following problem has been considered:

$$\frac{\partial u}{\partial t} - \epsilon \frac{\partial^2 u}{\partial x^2} + a(x, t, u)u_x = f(x, t, u)u, \quad (x, t) \in D,$$

with boundary conditions defined as

$$\begin{aligned} u(0, t) &= f(t), \quad t \geq 0, \\ u(1, t) &= g(t), \quad t \geq 0, \end{aligned}$$

and initial condition as

$$u(x, 0) = u_0(x), \quad 0 \leq x \leq 1,$$

with  $D = \Omega \times (0, 1)$ ,  $\Omega = (0, 1)$  and  $\epsilon$  is the singular perturbation parameter satisfying  $0 < \epsilon \ll 1$ . Here  $a(x, t, u)$  and  $f(x, t, u)$  are assumed to be smooth functions. Bellman and Kalaba[22] quasilinearization process has been considered to deal with nonlinearity occurring in the problem. Further, finite element method and SUPG technique has been used for spatial discretization based on exponentially fitted splines. Shishkin mesh has been used to capture sharp boundary layers arising in the solution. Stability analysis has been carried out. Numerical tests have been performed which shows that both the schemes works efficiently for solving the singularly perturbed problems and the numerical solution obtained by using the schemes agree with the exact solution.

### **Chapter 3: A posteriori error estimates for Hughes stabilized SUPG technique and adaptive refinement strategy for two-dimensional singularly perturbed problems**

This Chapter is devoted to the study of singularly perturbed convection-diffusion problems in two-dimensions. The convection-diffusion problem under consideration

is given by

$$\begin{aligned} -\nabla \cdot \epsilon \nabla u + \mathbf{a} \cdot \nabla u + bu &= f \quad \text{in } \Omega, \\ u &= 0 \quad \text{on } \partial\Omega_D, \\ \epsilon \frac{\partial u}{\partial n} &= g \quad \text{on } \partial\Omega_N, \end{aligned}$$

where  $\Omega \subset \mathbb{R}^2$  is a bounded domain with Lipschitz-continuous boundary  $\partial\Omega = \partial\Omega_D \cup \partial\Omega_N$ ,  $\epsilon$  is singular perturbation parameter satisfying  $0 < \epsilon \ll 1$ , and  $\mathbf{a}$ ,  $b$  and  $f$  are sufficiently smooth. Here  $\partial\Omega_D$  and  $\partial\Omega_N$  denote the Dirichlet and Neumann boundaries of the domain accordingly.

It has been observed that for small values of the singular perturbation parameter, the problem under consideration displays boundary layers in the small subregions near the boundary. Hughes[27] stabilization strategy along with the Streamline upwind/Petrov-Galerkin (SUPG) method has been proposed to solve the problem. Reliable a posteriori error estimates in energy norm on anisotropic meshes[111] have been derived. But these estimates prove to be singular perturbation parameter dependent. Therefore, to overcome the difficulty of oscillations in the solution, a robust and efficient adaptive anisotropic mesh refinement[99] algorithm has been proposed. Numerical experiments have been performed to test the theoretical findings.

#### **Chapter 4: A posteriori error estimates for Hughes stabilized SUPG method for three-dimensional singularly perturbed problems**

The fourth Chapter deals with the singularly perturbed convection-diffusion problem in three-dimensions. The convection-diffusion problem is considered in the following form:

$$\begin{aligned} -\nabla \cdot \epsilon \nabla u + \mathbf{b} \cdot \nabla u + cu &= f \quad \text{in } \Gamma, \\ u &= 0 \quad \text{on } \partial\Gamma_D, \end{aligned}$$

$$\frac{\partial u}{\partial n} = g \quad \text{on } \partial\Gamma_N,$$

where  $\Gamma \subset \mathbb{R}^3$  is a bounded domain with Lipschitz-continuous boundary  $\partial\Gamma$ . It has been assumed that  $\partial\Gamma = \partial\Gamma_D \cup \partial\Gamma_N$  with  $\partial\Gamma_D \cap \partial\Gamma_N = \emptyset$ , and  $\mathbf{b}$ ,  $c$  and  $f$  are sufficiently smooth.  $\partial\Gamma_D$  and  $\partial\Gamma_N$  denote the Dirichlet and Neumann boundaries of the domain respectively. Hughes stabilized Streamline upwind/Petrov-Galerkin (SUPG)[96] method has been proposed to approximate the solution of the problem. Reliable a posteriori error estimates in energy norm on anisotropic meshes have been developed for the proposed method.

### Chapter 5: Applications of singularly perturbed problems

In this Chapter, two realistic model phenomenon arising during the analysis of biological systems, heat transfer process, etc., and governed by singularly perturbed problems have been considered. An efficient adaptive numerical scheme has been proposed for approximating the solutions of these problems. The first considered model problem is the time dependent singularly perturbed Burgers-Fisher problem[174] given by:

$$u_t = \epsilon u_{xx} - \alpha u u_x + \beta u(1 - u), \quad 0 < x < 1, t > 0.$$

with initial and boundary conditions defined as

$$u(x, 0) = \phi(x), \quad x \in \Omega = (0, 1)$$

and

$$u(0, t) = f(t), \quad t > 0,$$

$$u(1, t) = g(t), \quad t > 0.$$

The second model problem is the time dependent singularly perturbed Burgers-Huxley problem[110]:

$$u_t = \epsilon u_{xx} - \alpha u u_x + \beta u(1 - u)(u - \gamma), \quad 0 < x < 1, t > 0.$$

with some non-zero initial and boundary conditions. The two model problems taken into consideration represents the traveling wave phenomenon. Both the problems are defined over the domain  $D = \Omega \times T = (0, 1) \times (0, \infty)$ .  $\alpha$  and  $\beta$  are parameters such that  $\alpha, \beta \geq 0$ , and  $\epsilon$  is the singular perturbation parameter satisfying  $0 < \epsilon \ll 1$ . Since both the problems are non-linear, quasilinearization process has been utilized to deal with the nonlinearity occurring in the problems. Time discretization has been performed using implicit Euler method and spatial discretization has been carried out using finite element technique based on exponentially fitted splines[174] on piecewise uniform Shishkin mesh. Stability analysis has been carried out. At the end, it has been shown numerically that the proposed method is very much effective for capturing sharp boundary layers arising in the solutions as singular perturbation parameter  $\epsilon \rightarrow 0$ .

---

# List of Research Papers

---

1. Vivek Sangwan and Brehmit Kaur, An exponentially fitted numerical technique for singularly perturbed Burgers-Fisher equation on a layer-adapted mesh, *International Journal of Computer Mathematics*, 96(7):1502-1513, 2019. (**SCIE, impact factor- 1.6**).
2. Brehmit Kaur and Vivek Sangwan, A Posteriori Error Estimates for Hughes Stabilized SUPG Technique and Adaptive Refinement for a Convection-Diffusion Problem, *Advances in Mathematical Physics*, 2020. (**SCIE, impact factor- 1.130**).
3. Brehmit Kaur and Vivek Sangwan, A Survey on the developments of adaptive finite element techniques. (**Communicated**)
4. Brehmit Kaur and Vivek Sangwan, Robust adaptive numerical scheme for Klein-Gordon equation. (**Communicated**)

---

# List of Figures

---

|      |   |    |
|------|---|----|
| 2.1  | Comparison of numerical solution profile for $\epsilon = 2^{-16}$ using FEM and SUPG method . . . . . | 67 |
| 2.2  | Grid validation test for $\epsilon = 2^{-8}, 2^{-18}$ . . . . .                                       | 67 |
| 2.3  | $\epsilon$ - effect at different time levels . . . . .  | 68 |
| 2.4  | Time-effect for $\epsilon = 2^{-12}, 2^{-16}$ . . . . .   | 68 |
| 2.5  | The numerical solution profile for $\epsilon = 2^{-26}$ . . . . .                                     | 69 |
| 2.6  | Stability region for non-linear singularly perturbed problem . . . . .                                | 75 |
| 2.7  | Grid validation test for $\epsilon = 2^{-12}, 2^{-22}$ . . . . .                                      | 77 |
| 2.8  | $\epsilon$ - effect at $t = 0.5, 1$ . . . . .   | 77 |
| 2.9  | Temporal-effect on the FEM sol. . . . .   | 78 |
| 2.10 | FEM solution profile for $\epsilon = 2^{-25}$ over the time-domain $[0,1]$ . . . . .                  | 78 |
| 2.11 | SUPG solution at $t=1$ for different values of $\epsilon$ . . . . .                                   | 78 |
| 2.12 | $\epsilon$ -effect on the FEM sol. . . . .  | 80 |
| 2.13 | Time-effect on the sol. for $\epsilon = 2^{-12}$ and $2^{-15}$ . . . . .                              | 80 |
| 2.14 | FEM solution profile for $k = 0.0001, \epsilon = 2^{-14}$ over the time-domain $[0,1]$                | 81 |
| 3.1  | Orthogonality condition . . . . .   | 87 |
| 3.2  | Triangle K . . . . .  | 90 |
| 3.3  | Portion of adaptive mesh for $\epsilon = 2^{-3}$ with DOF = 187,224 . . . . .                         | 98 |

|      |  |     |
|------|--|-----|
| 3.4  | Portion of adaptive mesh for $\epsilon = 2^{-5}$ with DOF = 559,587 . . . . .                    | 98  |
| 3.5  | Numerical Solution Profile for $\epsilon = 2^{-3}$ . . . . .                                     | 99  |
| 3.6  | Numerical Solution Profile for $\epsilon = 2^{-5}$ . . . . .                                     | 99  |
| 3.7  | Error $   v - v_h   $ and Error estimator for $\epsilon = 2^{-5}$ . . . . .                      | 100 |
| 3.8  | $\psi$ (Effectivity Index) for $\epsilon = 2^{-5}$ . . . . .                                     | 100 |
| 4.1  | Tetrahedron $T$ . . . . .  | 108 |
| 5.1  | Stability region for singularly perturbed Burgers-Fisher equation . . .                          | 121 |
| 5.2  | Grid validation test for $\epsilon = 2^{-11}, 2^{-14}$ . . . . .                                 | 123 |
| 5.3  | $\epsilon$ - effect at different time levels $t = 0.5, 1.0$ . . . . .                            | 124 |
| 5.4  | Time-effect at different values of $\epsilon = 2^{-12}, 2^{-15}$ . . . . .                       | 124 |
| 5.5  | The numerical solution profile for $\alpha = 0.01, \beta = 0.01, \delta = 1, \epsilon = 2^{-12}$ | 125 |
| 5.6  | Stability region for singularly perturbed Burgers-Huxley equation . .                            | 127 |
| 5.7  | Grid validation test for $\epsilon = 2^{-12}, 2^{-14}$ . . . . .                                 | 128 |
| 5.8  | $\epsilon$ - effect at different time levels = 0.5,1.0 . . . . .                                 | 128 |
| 5.9  | Time-effect on the sol. at $\epsilon = 2^{-14}$ and $2^{-18}$ . . . . .                          | 129 |
| 5.10 | Numerical solution profile for $\alpha = 3, \beta = 9.8, \gamma = 0.7, \epsilon = 2^{-15}$ . . . | 129 |
| 5.11 | Grid validation test for $\epsilon = 2^{-7}, 2^{-12}$ . . . . .                                  | 130 |
| 5.12 | $\epsilon$ -effect at $t = 0.5$ and $t = 1$ . . . . .  | 130 |
| 5.13 | Time-effect on the sol. at $\epsilon = 2^{-15}$ and $2^{-17}$ . . . . .                          | 130 |

---

# List of Tables

---

|     |  |     |
|-----|--|-----|
| 2.1 | Maximum pointwise errors $E_\epsilon^{N,\Delta t}$ for Example 1 on piecewise uniform Shishkin mesh . . . . .                | 66  |
| 2.2 | Maximum pointwise errors $E_\epsilon^{N,\Delta t}$ for Example 1 on piecewise uniform Shishkin mesh . . . . .                | 66  |
| 2.3 | Maximum SUPG pointwise errors $E_\epsilon^{N,\Delta t}$ for the Example 2 on piecewise uniform Shishkin mesh . . . . .       | 76  |
| 2.4 | Numerical results for Example 3 for $k = 6$ , $\epsilon = 1$ and $\Delta t = 0.001$ , $T = 0.01$ . . . . .                   | 79  |
| 5.1 | Maximum absolute errors in Example 1 for $\alpha = 0.01$ , $\beta = 0.01$ , $\epsilon = 1$ and $\Delta t = 0.0002$ . . . . . | 122 |
| 5.2 | Maximum pointwise errors and order of convergence in Example 1 with $\alpha = 0.01$ , $\beta = 0.01$ . . . . .               | 132 |

---

# Contents

---

|  |            |
|--|------------|
| <b>Certificate</b>   | <b>i</b>   |
| <b>Declaration</b>   | <b>ii</b>  |
| <b>Acknowledgement</b>   | <b>iii</b> |
| <b>Abstract</b>  | <b>v</b>   |
| <b>List of Research Papers</b>   | <b>xi</b>  |
| <b>List of Figures</b>   | <b>xii</b> |
| <b>List of Tables</b>  | <b>xiv</b> |
| <b>1 Introduction</b>  | <b>1</b>   |
| 1.1 Need of adaptive finite element strategies . . . . .                                     | 1          |
| 1.2 Some of the real world models . . . . .  | 3          |
| 1.3 Overview towards the development of various adaptive finite element<br>methods . . . . . | 8          |
| 1.4 Brief survey of adaptive techniques based on finite element framework                    | 11         |
| 1.4.1 $h$ -adaptive strategies . . . . .   | 12         |
| 1.4.2 $p$ -adaptive strategies . . . . .   | 13         |
| 1.4.3 $h - p$ -adaptive strategies . . . . .   | 14         |
| 1.4.4 $h - p - q$ -adaptive strategies . . . . .   | 25         |
| 1.4.5 $r - h$ -adaptive strategies . . . . .   | 25         |
| 1.4.6 Adaptive strategies based on layer adaptive mesh . . . . .                             | 26         |
| 1.4.7 Adaptive strategies based on error estimates . . . . .                                 | 28         |
| 1.5 Conclusion . . . . .   | 56         |

|          |   |            |
|----------|---|------------|
| <b>2</b> | <b>Adaptive finite element scheme for one-dimensional singularly perturbed parabolic problems</b>   | <b>58</b>  |
| 2.1      | Introduction . . . . .  | 58         |
| 2.2      | Singularly perturbed linear parabolic partial differential equation . .   | 60         |
| 2.3      | Construction of adaptive numerical scheme . . . . .   | 61         |
| 2.3.1    | Temporal discretization . . . . .   | 61         |
| 2.3.2    | Shishkin mesh methodology . . . . .   | 61         |
| 2.3.3    | Exponentially fitted finite element method . . . . .  | 62         |
| 2.3.4    | Streamline upwind/Petrov-Galerkin (SUPG) method . . . . .   | 64         |
| 2.4      | Numerical results . . . . .   | 64         |
| 2.5      | Non-linear singularly perturbed parabolic partial differential equation   | 69         |
| 2.6      | Proposed numerical strategy . . . . .   | 69         |
| 2.6.1    | Time semi-discretization . . . . .  | 69         |
| 2.6.2    | Quasilinearization process and its convergence . . . . .  | 70         |
| 2.7      | Absolute stability . . . . .  | 73         |
| 2.8      | Numerical results . . . . .   | 74         |
| 2.9      | Conclusion . . . . .  | 80         |
| <b>3</b> | <b>A posteriori error estimates for Hughes stabilized SUPG technique and adaptive refinement strategy for two-dimensional singularly perturbed problems</b> | <b>83</b>  |
| 3.1      | Introduction . . . . .  | 83         |
| 3.2      | Continuous problem . . . . .  | 85         |
| 3.2.1    | Hughes stabilization strategy . . . . .   | 87         |
| 3.3      | Some important notations and tools . . . . .  | 89         |
| 3.3.1    | Notations . . . . .   | 89         |
| 3.3.2    | Interpolation . . . . .   | 90         |
| 3.4      | Residual error estimates . . . . .  | 91         |
| 3.5      | Adaptive refinement strategy . . . . .  | 96         |
| 3.6      | Numerical results and discussion . . . . .  | 97         |
| 3.7      | Conclusion . . . . .  | 98         |
| <b>4</b> | <b>A posteriori error estimates for Hughes stabilized SUPG method for three-dimensional singularly perturbed problems</b>                                   | <b>101</b> |
| 4.1      | Introduction . . . . .  | 101        |

|          |  |            |
|----------|--|------------|
| 4.2      | Hughes stabilized SUPG technique . . . . .                         | 104        |
| 4.2.1    | SUPG method . . . . .  | 105        |
| 4.2.2    | Hughes stabilized SUPG technique . . . . .                         | 105        |
| 4.3      | Some auxiliary tools . . . . .                                     | 106        |
| 4.4      | Interpolation . . . . .  | 108        |
| 4.4.1    | Residual error estimates . . . . .                                 | 109        |
| 4.5      | Conclusion . . . . .   | 114        |
| <b>5</b> | <b>Applications of singularly perturbed problems</b>               | <b>115</b> |
| 5.1      | Introduction . . . . .   | 115        |
| 5.2      | Singularly perturbed generalized Burgers-Fisher equation . . . . . | 119        |
| 5.3      | Numerical results . . . . .  | 121        |
| 5.4      | Singularly perturbed generalized Burgers-Huxley equation . . . . . | 125        |
| 5.5      | Numerical results . . . . .  | 126        |
| 5.6      | Conclusion . . . . .   | 131        |
|          | <b>Future work</b>   | <b>133</b> |
|          | <b>Bibliography</b>  | <b>134</b> |

*DEDICATED  
TO  
MY FAMILY*

# Introduction

---

Around 1940's, with the advent of computer simulations, numerical methods came into existence. Scientists and researchers observed that analytical methods work efficiently for well-defined problems but for differential equations defined on complicated domains or which have complicated coefficients or which are non-linear in nature, it is not always feasible to apply these techniques. It has been observed that many times transformation of a continuum model to a discretized system may not effectively capture the whole information embodied in the models. As a result of which, at that time, one big question arose that how the approximation error can be effectively measured and minimized during computer simulations. Thanks to the efforts of researchers, scientists and mathematicians, today we have reached at a stage, where most of mathematical models of applied science and engineering can be numerically solved within the desired precision.

## 1.1 Need of adaptive finite element strategies

Finite element techniques are numerical techniques for simulating various realistic model problems described by differential equations or originating due to functional minimization and for approximating the sols. of initial or boundary value problems. Under a general framework, these techniques have been widely utilized

for solving many problems. From early 1950's to late 1970's, with the pioneering works of Courant[51], Hrennikoff[88], Feng[66], Argyris[7], Clough[48], Zeinkiewicz et al.[211, 212, 213], Ciarlet[42] and Gallagher et al.[72], etc., finite element methods became very popular and powerful techniques for solving differential problems. The researchers widely began to use these techniques for solving structural problems arising in civil and aeronautical engineering. During numerical simulations of realistic problems, one often faces the hurdle that the overall precision of numerical solutions is drastically affected due to the presence of local singularities e.g. interior or boundary layers, shocks or re-entrant corners[180], etc. In order to tackle this difficulty, one of the obvious ways is to identify the critical regions and then to refine the mesh in these regions to achieve more accurate numerical solutions. During 1980's-1990's, adaptive finite element techniques obtained its real impetus with the revolutionary work of Babuška et al.[13], Ainsworth et al.[5], Verfürth[193] and Eriksson et al.[62]. With the passage of time, these techniques became very popular and effective, and many researchers and scientists started using these techniques for finding numerical solutions of differential equations. These techniques are generally based on four successive steps:

**SOLVE**→**ESTIMATE**→**MARK**→**REFINE**.

In adaptive techniques based on a posteriori estimates, firstly, the problem under consideration is solved and then error estimates are proposed followed by the marking of elements that require refinements[193]. At the end, adaptive algorithm is proposed for refining the meshes and to obtain the admissible numerical solution within the desired accuracy. Since error estimation is a basic component in the development of adaptive strategies, therefore, the need of error estimates becomes essential. Broadly, error estimates can be categorized into two categories, namely, a priori error estimates and a posteriori error estimates. It is seen that a priori error estimates provide crude information only about the asymptotic behavior of the solution and involves regu-

larity conditions which are very difficult to achieve in case of singularities, whereas, a posteriori error estimates provide information about the quantitative behavior of the solution expected and can be derived using information about the computed numerical solution. The main goal of a priori error estimates is to obtain a reasonable measure about the order of convergence and the efficiency of the developed scheme. In this Chapter, a detailed survey of different adaptive techniques based on finite element methods has been presented. These methods have been developed to study partial differential equations which occur during the analysis of biological systems, heat transfer process, etc. Some realistic model problems e.g. Navier-Stokes problem, quasi-linear elliptic problems, Maxwell's equation, Helmholtz equation, bifurcation problem, frictional problems, etc., have also been presented in this Chapter.

The Chapter is organised as follows.

In Section 1.2, we have presented some real world problems from applied science and engineering which have been analyzed using various adaptive finite element techniques. In Section 1.3, an overview towards the developments of various adaptive techniques from 1970 to 2009 has been discussed. The literature survey of recently developed adaptive techniques, mostly based on a posteriori error estimates, gaps in literature and objectives of the thesis have been presented in Section 1.4. In the last Section, conclusion has been presented.

## **1.2 Some of the real world models**

In this Section, we present some of the realistic model problems for which various adaptive finite element techniques have been applied by researchers. Some of the mathematical models occurring frequently in fluid mechanics, financial mathematics, modeling of gas dynamics, ecology, physiology, combustion, crystallization, plasma physics, phase transition, etc., have been presented below in brief.

### **1. Anisotropic biphasic model of tissue-equivalent mechanics**

The anisotropic biphasic model of tissue-equivalent mechanics[150] can be represented as:

$$\begin{aligned} \frac{1}{2G}\dot{\sigma} + \frac{1}{2\mu}\sigma &= \frac{1}{2}[\nabla\mathbf{v} + (\nabla\mathbf{v})^T] + \frac{\nu}{1-2\nu}(\nabla \cdot \mathbf{v})\mathbf{I}, \\ \nabla \cdot [\theta(\sigma + \tau c\Omega_c) - P\mathbf{I}] &= 0, \\ \frac{Dc}{Dt} + c(\nabla \cdot \mathbf{v}) &= \nabla \cdot (D_o\Omega_c \cdot \nabla c) + k_o c, \\ \frac{D\theta}{Dt} + \theta(\nabla \cdot \mathbf{v}) &= 0, \\ -\nabla \cdot \left[ \frac{(1-\theta)}{\theta}\nabla P + \phi_o\nabla \cdot \mathbf{v} \right] &= 0, \end{aligned}$$

where

$$\dot{\sigma} \equiv \frac{D\sigma}{Dt} - \nabla\mathbf{v} \cdot \sigma - \sigma \cdot (\nabla\mathbf{v})^T.$$

Here  $\frac{D}{Dt}$  denotes material derivative,  $\mathbf{I}$  is the identity tensor,  $\theta$  is the collagen network volume fraction,  $\mathbf{v}$  is the network velocity,  $c$  denotes cell concentration,  $\sigma$  is the stress tensor,  $P$  is the pressure,  $G$  is the modulus representing material property associated with the collagen network,  $\mu$  the viscosity,  $\nu$  the Poisson's ratio,  $\phi_o$  represents interstitial flow resistance,  $D_o$  is the diffusivity,  $k_o$  is the growth rate constant,  $\Omega_c$  represents the cell orientation tensor and  $\tau$  is the traction parameter given as  $\tau \equiv \tau_o \cdot \frac{t^{X_A}}{t^{X_A+X_B}} \cdot \frac{1}{1+\lambda c^2}$  where  $\tau_o$ ,  $X_A$ ,  $X_B$  and  $\lambda$  are constants.

## 2. American-style option pricing problem

The American-style option pricing problem based on Black-Scholes model[204] is defined as

$$\begin{aligned} \frac{\partial V}{\partial t} + \frac{1}{2}\sigma^2 S^2 \frac{\partial^2 V}{\partial S^2} + rS \frac{\partial V}{\partial S} - rV &= 0 & \forall S > S_f(t) & \quad t \in [0, T], \\ V(S, t) &= P(S) & \forall 0 \leq S \leq S_f(t) & \quad t \in [0, T], \end{aligned}$$

subjected to initial and boundary conditions

$$\begin{aligned}
V(S, T) &= P(S) & S \geq 0, \\
V(S_f(t), t) &= P(S_f(t)) & 0 < t \leq T, \\
\frac{\partial V}{\partial S}(S_f(t), t) &= -1 & 0 < t \leq T, \\
\lim_{S \rightarrow \infty} V(S, t) &= 0 & 0 \leq t \leq T,
\end{aligned}$$

where  $S(t)$  represents the underlying stock price,  $V(S, t)$  is the American put option price at time  $t$ ,  $\sigma$  is the volatility of the underlying stock,  $r$  the interest rate,  $S_f(t)$  the exercise boundary at time  $t$  and  $P(S)$  is the pay-off function.

### 3. One dimensional water column model

One dimensional water column model[83] with unknowns horizontal velocity  $\mathbf{u} = (u, v)$  and  $b$  as buoyancy is given by:

$$\begin{aligned}
\frac{\partial \mathbf{u}}{\partial t} + f \mathbf{e}_z \times \mathbf{u} &= \frac{\partial}{\partial z} \left( K_u \frac{\partial \mathbf{u}}{\partial z} \right), \\
\frac{\partial b}{\partial t} &= \frac{\partial}{\partial z} \left( K_b \frac{\partial b}{\partial z} \right),
\end{aligned}$$

subjected to initial and boundary conditions

$$\begin{aligned}
[\mathbf{u}, b]_{t=0} &= [0, N_0^2 z], \\
[q^2, q^2 l]_{t=0} &= [q_{\min}^2, (q^2 l)_{\min}], \\
\left[ K_u \frac{\partial \mathbf{u}}{\partial z}, K_b \frac{\partial b}{\partial z} \right]_{z=0} &= [|\mathbf{u}_*| \mathbf{u}_*, 0], \\
[q^2, q^2 l]_{z=0} &= [6.5074 \mathbf{u}_*^2, 0]
\end{aligned}$$

defined over model domain that varies from  $z = -h$  to sea surface ( $z = 0$ ) assuming that all variables are horizontally homogeneous. In the above equations,  $f$  represents Coriolis factor,  $z$  is the vertical coordinate (increasing upwards),  $\mathbf{e}_z$  the vertical unit vector,  $K_u$  the eddy viscosity,  $K_b$  the eddy diffusivity,  $b = -g(\rho - \rho_0)/\rho_0$  is the buoyancy,  $g$  the gravitational acceleration,  $\rho$  the water density,  $\rho_0$  the reference value of density,  $N_0$  the initial Brunt-Väisälä frequency,  $\mathbf{u}_*$  is the surface friction velocity,

$l$  the turbulence macroscale,  $q$  the velocity scale,  $q_{\min}^2 = 5 \times 10^{-7} m^2 s^{-2}$ ,  $(q^2 l)_{\min} = 10^{-5} m^3 s^{-2}$  and  $\|\mathbf{u}_*\| = 10^{-2} m s^{-1}$ .

#### 4. Fokker-Planck equation

The drift-diffusion partial differential equation, also known as the Fokker-Planck equation[49] is given by

$$\mathbf{div}[D(\mathbf{x})\nabla p(\mathbf{x}) - v(\mathbf{x})p(\mathbf{x})] = 0,$$

where  $\mathbf{x} = (x_1, x_2, \dots, x_N) \in \mathbb{R}^N$  is a vector of concentration of  $N$  chemical species,  $D \equiv D(\mathbf{x}) : \Omega \rightarrow \mathbb{R}^{N \times N}$  is the diffusion matrix,  $v \equiv v(\mathbf{x}) : \Omega \rightarrow \mathbb{R}^N$  is the drift term,  $p \equiv p(\mathbf{x})$  represents the  $N$ -dimensional probability distribution function and  $\mathbf{div}$  is the divergence operator.

#### 5. Model representing transport of contaminated groundwater flow in saturated and unsaturated porous media

The model representing multi-dimensional, time dependent transport of contaminated groundwater flow[155] is defined as

##### Saturated porous media

$$\begin{aligned} R_d \frac{\partial C}{\partial t} + \mathbf{V} \cdot \nabla C &= \nabla \cdot (\mathbf{D} \cdot \nabla C) + S, \\ S_h \frac{\partial h}{\partial t} &= \nabla \cdot (\mathbf{k} \cdot \nabla h) + Q, \end{aligned}$$

where  $\mathbf{D}$  ( $\equiv d_{ij}$ ) represents hydrodynamic dispersion tensor given as

$$\begin{aligned} d_{ij} &= \delta_{ij} \alpha_T |\mathbf{V}| + (\alpha_L - \alpha_T) \frac{\mathbf{V} \mathbf{V}^T}{|\mathbf{V}|} + \delta_{ij} \mu, \\ \mathbf{V} &= -\mathbf{k} \cdot \nabla h / \theta. \end{aligned}$$

##### Unsaturated porous media

$$\begin{aligned} \frac{\partial C}{\partial t} + \mathbf{V} \cdot \nabla C &= \nabla \cdot [\mathbf{D}(\psi) \cdot \nabla C] + S_\psi, \\ C_\psi \frac{\partial \psi}{\partial t} &= \nabla \cdot (\mathbf{k}(\psi) \cdot \nabla \psi) + Q_\psi. \end{aligned}$$

The parameters used in the above models are defined in [155].

## 6. Magnetotelluric excitation model

The set of partial differential equations arising due to two independent modes (TE-transverse electric and TM-transverse magnetic) of magnetotelluric excitation (MT)[103] are represented as:

$$\begin{aligned} TE : -\nabla \cdot \nabla E_x + i\omega u_0 \sigma E_x &= -i\omega u_0 J_0, \\ TM : -\nabla \cdot \frac{1}{\sigma} \nabla H_x + i\omega u_0 H_x &= -i\omega u_0 M_0, \end{aligned}$$

where  $\omega$  is the angular frequency,  $u_0 = 4\pi \times 10^{-7}$  H/m is the uniform magnetic permeability,  $J_0(z)$  represents the uniform electric source,  $M_0(z)$  is the uniform magnetic source located above earth' surface,  $\sigma$  the electrical conductivity,  $E_x$  the electric field and  $H_x$  is the magnetic field.

## 7. Poisson-Boltzmann equation

Poisson-Boltzmann equation[87] is used to study the electrostatic interaction between molecules in ionic solution and is given by

$$-\nabla \cdot (\epsilon \nabla \phi) = \frac{4\pi}{\epsilon_0} (\rho_m + \rho_f),$$

where  $\phi = \phi(x)$  is the electrostatic potential,  $\epsilon = \epsilon(x)$  is the spatially varying dielectric constant,  $\epsilon_0$  is the dielectric permittivity constant of vacuum,  $\rho_m$  represents mobile charge distribution and  $\rho_f$  is the fixed charge distribution. The expression for  $\rho_m$  and  $\rho_f$  are defined as

$$\rho_m = \sum_{j=1}^M c_j q_j e^{\frac{-q_j \phi}{kT}}, \quad \rho_f = \sum_{i=1}^N q_i \delta(x_i), \quad x_i \in \Omega_m,$$

where  $M$  is the number of ion species,  $c_j$  is the bulk concentration,  $q_j$  is the charge of  $j^{th}$  ion,  $k$  represents Boltzmann constant,  $T$  is the absolute temperature,  $q_i$  the carrying charge,  $\delta(x_i)$  the delta function centered at  $x_i$  and  $N$  represents number of charges located at  $x_i$  in the molecular region  $\Omega_m$ .

## 8. Models representing autocatalytic chemical reaction

The model representing autocatalytic chemical reaction (Gray-Scott model)[105] is given by

$$\begin{aligned} \frac{\partial \mathbf{u}}{\partial t} &= d_u \Delta \mathbf{u} - \mathbf{u} \mathbf{v}^2 + A(1 - \mathbf{u}) && \text{in } \Omega \times (0, T), \\ \frac{\partial \mathbf{v}}{\partial t} &= d_v \Delta \mathbf{v} + \mathbf{u} \mathbf{v}^2 - \lambda \mathbf{v} && \text{in } \Omega \times (0, T), \\ \frac{\partial \mathbf{u}}{\partial \nu} &= 0, \quad \frac{\partial \mathbf{v}}{\partial \nu} = 0 && \text{on } \partial \Omega, \\ \mathbf{u}(x, 0) &= \mathbf{u}_0(x), \quad \mathbf{v}(x, 0) = \mathbf{v}_0(x) && x \in \Omega, \end{aligned}$$

where  $d_u, d_v, \lambda > 0, A \geq 0$  are constants and  $\mathbf{u}, \mathbf{v}$  represent concentration of chemical reactants.

### 1.3 Overview towards the development of various adaptive finite element methods

During 1978, Babuška and Rheinboldt[9] made remarkable contributions in this emerging field by developing a posteriori error estimates for two point elliptic boundary value problems. In 1984, at the Lisbon conference on adaptive refinement techniques and error estimates, emphasize was given on new techniques[12], such as element residual method, for the development of a posteriori error estimates. With the aim to get effective adaptive techniques, many a priori and interpolation estimates[53] came into existence. Different a posteriori error estimation techniques such as residual estimation method, duality method, subdomain residual method, post-processing method, etc., were discussed. These interpolation estimates proved to be efficient for some specific problems of computational fluid dynamics in which solution exhibits surfaces of discontinuity and rarefaction waves, but failed badly for problems whose solutions display boundary layers. In 1989, Demkowicz et al.[54, 148] proposed a posteriori error estimates and adaptive strategies for linear elliptic boundary value problem using  $h-p$ -FEM(“finite element method”). In 1990, Wu et al.[198] proposed

adaptive technique based on Zienkiewicz and Zhu error estimates and semi-implicit time marching scheme for Navier-Stokes incompressible fluid flow problems.

After the development of basic strategies for a posteriori error estimation, the attention of researchers diverted towards the application of these estimates to general classes of problems. Verfurth[192] derived error estimates for Stokes and Navier-Stokes problems. By the end of 1990, researchers started making efforts to formulate a posteriori error estimates based on  $h$ -,  $p$ - and  $h - p$ -finite element methods for different practical problems. Ainsworth and Oden[4] developed a posteriori error estimates for elliptic problems using element residual method. Further, authors formulated a posteriori error estimates and adaptive techniques based on  $h - p$ -finite element approximations for solving incompressible Navier-Stokes problem.

In 1998, Picasso[157] proposed a posteriori error estimates for the heat equation. The author used backward Euler scheme for time discretization and finite element scheme with linear triangular finite elements for space discretization. Becker and Rannacher[20] discussed adaptive strategy based on Galerkin FEM. A posteriori error estimates were derived using duality technique. Zienkiewicz and Zhu[213] proposed a simple and accurate error estimator for estimation of local and global energy norm errors for different engineering problems. Bergam et al.[23] developed a posteriori error estimates for linear and semilinear parabolic problems. Implicit Euler scheme was considered for time discretization followed by space discretization under finite element framework.

Verfurth[194] proposed a posteriori error estimates for the convection-diffusion problem

$$\begin{aligned}
 -\epsilon \Delta u + \mathbf{a} \cdot \nabla u + bu &= f \text{ in } \Omega \subset \mathbb{R}^n, \\
 u &= 0 \text{ on } \Gamma_D, \\
 \epsilon \frac{\partial u}{\partial \mathbf{n}} &= g \text{ on } \Gamma_N,
 \end{aligned}$$

based on finite element method using locally refined isotropic meshes over a bounded polygonal domain  $\Omega$ . By the end of 2000, the concept of error estimation for FE (“finite element”) methods reached its maturity. As a result, researchers shifted their focus towards the development of marking and refining strategies essential to obtain adaptive procedures. Eriksson et al.[62] in their work stressed over the need of introducing the concept of adaptivity for FE methods. In 1996, Dörfler[60] proposed crucial marking and refinement strategy based on error estimates for marking the triangles which need refinements to get new triangulations.

Mesh refinement can be achieved by coarsening or local refinement of the mesh ( $h$ -refinement), moving or relocating a mesh ( $r$ -refinement) and by local variation of the degree of polynomials in the basis ( $p$ -refinement). It has been observed that  $r$ -refinement techniques are quite effective in dealing with transient problems whereas  $p$ -refinement techniques result in increase in rate of convergence for problems with smooth solutions. Many  $h$ -refinement strategies also result in an increase in convergence rate for problems exhibiting singularities[11, 166]. Mitchell in his work[128] proposed various adaptive finite element refinement techniques for solving elliptic problems using piecewise linear basis functions. He emphasized on different strategies to determine triangles with largest error and on the techniques for division of triangles such as-regular division and bisection method. Later Rivara[166, 167] developed hybrid mesh refinement strategy based on the bisection of longest edge approach and newest node approach. Cliffe et al.[46] proposed DGFEM (“discontinuous Galerkin finite element method”) for solving bifurcation problems associated with steady Navier-Stokes equation. The authors proposed adaptive mesh refinement technique based on the derived a posteriori error estimates. Further, Cliffe et al.[45] presented a posteriori error estimates and adaptive mesh refinement strategy based on the discontinuous Galerkin method for eigenvalue problems used in channel and pipe geometries. Moore[137] proposed an adaptive higher order  $h$ -refinement technique

combined with continuation method to approximate solutions of three-dimensional singularly perturbed reaction-diffusion problems.

Lang[114] derived a priori error estimates based on interpolation technique for two-dimensional convection-diffusion SPP(“singularly perturbed problems”). An adaptive refinement strategy based on SDFEM(“streamline-diffusion finite element method”) was proposed. On the basis of  $h$ -,  $p$ - and  $r$ -refinement techniques, several new refinement strategies came into existence. Lang et al.[115] developed  $r - h$ -adaptive FEM for solving time-dependent partial differential equations.

Numerous good books were written by Verfurth[193], Ainsworth and Oden[5], Bangerth et al.[14], Babuska, etc., on a posteriori error estimation and adaptive mesh refinement techniques. Though the authors tried their bests to incorporate exclusive and wide varieties of adaptive techniques, but probably due to limited resources and availability of the research papers, some of the research papers could not have been included. The literature towards the development of adaptive FE methods is quite vast. In this Chapter, we present a recent survey with the aim to highlight the developments of adaptive techniques under finite element framework.

## **1.4 Brief survey of adaptive techniques based on finite element framework**

Here below, we present a survey of various finite element based adaptive strategies ( $h$ -,  $p$ -,  $h - p$ -,  $h - p - q$ -,  $r$ -,  $r - h$ -, etc.) for different problems e.g. axisymmetric compressible flow problems, Navier-Stokes problems, quasi-linear elliptic problems, Maxwell’s equation, evolutionary convection dominated problems, singularly perturbed problems, Helmholtz equation, advection-diffusion-reaction problems, bifurcation problems, frictional problems, etc. The survey has been categorized as per different adaptive strategies.

### 1.4.1 $h$ -adaptive strategies

Bao et al. [17] considered the following Kohn Sham equation representing density functional theory model

$$H\psi_i(\vec{x}) = \epsilon_i\psi_i(\vec{x}),$$

where  $H = -\frac{1}{2}\nabla^2 + V_{ext}(\vec{x}) + V_{Hartree}[n](\vec{x}) + V_{xc}[n](\vec{x})$ ,

subjected to Dirichlet boundary conditions, where  $H$  is the Hamiltonian operator,  $\psi_i(\vec{x})$  is the wavefunction or the eigenfunction,  $\epsilon_i$  is the eigen energy,  $-\frac{1}{2}\nabla^2$  is the kinetic energy operator,  $n$  is the electron density,  $V_{ext}(\vec{x})$  is the external potential,  $V_{xc}$  is the exchange-correlation potential and  $V_{Hartree}$  is the Hartree (electrostatic) potential. In the beginning, the authors have used self-consistent field iteration for discretization of considered equation based on linear finite element method using tetrahedron meshes. Further, Hartree potential is computed by solving Poisson equation using algebraic multigrid method. Boundary values are obtained using multipole expansion method. Locally optimal block preconditioned conjugate gradient method is considered to solve the generalized eigenvalue problem. An efficient error indicator based on normalization of indicator for each orbital has been presented. Further,  $h$ -adaptive algorithm based on error indicator and hierarchy of the geometry tree for mesh refining and coarsening has been presented. The efficiency of adaptive technique has been tested through numerical experiments involving simulation of atoms and molecules. Experimentally, it has been shown that the numerical solutions obtained using the adaptive technique are efficient for the pseudo-potential and the all-electron calculations.

In 2013, Paszynski et al.[154] considered two-and three-dimensional problems displaying point singularities. With the aim to reduce the computational cost, the authors developed a direct adaptive algorithm based on  $h$ -refinement at point of singularities. It was shown that the proposed solver results in linear computational cost of  $O(N)$

with respect to the number of unknowns  $N$  in terms of memory usage and execution time.

Later on in 2013, Nicolas and Fouquet [147] proposed an adaptive  $h$ -refinement technique based on conformal finite element method on hexahedral mesh. Technique developed has been presented in three steps. In the first step, each mesh element in mesh having error indicator greater than same threshold value is refined by splitting its edges into two edges. In the second step, each mesh element with at least two refined neighbors is refined. In the third step, each mesh element with hanging nodes is refined. At the end, the efficiency of proposed adaptive technique has been tested numerically using HOMARD software.

### 1.4.2 $p$ -adaptive strategies

Nguyen et al.[144] proposed  $p$ -adaptive FEM for elliptic partial differential equations defined as:

$$-\nabla \cdot \mathbf{a}(x, y, u, \nabla u) + f(x, y, u, \nabla u) = 0 \text{ in } \Omega,$$

subjected to boundary conditions

$$\begin{aligned} u &= g_2(x, y) \quad \text{on } \partial\Omega_2, \\ \mathbf{a}(x, y, u, \nabla u) \cdot \mathbf{n} &= g_1(x, y, u) \quad \text{on } \partial\Omega_1, \end{aligned}$$

where  $\Omega \subseteq \mathbb{R}^2$  is a bounded domain,  $\mathbf{a} = (a_1, a_2)^T$ ,  $u$ ,  $\mathbf{a}(x, y, u, \nabla u) \cdot \mathbf{n}$  are continuous on  $\partial\Omega_0$  and  $a_1$ ,  $a_2$ ,  $f$ ,  $g_1$ ,  $g_2$  are the scalar functions. The following a priori error estimates:

$$\|u - u_p\|_{1, \Omega_0} \leq C(k, \epsilon) p^{-(k-1)+\epsilon} \|u\|_{k, \Omega_0},$$

is proposed. Here  $u \in H^k(\Omega_0)$ ,  $k > 1$ ,  $u_p \in P_p(\Gamma_h)$  is the finite element approximation,  $P_p(\Gamma_h)$  is the space of  $C^0$  piecewise polynomials of degree upto  $p$  and  $\Gamma_h$  is

the triangulation of  $\Omega_0$ . Error estimates based on the derivative recovery technique proposed by Bank and Xu [15, 16]

$$\|\nabla u - S_h^m Q_h \nabla u_h\|_{0,\Omega} \leq h (mh^{1/2} + \epsilon m) (\|u\|_{3,\Omega} + |u|_{2,\infty,\Omega}),$$

are discussed. Further,  $h - p$ -refinement indicator is discussed. Numerical validation shows that the combination of  $h$ -and  $p$ -refinement indicators results in optimal meshes. Exponential rate of convergence on adaptive meshes is shown.

### 1.4.3 $h - p$ -adaptive strategies

Dörsek and Melenk [61] considered the problem of frictional contact arising in linear elasticity. In the beginning, the considered problem is approximated using  $h - p$ -finite element method. Further, a priori error estimates based on  $h - p$ -mortar projection operator are proposed in two-and three-dimensions. A residual based error indicator in two-dimensions is proposed as defined by Melenk and Wohlmuth[126]. At the end, based on the derived error estimates an adaptive  $h - p$ -finite element algorithm is proposed and it is shown to be efficient on the basis of different numerical tests.

In 2010, Paszyński et al.[152] proposed self-adaptive  $h - p$ -finite element method to study petroleum engineering problems (3D Direct Current (DC) resistivity logging measurements in deviated well) modeled by

$$\nabla \cdot (\sigma \nabla u) = -f,$$

where  $\sigma$  is the conductivity of media and  $f$  is the load. Starting with an arbitrary initial two-dimensional rectangular mesh, the mesh is refined with the aim to reduce the numerical error of the solution. It has been observed that size of elimination tree (number of degrees of freedom) increases as mesh refinement is performed and consequently the computation time also increases. In this work, a new parallel direct solver on the basis of three level elimination trees i.e. sub-domains, initial mesh elements, and refinement trees is proposed. Based on history of refinements, the new solver

involves construction of the third level elimination tree. The proposed solver involves elimination of interior of  $h - p$ -finite elements which are computationally most expensive and have less connected nodes. Exponential convergence of the numerical error with respect to degrees of freedom and CPU time on adaptive mesh is shown. Both regular and irregular mesh i.e. adaptive meshes with very large degrees of freedom are considered to measure computational cost and the execution time of the proposed solver numerically.

In his paper[197], Wihler proposed  $h - p$ -adaptive strategy based on continuous Sobolev embedding for one-dimensional elliptic BVP(“boundary value problems”) of the type

$$\begin{aligned} -au'' + du &= f \quad \text{on } \Omega = (0, 1) \subset \mathbb{R}, \\ u(0) &= u(1) = 0, \end{aligned}$$

where  $a > 0$  and  $d \geq 0$ . Reliable and efficient upper and lower a posteriori error bound are proposed. The **upper bound** is

$$\|u - u_{hp}\|_{E,(0,1)}^2 \leq \sum_{j=1}^N \eta_{K_j}^2 + \frac{1}{ap_j(p_j+1)} \|(f - \pi_N f)w_j^{1/2}\|_{0,K_j}^2$$

where

$$\eta_{K_j} = \frac{1}{\sqrt{ap_j(p_j+1)}} \|(\pi_N f + au''_{hp} - du_{hp})w_j^{1/2}\|_{0,K_j}.$$

Here  $\eta_{K_j}$  is the local error estimator on  $K_j$ ,  $j = 1, 2, \dots, N$ ,  $\pi_N$  represents  $L^2$ - projection onto  $V(\gamma_N, \mathbf{p}_N)$ ,  $w_j$  is a non-negative weight function on  $K_j$ . Define  $K_j = (x_{j-1}, x_j)$ ,  $w_j(x) = (x_j - x)(x - x_{j-1})$ ,  $u \in H_0^1(0, 1)$  represents solution,  $u_{hp} \in V(\gamma_N, \mathbf{p}_N)$  is  $h - p$  finite element solution on mesh  $\gamma_N$ ,  $\gamma_N = \{K_j\}_{j=1}^N$  and  $\mathbf{p}_N$  is polynomial degree vector defined as  $\mathbf{p}_N = (p_1, p_2, \dots, p_N)$ . The **lower bound** is

$$\eta_{K_j} \leq c \left( a \|u' - u'_{hp}\|_{0,K_j}^2 + d \|u - u_{hp}\|_{0,K_j}^2 \right)^{1/2} + \frac{1}{\sqrt{ap_j(p_j+1)}} \|(f - \pi_N f)w_j^{1/2}\|_{0,K_j}^2,$$

for  $j = 1, 2, \dots, N$  and  $c > 0$  is a constant. The author proposed new smoothness estimation technique using a posteriori error estimates. Exponential convergence is

proved experimentally for the proposed  $h-p$ -adaptive strategy for the elliptic boundary value problems. The advantage of proposed algorithm is that it helps to locate and resolve the local irregularities arising in the solution.

Schillinger and Rank [176] introduced B-spline finite element method to study interface problems with complex geometry. An unfitted adaptive refinement of interfaces based on hierarchically contracted B-splines, which improves the resolution of corresponding discontinuities, is proposed. Numerically, it is shown that despite of the presence of discontinuities, proposed  $h-p$ -adaptive refinement strategy, which involves simultaneous increase in the polynomial degree of B-spline basis and the levels of refinement around interfaces, results in exponential rate of convergence. The performance of proposed adaptive strategy is tested for two- and three-dimensional interface problems.

In 2011, Armentano et al. [8] proposed  $h-p$ -adaptive FEM to solve a two-dimensional Laplace model, arising from fluid-solid vibrations.  $h-p$ -FEM is used to find the approximate solution of the considered model problem. Convergence analysis of the proposed method is presented. A priori error estimates for eigenvalues and eigenfunctions are derived. Residual type a posteriori error estimates are proposed. Authors derived the global error estimate given as:

$$\eta_{\Omega} \leq C_{\delta}(\max \mathbf{p})^{1+\delta}(|e|_{H^1(\Omega)}^2 + \text{higher order terms})^{1/2},$$

where  $\delta > 0$ ,  $C_{\delta} > 0$  is a positive constant,  $\eta_{\Omega}$  represents global error estimator and  $e$  is the error. Further, the reliability and efficiency of the derived estimates have been proved by showing it to be equivalent to the  $e$  in energy norm. An adaptive algorithm has been developed based on the proposed a posteriori error estimates. The proposed an adaptive algorithm results in refining of some of the elements and increasing the polynomial degree at each step. At the end, numerical experiments have been carried out which show that the proposed scheme results in exponential convergence.

Solin and Kuraz [184] analysed time-dependent Darcian flow problem (Richards equa-

tion) using  $h-p$ -adaptive finite element method. Convergence of new proposed adaptive approach has been tested numerically by considering different problems with known exact solution, non-stationary groundwater seepage into dry lysimeter box with time-dependent boundary conditions and non-stationary problem of capillary under intense infiltration.

Paszyńska et al.[153] developed programmable graph grammar model for self-adaptive two-dimensional  $h-p$ -FEM based on mixed triangular and rectangular elements. In the beginning,  $h-p$ -adaptive finite element strategy is discussed. Further modelling of the proposed method by graph grammars has been presented.

Hakula [82] analyzed two- and three-dimensional elliptic BVPs, given in [82], using  $h-p$  adaptive finite element method. The author proposed error indicators for the model and then based on these error indicators, developed an  $h-p$ -adaptive algorithm. Error indicators based on the internal shape functions of the elements have been developed. The effectivity and convergence of the proposed adaptive algorithm have been observed numerically by applying it to square and L-shaped domains.

Revuelto et al.[165] studied the following discontinuity problem in rectangular waveguide technology

$$\nabla \times \frac{1}{\epsilon_r} \nabla \times \mathbf{H} - k_0^2 \mu_r \mathbf{H} = 0,$$

subject to boundary conditions

$$\begin{aligned} \mathbf{n} \times \mathbf{H} &= 0 \text{ at perfect magnetic conductors } (\Gamma_D), \\ \mathbf{n} \times \frac{1}{\epsilon_r} \nabla \times \mathbf{H} &= 0 \text{ at perfect electric conductors } (\Gamma_N), \\ \mathbf{n} \times \frac{1}{\epsilon_r} \nabla \times \mathbf{H} + j \frac{k^2}{\epsilon_r \beta_{10}} \mathbf{n} \times \mathbf{n} \times \mathbf{H} &= \mathbf{U}^{in} \text{ at port boundaries } (\Gamma_p), \end{aligned}$$

where  $\mathbf{H}$  represents magnetic field intensity vector,  $\epsilon_r = \epsilon/\epsilon_0$ ,  $\mu_r = \mu/\mu_0$ ,  $\epsilon$  is electrical permittivity,  $\mu$  is magnetic permeability of the medium,  $k_0 = w\sqrt{\epsilon_0\mu_0}$ ,  $\epsilon_0$  corresponds to electrical permittivity in vacuum medium,  $\mu_0$  is magnetic permeability of vacuum

medium,  $\mathbf{U}^{in} = 2j \frac{k^2}{\epsilon_r \beta_{10}} \mathbf{n} \times \mathbf{n} \times \mathbf{H}^{in}$ , with  $\mathbf{H}^{in}$  being incident magnetic field at the port. An adaptive  $h-p$ -FEM supporting anisotropic refinements on irregular meshes with hanging nodes, and isoparametric elements is developed. Similar type of three-dimensional self-adaptive  $h-p$ -strategy was first proposed for elliptic problems by Demkowicz and Buffa[55]. Numerical experiments are performed which show that the approximation error in energy norm converges exponentially on  $h-p$ -meshes.

Later on in 2014, Giani et al.[76] proposed  $h-p$ -adaptive discontinuous Galerkin (DG) method for singularly perturbed convection-diffusion problem in 2D on anisotropically refined meshes. Firstly, the considered equation is discretized using  $h-p$ -version interior penalty DG FEM on anisotropically refined meshes. A posteriori error estimates have been derived. Based on these derived estimates, global upper and lower bounds of error, expressed in terms of natural norm associated with diffusion and semi-norm associated with convection, have been proposed. It has been shown that the proposed lower bound of error does not depend on singular perturbation parameter and mesh size whereas global error upper bound is based on anisotropic interpolation. Further,  $h-p$ -adaptive algorithm has been developed. In order to test the reliability and efficiency of proposed adaptive strategy, various numerical experiments have been carried out which shows that internal and boundary layers occurring in numerical solutions are easily captured and resolved with exponential rate of convergence.

Aramberri et al.[6] analyzed the round-off errors during the computation of numerical solution of Poisson equation

$$-\Delta u = f,$$

using  $h-p$ -adaptive finite element method. Earlier, it was considered that the behavior of round-off errors can be analyzed only using the condition number. In this paper, it has been shown that through suitable eigenvalue analysis, suitable choice of right-hand side of considered equation can also result in small round-off errors despite the presence of large condition number. While performing  $p$ -refinements, authors proved

that suitable choice of basis functions also affects the round-off errors. Different basis functions such as hierarchical Peano and integrated Legendre polynomials (ILP) have been considered and it has been shown numerically that ILP produces better results as compared to hierarchical Peano basis functions and small number of elements.

Giani et al. [75] studied the following eigen value problem:

$$\begin{aligned} Au &:= -\nabla \cdot (\mathbf{A}\nabla u) + Vu = \lambda u \quad \text{on } \Omega, \\ u &= 0 \quad \text{on } \partial\Omega, \end{aligned}$$

where  $\Omega \subset \mathbb{R}^2$  is a bounded domain,  $A$  is a self-adjoint and satisfies some conditions[75]. Such type of equations represent a class of jumping coefficient problems. The considered problem has been analyzed using discontinuous Galerkin method. Since dual weighted residual (DWR)[46, 45] approach is flexible and effective, goal oriented a posteriori error estimates have been derived using DWR approach based on associated dual of the considered problem. In order to estimate the error, authors proposed the following result

$$|J(\hat{u}) - J(\hat{u}_n)| \leq \sum_{K \in \gamma_n} |\eta_K|$$

in terms of the goal functional. Here  $\eta_K$  represents the residual defined as:

$$\begin{aligned} \eta_K &= \int_K -(\lambda_n u_n + \nabla \cdot (\mathbf{A}_K \nabla u_n) - Vu_n)(z - z_n) - \frac{1}{2} \int_{\partial K/\Gamma} \{ \{ \mathbf{A} \nabla (z - z_n) \} \} [[u_n]] \\ &\quad + \frac{1}{2} \int_{\partial K/\Gamma} [[\mathbf{A} \nabla u_n]] \{ \{ z - z_n \} \} + \frac{1}{2} \int_{\partial K/\Gamma} c[[u_n]][[z - z_n]] - \int_{\partial K \cap \Gamma} \mathbf{A}_K \frac{\partial(z - z_n)}{\partial \mathbf{n}} u_n \\ &\quad + \int_{\partial K \cap \Gamma} c u_n (z - z_n), \end{aligned}$$

where  $\hat{u}$  is exact solution and  $\hat{u}_n$  is approximate solution of corresponding dual problem. The  $h-p$ -adaptive algorithm has been developed to reduce the eigen value error. Numerical experiments have been performed on different test problems having jump discontinuities and it has been shown that the developed adaptive scheme results in exponential convergence of eigenvalue error.

Bürg [28] developed an automatic  $h-p$ -adaptive FE methodology for numerical simulation of Maxwell's equation representing the electric field. Firstly, the author carried out finite element formulation and proposed the following a posteriori error estimates:

$$\|u - u_N\|_{\Omega}^2 \leq C_1 \sum_{K \in \mathbf{K}} (p_K + 1)^{2\epsilon} (\eta_K^2 + \frac{h_K^2}{(p_K+1)^2} \|f - f_{p_{K+1}}\|_{L^2(K)}^2),$$

where

$$\eta^2 \leq C_2(\epsilon) \sum_{K \in \mathbf{K}} (p_K + 1)^{2(2+\epsilon)} (\|u - u_N\|_{w_K}^2 + \frac{h_K^2}{(p_K+1)^2} \|f - f_{p_{K+1}}\|_{L^2(w_K)}^2).$$

Here the constants  $C_1$  and  $C_2(\epsilon) > 0$  are independent of  $h$ , the mesh size vector and  $p$ , the polynomial degree vector. Further,  $h-p$ -adaptive refinement technique has been developed. It has been shown that the proposed  $h-p$ -adaptive refinement strategy is uniformly convergent as energy error decreases with each refinement step of the algorithm. At the end, efficiency of proposed algorithm is tested using various numerical examples.

In the same year 2013, Cliffe et al. [47] developed goal oriented a posteriori estimates based on dual weighted residual strategy for the DGFEM (“discontinuous Galerkin finite element method”) for the nonlinear time dependent bifurcation problem given as:

$$\frac{\partial u}{\partial t} + F(u, \lambda) = 0,$$

where  $\lambda$  is unknown parameter (Reynolds number),  $u$  is state variable and  $F$  represents the incompressible Navier-Stokes equation defined on open domain  $\Omega \subset \mathbb{R}^d$  ( $d = 2,3$ ). The concept of  $Z_2$  or  $O(2)$  symmetry is introduced to reduce the computational difficulty. After that  $h-p$ -adaptive refinement strategy based on 1-irregular quadrilateral elements has been proposed. At the end, efficiency of proposed adaptive scheme has been tested using numerical experiments.

Dolejší [58] studied the following nonlinear problem

Find  $u: \Omega \rightarrow \mathbb{R}$  such that

$$\begin{aligned}\nabla \cdot \mathbf{f}(u) - \nabla \cdot (\mathbf{K}(u)\nabla u) &= g(x), \\ u|_{\partial\Omega_D} &= u_D, \\ \mathbf{K}(u)\frac{\partial u}{\partial \mathbf{n}}|_{\partial\Omega_N} &= g_N,\end{aligned}$$

where  $\Omega \subseteq \mathbb{R}^d$  ( $d = 2,3$ ) is polygonal domain with boundary  $\partial\Omega = \partial\Omega_D \cup \partial\Omega_N$ ,  $\mathbf{n}$  is unit outer normal to  $\partial\Omega$ ,  $\mathbf{f}(u) = (f_1(u), \dots, f_d(u)): \mathbb{R} \rightarrow \mathbb{R}^d$  and  $\mathbf{K}(u) = \{K_{ij}(u)\}_{i,j=1}^d: \mathbb{R} \rightarrow \mathbb{R}^{d \times d}$  are nonlinear functions. In the beginning, the model problem is discretized using DGFEM. The system of discrete equations are then solved using damped Newton-like method. In order to estimate the discretization and algebraic errors, some residuum-nonconformity estimator is proposed. Author proposed the following global residuum-nonconformity estimator

$$\eta_h := (\rho_h(u_h)^2 + N_h(u_h)^2)^{1/2},$$

defined in terms of algebraic residuum estimator and local variant. Further, regularity indicator based on inter-element jumps of the approximate solution computed over the element boundary is discussed. The  $h-p$ -adaptive strategy based on combination of derived residuum-nonconformity estimator and regularity indicator is proposed. At the end, accuracy of the proposed strategy is verified numerically.

Fankhauser et al. [64] considered a linear elliptic problem defined over some bounded Lipschitz polygonal domain  $\Omega$  in  $\mathbb{R}^2$ . Some smoothness indicators are proposed. Based on isotropic embedding,  $h-p$ -adaptive strategy has been developed. Numerical tests are performed to check the effectivity of proposed adaptive scheme. It has been shown that the proposed technique results in exponential rate of convergence.

Giani [74] considered the following eigenvalue problem for two-dimensional periodic photonic crystals

$$\nabla \cdot (A\nabla u) + \lambda Bu = 0,$$

defined over  $\mathbb{R}^2$  with periodic coefficients to determine band structure arising from it. The  $h - p$ -version of symmetric interior penalty FEM has been implemented to discretize the considered problem. A reliable and efficient residual based error estimator has been presented. Author proposed the following bound on error estimator

$$\eta_j \lesssim \text{dist}(u_{j,hp}, E_1(\lambda_j))_{E,\Gamma} + h \|\lambda_{j,hp} u_{j,hp} - \lambda_j u_j\|_{0,\beta} + hs \|u_{j,hp} - u_j\|_{0,\beta}.$$

Here  $u_j$  represents an eigenvalue and  $u_{j,hp}$  be its corresponding discontinuous Galerkin approximation. Based on these estimates,  $h - p$ -adaptive strategy has been developed. Two numerical tests have been performed based on fully periodic crystals and crystal with defects which show that the proposed strategy results in exponential rate of convergence for computed eigenvalues on single cell and supercell. Author also proved that the computed eigenvalue converges to true eigenvalue as error estimator converges to zero.

Matuszyk et al.[124] in their paper analyzed a non-stationary two dimensional heat transfer problem over some bounded domain  $\Omega \subseteq \mathbb{R}^2$ . Time discretization has been performed based on Crank-Nicolson scheme. Further, space discretization has been performed using finite element method over quadrilateral elements at each time step. A self-adaptive  $h - p$ -FEM has been presented. At the end, numerical solution of non-stationary heat transfer problem over L-shaped domain has been analyzed to test the efficiency of proposed adaptive algorithm.

Klimczak et al.[106] studied the following viscoelastic problem with Burgers constitutive equation

$$\mathbf{div} \dot{\sigma} + \dot{X} = 0 \quad \forall t, x \in w_i \subset \Omega,$$

$$\dot{\sigma} = C[\dot{\varepsilon}(\dot{u}) - \dot{\varepsilon}^*],$$

$$\dot{\varepsilon} = \frac{1}{2}[\nabla \dot{u} + (\nabla \dot{u})^T],$$

$$\dot{\varepsilon}^* = f(\sigma, \chi, \dots),$$

subjected to initial, boundary and continuity conditions. Here  $\sigma$  is stress tensor,  $u(x, t)$  is the displacement vector,  $X$  is the body force,  $C$  is the tensor of material parameters,  $\chi$  is the internal variable and  $\dot{\epsilon}^*$  is inelastic strain rate. An adaptive strategy based on local numerical homogenization approach and  $h - p$ -adaptive FEM has been proposed. The authors discussed the projection based interpolation error estimates. Then anisotropic refinements were considered to obtain the optimal mesh. At the end, effectiveness of proposed adaptive scheme has been validated numerically. Oleksy et al.[151], in 2015, proposed an adaptive strategy based on two scale approach for modeling of inelastic heterogenous materials with periodic microstructure. The authors considered two problems, namely the macro-scale problem for heterogenous material defined over heterogenous domain and the micro-scale problem for heterogenous material defined over representative volume elements. It is seen that in case of inelastic deformations, numerical computations become expensive. In order to reduce the computational cost, computational homogenization is taken into consideration. Error estimation based on residuum has been discussed. Further, an automatic  $h - p$ -adaptive FEM has been proposed to reduce the approximation error. Efficiency of the proposed strategy has also been tested numerically.

Tsuchida et al.[191] gave an adaptive finite element strategy for large scale atomistic simulations. FEMTECK code based on density functional theory is considered for effective simulation. Comparison has been made for computation of the Kohn-Sham total energy of methane molecule using FEMTECK and ABINIT on uniform and adaptive mesh. At the end, accuracy of the proposed adaptive strategy has been verified numerically using example of polymer electrolyte membranes for fluid cells.

Abas et al.[1] studied the following fluid-structure interaction problem

Find  $\{u, v, w, p\} \in \{v_D + V\} \times V \times V \times L$

$$\begin{aligned} \left( \rho \frac{\partial \mathbf{v}}{\partial t} \Big|_{x_0} + \rho([\mathbf{v}-\mathbf{w}] \cdot \nabla) \mathbf{v}, \psi^v \right) + (\nabla \cdot \sigma, \psi^v) &= (g_1, \psi^{v,p}) \Big|_{\partial\Omega} + (f_1, \psi^{v,p}), \\ (\nabla \cdot \mathbf{v}, \psi^v) &= 0, \\ (\nabla \cdot C : \epsilon(u), \psi^u) &= 0 \quad \forall \psi \in V, \end{aligned}$$

where

$$\begin{aligned} \sigma &= \sigma_f + \sigma_s, \\ \sigma_f &= -pI + 2\rho_f v_f \epsilon(\mathbf{v}), \\ \sigma_s &= JF^{-1}(\lambda_s(\text{tr}(E))I + 2\mu_s E)F^{-T}, \\ C : \epsilon(u) &= 2\mu\epsilon + \lambda(\text{tr}(\epsilon))I, \\ \epsilon &= \frac{1}{2}(F^T F - I), \\ F &= (I - \nabla u)^{-1}. \end{aligned}$$

The parameters used in the above problem have been defined in [1]. The authors derived the following residual based a posteriori error estimates in terms of weighted sum of elements and edge contributions

$$\sum_{R,K} \eta_{R,K}^2 = \eta_K(u_h)^2 + \eta_{E,\Omega}(u_h)^2 + \eta_{E,\Gamma_N}(u_h)^2,$$

where

$$\begin{aligned} \eta_K(u_h)^2 &= \frac{h_K^2}{p_K} \int_K |\nabla \cdot q_h^l + f|^2 d\Omega, \\ \eta_{E,\Omega}(u_h)^2 &= \sum_{e \text{ in } \Omega} \frac{h_E}{2p_K} \int_e |[q_h^e \cdot \mathbf{n}_e]|^2 d\Gamma, \\ \eta_{E,\Gamma_N}(u_h)^2 &= \sum_{e \text{ in } \Gamma} \frac{h_E}{2p_K} \int_e |q_h^b \cdot \mathbf{n}_e - g|^2 d\Gamma. \end{aligned}$$

Here  $K$  represents element number,  $u_h$  is value of velocity in fluid domain,  $q_h$  is flux vector,  $\Omega$  is considered mesh,  $h_K$  is size of element,  $h_E$  is size of edge and  $\mathbf{n}_e$  is the unit normal to the edge. Based on these proposed error estimates,  $h - p$  adaptive strategy is proposed. Further, domain decomposition parallelization scheme

is adopted to reduce the computational time. Numerical tests are carried out to check the performance proposed adaptive finite element method.

#### **1.4.4 $h - p - q$ -adaptive strategies**

Zboinski [201] developed  $h - p - q$ -adaptive FEM for analysis of complex structures. The proposed adaptive strategy is applied to simulate a hierarchy of 3D-based mechanical models, first-order Reissner-Mindlin shell theory, higher-order hierarchical shell models and 3D elasticity models. Residual equilibration method is considered for a posteriori error estimation. The performance of adaptive algorithm is tested through numerical experiments.

Zboinski [202] proposed an adaptive  $h - p - q$ -finite element method for solving complex 3D-models based on elastic structures. The a posteriori error estimates based on residual equilibrated method proposed by Ainsworth and Oden [5] are derived. An adaptive technique based on Texas three step strategy is developed. Various numerical tests are performed by the author to test the effectiveness and reliability of proposed adaptive scheme.

#### **1.4.5 $r - h$ -adaptive strategies**

Kardani et al. [98] studied large deformation problems of geomechanics. The authors developed combined  $r - h$ -adaptive FEM for numerical simulation. In the proposed  $r - h$ -adaptive strategy,  $h$ -adaptivity helps to obtain more accurate solution and  $r$ -adaptivity (Arbitrary Lagrangian-Eulerian method) helps to refine the mesh distortion without changing number of elements and nodes.

### 1.4.6 Adaptive strategies based on layer adaptive mesh

Franz et al.[68] considered the following singularly perturbed convection-diffusion equation

$$\begin{aligned} -\epsilon\Delta u - bu_x + cu &= f & \text{in } \Omega = (0,1)^2, \\ u &= 0 & \text{on } \partial\Omega, \end{aligned}$$

where  $0 < \epsilon \ll 1$  is small perturbation parameter,  $b \geq \beta$  on  $\bar{\Omega}$  and  $\beta$  is positive constant. In this paper, the considered equation is discretized using standard Galerkin FEM and local projection stabilization FE method on layer-adapted mesh. Numerical validation of proposed scheme is done using both bilinear finite elements and higher order finite elements. It is shown that for bilinear finite elements, first order convergence in energy norm for Galerkin method and local stabilization scheme is achieved. Higher order elements results in convergence of order  $p + 1$  for both Galerkin and local stabilization methods.

Kumar et al.[110] considered the following singularly perturbed generalized Burgers-Huxley equation

$$u_t + \alpha u^\delta u_x - \epsilon u_{xx} = \beta u(1 - u^\delta)(u^\delta - \gamma) \quad 0 \leq x \leq 1, t \geq 0,$$

subjected to initial and boundary conditions

$$\begin{aligned} u(x, 0) &= f(x) \quad 0 \leq x \leq 1, \\ u(0, t) &= u_0 \quad 0 \leq t \leq 1, \\ u(1, t) &= u_1 \quad 0 \leq t \leq 1, \end{aligned}$$

where  $\alpha, \beta, \gamma, \delta$  and  $\epsilon$  are parameters s.t.  $\alpha \geq 0, \beta \geq 0, \gamma \in (0, 1), \delta = 1, 2, 3$  and  $\epsilon \ll 1$ . An efficient numerical scheme based on three-step Taylor Galerkin method is proposed. In the beginning, time discretization is performed using forward-time Taylor series expansion. Shishkin mesh has been considered for mesh discretization.

Standard Galerkin FEM is used for spatial discretization. Stability analysis of proposed scheme has been discussed in detail. It has been shown that the proposed numerical scheme is robust and efficient in capturing sharp boundary layers as singular perturbation parameter becomes small numerically.

Franz[69] studied the following singularly perturbed convection-diffusion problem

$$\begin{aligned} -\epsilon\Delta u - bu_x + cu &= f \text{ in } \Omega = (0, 1)^2, \\ u &= 0 \text{ on } \partial\Omega, \end{aligned}$$

where  $0 < \epsilon \ll 1$  is small perturbation parameter and  $b \geq \beta > 0$ . Shishkin mesh is considered for domain discretization. Superconvergence analysis for higher-order SDFEM is presented. The author established the following estimates

$$|||u - u^N|||_\epsilon \leq C(N^{-1} \ln N)^p,$$

for the convergence analysis of the general higher-order element space. Here  $u^N$  is the streamline diffusion solution and  $u$  is the exact solution.

In [70], the author considered the following convection dominated problem

$$\begin{aligned} -\epsilon\Delta u - b\nabla u + cu &= f \text{ in } \Omega = (0, 1)^2, \\ u &= 0 \text{ on } \partial\Omega, \end{aligned}$$

defined over domain  $\Omega$ . The authors derived the following supercloseness estimates based on higher-order Galerkin finite element on Shishkin mesh:

$$|||P^N u^N - u|||_\epsilon \leq (N^{-1} \ln N)^{p+1} + N^{-(p+1/4)},$$

where  $P^N$  is postprocessing operator and  $P^N u^N$  is the numerical solution.

Liu et al.[121] studied the following singularly perturbed problem:

$$\begin{aligned} -\epsilon\Delta u + \mathbf{b} \cdot \nabla u + cu &= f \text{ in } \Omega = (0, 1)^2, \\ u &= 0 \text{ on } \partial\Omega. \end{aligned}$$

The authors discussed some bounds on the solution of the continuous problem and its derivatives. Further, Galerkin FEM on Shishkin triangular mesh and hybrid mesh has been discussed. The authors derived anisotropic interpolation bounds on Shishkin mesh followed by error estimation on Shishkin mesh and hybrid mesh. Numerical tests are carried out and it is shown that the proposed scheme is  $\epsilon$ -uniform convergent with respect to diffusion parameter. Increase in order of convergence of computed solution on hybrid mesh is shown as compared to Shishkin mesh.

Sangwan et al.[174] proposed mesh adaptive strategy for computing numerical solution of time dependent singularly perturbed Burger-Fisher equation defined as:

$$u_t + \alpha u^\delta u_x = \epsilon u_{xx} + \beta u(1 - u^\delta) \quad a \leq x \leq b, t \geq 0,$$

where  $u$  represents traveling wave phenomena,  $\epsilon$  is the diffusion coefficient,  $\alpha$ ,  $\beta$  and  $\delta$  are parameters satisfying  $\alpha, \beta \geq 0$ ,  $\delta > 0$  and  $0 < \epsilon \leq 1$ . Firstly, time semi-discretization is performed using implicit Euler method. Quasilinearization process is used to handle the nonlinearity. Further its convergence has been discussed. Spatial discretization is carried out using finite element procedure. Exponentially fitted splines on piecewise Shishkin mesh is considered for discretization in spatial direction. Stability of proposed adaptive scheme is analyzed. Numerical experiments are performed and it is shown that the proposed adaptive scheme is quite effective in capturing sharp boundary layers.

#### 1.4.7 Adaptive strategies based on error estimates

Ren et al.[164] studied the three-dimensional DC resistivity boundary value problem. Gradient recovery based a posteriori error estimates originally developed by Zienkiewicz and Zhu (1987) have been discussed. The authors considered the following two estimators  $\bar{\eta}_e$ (average element error percentage) and  $\eta$  (global error percentage) to propose mesh adaptive scheme defined as:

$$\bar{\eta}_e = \left[ \frac{1}{m} \sum_{k=0}^{m-1} \left( \frac{\|e\|_k}{\|R\nabla u_h\|_k} \right)^2 \right]^{1/2} \times 100\%,$$

and

$$\eta = \frac{\|e\|}{\|R\nabla u_h\|} \times 100\%,$$

where  $\|e\| = \sum_{k=0}^{m-1} \|e_k\|$ ,  $\|R\nabla u_h\| = \sum_{k=0}^{m-1} \|R\nabla u_h\|_k$ ,  $m$  is the number of elements,  $\|e_k\|$  is the element error and  $R\nabla u_h$  is the recovered gradient. To test the accuracy and efficiency of proposed adaptive strategy, numerical experiments for two synthetic models and one valley model have been performed .

Chen et al.[41] considered the following eddy current model with voltage excitations for complicated 3D structures

$$\begin{aligned} \nabla \times \nabla \times \mathbf{A} + iw\sigma\mu\mathbf{A} &= -\sigma\mu\nabla\phi_0 + \mu J_s \text{ in } \Omega, \\ \mathbf{A} \times \mathbf{n} &= 0 \quad \text{on } \Gamma, \end{aligned}$$

defined on domain  $\Omega$  with boundary  $\Gamma$ .  $\mathbf{A}$  is assumed to be the magnetic vector potential,  $J_s$  is the applied current density satisfying  $\mathbf{div}J_s = 0$ ,  $\mu$  is the magnetic permeability,  $w$  is frequency,  $\sigma$  is the electric conductivity and  $\phi_0 \in H^1(\Omega)$  satisfying  $\phi_0 = U_j$  on  $S_j$ ,  $j = 1, \dots, N$ . Using Scott-Zhang and Beck-Hiptmair-Hoppe-Wohlmuth interpolants, the authors proposed the adaptive FEM and derived the following error upper bounds

$$\eta_T \leq C(\|\nabla \times (\mathbf{A} - \mathbf{A}_h)\|_{L^2(\tilde{T})} + \alpha^2\|\mathbf{A} - \mathbf{A}_h\|_{L^2(\Omega_C \cap \tilde{T})} + \sum_{T \subset \tilde{T}} h_T \|f - Q_h f\|_{L^2(T)}),$$

where  $\tilde{T}$  is the union of  $T$  and the adjacent elements of  $T$ ,  $f = s^2\mu(J_s - s^{-1}\sigma\nabla\phi_0)$ ,  $Q_h : L^2(T) \rightarrow P_1(T)$  is the  $L^2$  projection to the space of linear functions on  $T$ ,  $\mathbf{A}$  is the analytical solution of the considered problem and  $\mathbf{A}_h$  is its finite element approximation. Based on these a posteriori error estimates, an adaptive algorithm is developed. A parallel adaptive finite element package i.e. parallel hierarchical grid (PHG) is considered for numerical validation of the proposed adaptive scheme.

Mao et al. [123] developed simple adaptive nonconforming finite element method using Dörfler marking strategy [60] for a second order elliptic problem. Firstly, nonconforming  $P_1$  finite element space (Crouzeix-Raviart element) is considered for domain

discretization. Further, efficient and reliable residual type a posteriori error estimates are developed. Mesh refinement technique is so employed that the family of meshes obtained are conforming and shape regular. At last, optimal convergence of the proposed adaptive algorithm is tested numerically.

Guaily and Megahed [81] considered the following two dimensional planar and axisymmetric compressible flow problem

$$\mathbf{A}_t \frac{\partial Q}{\partial t} + \mathbf{A}_x \frac{\partial Q}{\partial x} + \mathbf{A}_y \frac{\partial Q}{\partial y} + \alpha \mathbf{A}_{axis} Q = 0,$$

where  $\mathbf{Q}^T = (\rho, u, v, p)$  is the vector of unknowns and  $A_x, A_y, A_t, A_{axis}$  are some matrices,  $\rho$  is the spatial density,  $\gamma$  is the specific heat ratio,  $\mathbf{A}_t = I$  is identity matrix,  $\alpha = 1$  for axisymmetric flow and  $\alpha = 0$  for planar flow. In the beginning, least square FEM combined with Newton-Raphson method is considered for approximation of solution. Edge based error estimates are discussed. Further, grid smoothening is performed to obtain the grid differentiable at all nodes. Based on error estimates, an adaptive algorithm on quadrilateral meshes is developed to achieve sharp resolution of discontinuities. Through numerical tests, it has been shown that the proposed technique is quite effective as compared to other existing techniques. The proposed scheme allows to use large time steps in order to reach steady state solution in very few iterations.

Solin et al. [183] considered the following time-dependent multiphysics model

$$\begin{aligned} c^{[TT]} \frac{\partial T}{\partial t} - d^{[TT]} \Delta T - d^{[Tw]} \Delta w &= 0, \\ c^{[ww]} \frac{\partial w}{\partial t} - d^{[wT]} \Delta T - d^{[ww]} \Delta w &= 0, \end{aligned}$$

defined over reactor vessel with boundary  $\partial\Omega = \Gamma_S \cup \Gamma_R \cup \Gamma_E$ ,  $\Gamma_S \cap \Gamma_R \cap \Gamma_E = \emptyset$ . Here  $T$  represents temperature,  $w$  relative humidity,  $d^{[TT]}$ ,  $d^{[wT]}$ ,  $d^{[Tw]}$ ,  $d^{[ww]}$  are the scalar conductivities,  $c^{[TT]}$ ,  $c^{[ww]}$  represents capacity properties,  $\Gamma_S$  is the axis of symmetry,  $\Gamma_R$  is reactor wall,  $\Gamma_E$  is exterior wall. Boundary conditions under consideration are

$$\frac{\partial T}{\partial \mathbf{n}} = 0, \quad \frac{\partial w}{\partial \mathbf{n}} = 0 \quad \text{on } \Gamma_S,$$

$q^{[w]} \cdot \mathbf{n} = 0$  and Dirichlet boundary condition for temperature  $T = \tilde{T}$  on  $\Gamma_R$ ,  
 $q^{[T]} \cdot \mathbf{n} = k^{[TT]}(T - T_{ext}) + k^{[Tw]}(w - w_{ext})$  on  $\Gamma_E$  (Newton Boundary condition),  
 $q^{[w]} \cdot \mathbf{n} = k^{[wT]}(T - T_{ext}) + k^{[ww]}(w - w_{ext})$  on  $\Gamma_E$  (Newton Boundary condition),  
 where  $k^{[Tw]}$ ,  $k^{[ww]}$ ,  $k^{[TT]}$ ,  $k^{[wT]}$  represent the transmission coefficients,  $T_{ext}$  is the temperature of environment,  $w_{ext}$  is the relative humidity of environment,  $q^{[T]}$  is heat flux and  $q^{[w]}$  is moisture flux. Time discretization is performed using Rothe's method followed by space discretization. Further, multimesh space and time adaptive higher-order FEM based on dynamical meshes is proposed. The proposed technique involves small low-degree elements on moving fronts and large high-degree elements where solution is smooth. At the end, it is shown numerically that the computed solution obtained from the proposed scheme is more reliable and efficient as compared to the results obtained from  $h$ -adaptive with quadratic elements and standard (single-mesh)  $h - p$  FEM.

Carstensen et al.[32] proposed an optimal adaptive FEM for Poisson model defined as:

$$\begin{aligned}
 p + \nabla u &= 0 \text{ and } \mathbf{div} p = f \text{ in } \Omega := (0, 1)^2, \\
 u &= 0 \text{ on } \partial\Omega.
 \end{aligned}$$

The problem has been approximated using Raviart-Thomas finite elements of the lowest order. The authors established the following edge-error estimator:  $\eta_e := \eta_e(E_e)$  where

$$\eta_e^2(M) := \sum_{E \in M} \eta_e^2(E) \text{ for } M \subseteq E_e,$$

with local contributions

$$\eta_e(E) := |E|^{1/2} \|[p]_E\|_{L^2(E)} \quad \forall E \in E_e.$$

Here  $T_l$  is the regular triangulation of  $\Omega$ ,  $E = T_+ \cap T_-$  represents edge shared by elements  $T_+$ ,  $T_- \in T_l$  and  $\eta_e(E)$  corresponds to the jump parallel to  $E$ . When

oscillations are small as compared to estimated error, edge-oriented Dörfler marking strategy has been performed, otherwise the thresholding second algorithm (TSA)[24] has been performed in order to reduce the oscillations. Adaptive mesh refinement has been performed based on Newest vertex bisection refinement technique. Later on, convergence of the proposed adaptive scheme has also been shown to be optimal. At the end, numerical tests have been presented to validate the theoretical findings. Key et al.[104] studied isotropic two-dimensional electrical conductivity model defined as

$$\begin{aligned} -\nabla \cdot (\mathbf{A}\nabla u) + \mathbf{C}u &= \mathbf{f} \text{ in } \Omega, \\ u &= 0 \text{ on } \partial\Omega, \end{aligned}$$

where parameters have been defined in [104]. Authors proposed a parallel goal-oriented adaptive finite element method for solving the problem under consideration. In the beginning, finite element formulation is presented. Goal oriented error estimates has been proposed using dual weighted residual (DWR) method. Authors established the following local element error indicator for any triangle  $\tau$ :

$$\mu_t = |F(\delta_n)_\tau - B(u_n, \delta_n)_\tau|,$$

where  $\delta_n \approx w - w_n$  is the discrete error in the dual solution. Here  $G(u) = B(u, w) = F(w)$  represents the functionals of the primal and dual solution  $u$  and  $w$ . Domain discretization is based on coarse Delaunay triangulation. Goal oriented error estimator based on dual weighted residual method has been considered. Further, iterative mesh refinement based on the relative error has been carried out. In order to save computational cost, parallel computation of different parameters such as wavenumber, frequency, etc., in the proposed adaptive algorithm has been considered. Performance of the proposed adaptive strategy has been tested numerically.

Tavakoli and Zarmehi [187] studied the Saint-Venant equations using adaptive finite element methods. The problem represents unsteady, one-dimensional flow in an open

channel with no lateral inlet or outlet. The authors proposed three adaptive FE schemes for solving the Saint Venant equation. In the first method, called as comparison adaptive finite element method (CAFE), the problem is initially solved on coarse grid followed by refinement of intervals. Further, the numerical solution is obtained on new coarse grid. Since in CAFE method, problem is solved several times in each time step which results in increase in CPU time, therefore, in the second proposed method known as the regression adaptive finite element method (RAFE), problem is solved for first few moments on fine mesh. Further, the solution is computed at next time level using regression method. In the third method, called as the heuristic adaptive finite element method (HAFE), the considered problem is solved for first few moments on fine mesh followed by computing numerical solution for next time levels. Numerical experiments are carried out for subcritical and supercritical flow problems to test the effectivity of the proposed adaptive methods.

Frutos et al. [71] considered the following evolutionary convection dominated problem defined as:

$$\begin{aligned}
u_t - \epsilon \Delta u + b \cdot \nabla u + cu &= f && \text{in } \Omega, \\
u &= g_1 && \text{on } \partial\Omega_D, \\
\frac{\partial u}{\partial \mathbf{n}} &= g_2 && \text{on } \partial\Omega_N, \\
u(0, x) &= u_0(x) && \text{in } \Omega,
\end{aligned}$$

where  $\Omega$  is bounded open domain in  $\mathbb{R}^n$  ( $n = 1,2,3$ ) with polygonal boundary  $\partial\Omega = \partial\Omega_D \cup \partial\Omega_N$ . In the beginning, temporal semi-discretization is performed. Further, spatial semidiscrete Galerkin finite element approximation is considered to compute approximate solution. On the basis of computed solution, a posteriori error indicator is proposed. An adaptive algorithm is developed based on refining of mesh using red-green refinement technique. At the end, numerical experiments are performed to validate the effectivity of developed algorithm.

Garau et al. [73] studied quasi-linear elliptic partial differential equation using discrete adaptive approximations based on Lagrange finite element space. Triangulation of the domain comprising of continuous functions vanishing on  $\partial\Omega$  is considered. An inexact adaptive FEM has been developed using Kačanov iteration and mesh adaptation. Convergence of the proposed scheme

$$\lim_{k \rightarrow \infty} \|\nabla(u_k - u_{k+1})\|_{\Omega} = 0,$$

and stability of local error indicators have been proved by showing

$$\eta_K(T) \lesssim \|\nabla u_k\|_{w_k(T)} + \|f\|_T \quad \forall T \in T_k \quad \forall k \in N,$$

where  $u_{k\{k \in N\}}$  represents the sequence of discrete solutions obtained using adaptive algorithm. The proposed adaptive strategy is based on adaptive technique for Stokes problem using Uzawa's Algorithm [52, 200]. At the end, the behavior of adaptive algorithm has been analyzed numerically by considering different nonlinear problems. Schwarzbach et al.[178] considered the following three-dimensional model of electromagnetics

$$\text{curl}(\mu^{-1} \text{curl} E_s) - iw(\sigma - iw\varepsilon)E_s = \text{curl}([\mu_p^{-1} - \mu^{-1}] \text{curl} E_p) - iw([\sigma_p - \sigma] - iw[\varepsilon_p - \varepsilon])E_p,$$

subject to homogenous Dirichlet condition

$$\mathbf{n} \times E_s = 0,$$

defined over domain  $\Omega$  with boundary  $\partial\Omega$ . Here  $\mu$  is magnetic permeability,  $\varepsilon$  is electrical permittivity,  $\sigma$  is electrical conductivity,  $E_p$  is primary electric field,  $E_s$  is secondary electric field and  $\mu_p$ ,  $\varepsilon_p$ ,  $\sigma_p$  are parameters. Finite element discretization based on tetrahedral meshes has been presented. Finite element library FEMSTER has been used for computation of finite element solution. A posteriori error estimates proposed by Beck and Hiptmair[19] have been discussed for the model under consideration. Based on these a posteriori error estimates, the local error indicator

$$\eta_{K_i} = \int_{K_i} \overline{(\hat{H}_s - \bar{H}_s)} \cdot \mu(\hat{H}_s - \bar{H}_s) d^3r,$$

defined in terms of a weighted norm of the difference between the two magnetic field approximations  $\hat{H}_s$  and  $\bar{H}_s$  over element  $K_i$  has been proposed and an adaptive mesh refinement procedure has been discussed. Convergence analysis has been carried out which clearly shows that the use of higher order polynomial is highly appreciated when solution is not globally smooth. Validation of code is done through numerical experiments.

Hoffman et al. [85] proposed an adaptive FEM for numerical simulation of Navier-Stokes equation

$$\begin{aligned} \dot{\mathbf{u}} + (\mathbf{u} \cdot \nabla) \mathbf{u} + \nabla p - \nu \Delta \mathbf{u} &= f & (x, t) \in \Omega \times I, \\ \nabla \cdot \mathbf{u} &= 0 & (x, t) \in \Omega \times I, \\ \mathbf{u}(x, 0) &= \mathbf{u}^0(x) & x \in \Omega, \end{aligned}$$

defined over  $\Omega \subseteq \mathbb{R}^3$ ,  $I = (0, T]$ . The considered equation is discretized using continuous Galerkin method in space as well in time. The authors derived the following estimates based on the solution of dual problem [62, 20, 77]:

$$\begin{aligned} |M(\hat{u}) - M(\hat{U})| &\leq \sum_{n=1}^N \left[ \int_{I_n} \sum_{K \in \Gamma_n} |R_1(\hat{U})|_K \cdot w_1 dt + \int_{I_n} \sum_{K \in \Gamma_n} |R_2(U)_K| \cdot w_2 dt \right. \\ &\quad \left. + \int_{I_n} \sum_{K \in \Gamma_n} R_3(U) \cdot w_3 dt + \int_{I_n} \sum_{K \in \Gamma_n} |SD_\delta^n(\hat{U}; \hat{\phi})_K| dt \right], \end{aligned}$$

where  $R_1$ ,  $R_2$  and  $R_3$  are defined in [85]. Robust and efficient adaptive algorithm based on a posteriori error estimates has been developed. At the end, the efficiency of proposed algorithm has been observed numerically by considering different problems arising in the field of aerodynamics and geophysics.

Chang and Chen [39] considered the following convection-diffusion problem in two spatial dimensions

$$\begin{aligned} -\beta \nabla \Phi + \langle \alpha, \nabla \Phi \rangle &= f \text{ on } \Omega, \\ \Phi &= g \text{ on } \Gamma, \end{aligned}$$

where  $\Omega$  is a unit square  $\{0 < x, y < 1\}$  with boundary  $\Gamma$ ,  $\beta$  is diffusion coefficient,  $\alpha$  represents convection,  $f$  and  $g$  are given functions. Authors proposed an adaptive algorithm to generate optimal grids using least squares finite element method. With the slight modifications to algorithm developed by Chen and Yang [40] for solving convection-diffusion problems, refinement strategy has been developed by the authors based on redistribution of grading function. Delaunay triangulation is considered to generate good quality triangular mesh. An unstructured local mesh smoothing is performed to avoid skewed mesh in optimal grids generated by proposed algorithm. At the end, effectiveness and optimal convergence of proposed strategy have been analyzed numerically by comparing it with the results obtained from Galerkin finite element method.

Tian et al. [189] considered the elliptic partial differential equation represented as:

$$\begin{aligned} -\nabla \cdot (a\nabla u) &= f \text{ in } \Omega, \\ u &= 0 \text{ on } \partial\Omega, \end{aligned}$$

where  $a(x) > 0$ ,  $\Omega \subseteq \mathbb{R}^2$  is rectangular domain with boundary  $\partial\Omega$ . The authors presented finite element discretization using polynomial basis over hierarchical T-meshes. It has been observed that polynomial splines over hierarchical T-meshes results in effective local refinement in adaptive computation. To perform an adaptive refinement, residual based a posteriori error estimates

$$\|e_h\|_E^2 \leq C \sum_{K \in \Gamma} h_K^2 \|r\|_{L^2(K)}^2,$$

has been proposed, where  $C$  is constant,  $e_h = u - u_h$  is the error in the approximation  $u_h$  and  $r = f + \nabla \cdot (a\nabla u_h)$ . Further, reliability and efficiency of the derived error estimates has been discussed. Numerical experiments have been performed to study the robustness of the proposed adaptive scheme.

Zhang et al. [205] considered the following stationary conduction-convection problem:

Find  $\mathbf{u} = (u_1, u_2)$ ,  $p$  and  $T$  such that

$$\begin{aligned} -\mu\Delta\mathbf{u} + (\mathbf{u} \cdot \nabla)\mathbf{u} + \nabla p &= \lambda j T \quad x \in \Omega, \\ \mathbf{div}\mathbf{u} &= 0 \quad x \in \Omega, \\ -\Delta T + \lambda\mathbf{u} \cdot \nabla T &= 0 \quad x \in \Omega, \\ \mathbf{u} = 0, T &= T_0 \quad x \in \partial\Omega, \end{aligned}$$

where  $\Omega \subset \mathbb{R}^2$  is bounded, connected domain with Lipschitz continuous boundary  $\partial\Omega$ ,  $\mathbf{u}$  is velocity vector,  $\lambda > 0$  is Groshoff number,  $j = (0,1)$  be the unit vector and  $\mu$  is viscosity. In the beginning, mixed FE formulation of given equation has been presented. Authors established the following residual based a posteriori error estimates based on Verfürth [193]

$$\begin{aligned} \{ \|u_* - u_h\|_{1,2}^2 + \|p_* - p_h\|_{0,2}^2 + \|T_* - T_h\|_{1,2}^2 \}^{1/2} &\leq C_8 \|DF(u_*, p_*, T_*)^{-1}\|_{Q(Y_D^*, X_D)} \left\{ \sum_{K \in \Gamma_{h,j}(\Omega)} \eta_K^2 \right\}^{1/2}, \\ \eta_K &\leq C_9 \|DF(u_*, p_*, T_*)\|_{Q(X, Y^*)} \{ \|u_* - u_h\|_{1,2;w_K}^2 + \|p_* - p_h\|_{0,2;w_K}^2 + \|T_* - T_h\|_{1,2;w_K}^2 \}^{1/2}, \end{aligned}$$

where  $C_8$  and  $C_9$  depend upon the polynomial degrees of the spaces  $M_h$ ,  $Q_h$ ,  $W_h$ , domain  $\Omega$  and on  $\frac{h_K}{Q_K}$ ,  $u_*$  represents a weak solution and  $u_h$  is an approximate solution of the equation  $F_h(u_h) = 0$ . Based on error estimates, an adaptive refinement strategy has been developed for solving the considered stationary conduction-convection equation. Two numerical tests have been performed to test the effectivity of the proposed adaptive strategy.

Vuong et al. [195] formulated hierarchical adaptive local refinement approach for isogeometric analysis based on hierarchical B-splines defined on nested approximation spaces for approximating the solution of the stationary heat conduction equation. Authors proposed the following error indicator defined as:

$$\tilde{\eta}(\phi) = \frac{1}{|S(\phi)|} \sum_{T \in S(\phi)} \eta(T),$$

where  $\tilde{\eta} : \Phi \rightarrow R_o^+$  and  $S(\phi) := \{T \in A | T \subset \text{supp } \phi\}$ . Effectiveness of hierarchical adaptive algorithm is tested using numerical experiments on problem with elastic plate with circular hole, stationary heat conduction equation with L-shaped domain and advection-diffusion problem.

Selim et al. [179] proposed an adaptive finite element splitting scheme for approximating the solution of incompressible Navier-Stokes equation. Standard splitting scheme (incremental pressure correction scheme) has been considered for time discretization. Finite element formulation has been used for space discretization of the considered problem and its dual. A posteriori estimates  $E = (E_h + E_k + E_c)$  expressed as sum of spatial discretization error, time discretization error and computational error have been derived. An adaptive algorithm has been developed to test the quality of the derived error estimates. Numerical experiments have been carried out and it has been shown that the proposed adaptive refinement strategy is optimal in approximating the solution of the considered problem.

Nazarov et al.[143] proposed a robust and efficient adaptive FEM for approximating numerical solution of turbulent compressible flow problem:

Find  $\hat{\mathbf{u}} \equiv (\rho, m, E)$

$$\begin{aligned} \partial_t \rho + \nabla \cdot (\rho \mathbf{u}) &= 0 \quad \text{in } Q, \\ \partial_t m + \nabla \cdot (m \otimes \mathbf{u} + pI) &= g \quad \text{in } Q, \\ \partial_t E + \nabla \cdot (E \mathbf{u} + p \mathbf{u}) &= 0 \quad \text{in } Q, \\ \hat{u}(\cdot, 0) &= \hat{\mathbf{u}}^0 \quad \text{in } \Omega, \end{aligned}$$

defined over fixed, open domain  $\Omega \subseteq \mathbb{R}^3$  with boundary  $\Gamma$  where  $I = [0, \hat{t}]$ ,  $\rho$  is density,  $\mathbf{m} = \rho \mathbf{u}$  is momentum,  $\mathbf{u} = (u_1, u_2, u_3)$  represents velocity,  $E = E(x, t)$  is total energy,  $(x, t) \in Q = \Omega \times I$ ,  $x = (x_1, x_2, x_3) \in \mathbb{R}^3$ ,  $I$  is identity matrix,  $g = (g_1, g_2, g_3)$  is given volume force,  $\otimes$  denotes tensor product,  $\hat{u}^0 = \hat{u}^0(x)$  and  $p = (\gamma - 1)\rho T$  is pressure,  $\gamma = c_p$  is adiabatic index and  $c_p$  is heat capacity under constant pressure. FEM

combined with residual based artificial viscosity for numerical stabilization, shock capturing and turbulence capturing is considered. Time discretization is carried out using explicit third-order Runge-Kutta method. Authors presented a posteriori error estimates based on solution of corresponding dual problem and are defined as:

$$|M(\hat{u}) - M(\hat{u}_h)| \leq \sum_n \sum_{K \in \Gamma_n} \int_{I_n} C_h h_K |R(\hat{u}_h)|_K \cdot |D\phi|_K + \sum_n \sum_{K \in \Gamma_n} \int_{I_n} |Vis(\hat{u}_h; \pi_h \phi)_K| dt + h.o.t,$$

where  $R(\hat{u}_h) = (R_\rho(\hat{u}_h), R_m(\hat{u}_h), R_E(\hat{u}_h))$  is the residual of Euler equations,  $M(\hat{u})$  is target functional,  $C_h = 1/2$  is interpolation constant,  $D\phi$  represents space-time derivative of  $\phi$  and  $Vis(\hat{u}_h; \pi_h \phi) = (\nabla \cdot f_{visc}(\hat{u}_h), \pi_h \phi)$  represents contribution from the residual based artificial viscosity in the finite element discretization. An adaptive algorithm is proposed by authors. Various two-and three-dimensional examples are considered for numerical validation of the proposed adaptive algorithm.

Belenki et al.[21] studied the following nonlinear Dirichlet problem

$$\begin{aligned} -\mathbf{div}(A(\nabla u)) &= f \text{ in } \Omega, \\ u &= 0 \text{ on } \partial\Omega, \end{aligned}$$

where  $\Omega$  is bounded, polyhedral domain in  $\mathbb{R}^d$ ,  $d \in \mathbb{N}$  and  $A : \mathbb{R}^d \rightarrow \mathbb{R}^d$ . The considered equation is discretized under finite element framework. Conforming and shape regular triangulation of domain is considered. Some residual based a posteriori error estimates are discussed. The author established the following error indicator on  $T \in \Gamma$ :

$$\eta^2(v, v_{\mathbf{T}}, T) := \int_T (\phi_{|\nabla v|}^* (h_T |f|)) dx + \sum_{\gamma \in \Gamma, \gamma \subset \partial T} \int_\gamma h_T |[F(\nabla v_{\mathbf{T}})]_\gamma|^2 dx,$$

where  $[F(\nabla v_{\mathbf{T}})]_\gamma$  represents jump of  $F(\nabla v_{\mathbf{T}})$  across the face  $\gamma \in \Gamma$ . Here 1st term in the right hand side of above expression denotes element indicator and second term as jump indicator. Based on error indicator, an adaptive refinement strategy is proposed. Dörfler marking strategy is used for selection of elements for further

refinement. Refinement is done using bisection method. Optimal rate of convergence of discrete solution obtained from adaptive algorithm is proved. Numerical tests over L-shaped and crack domain are carried out to analyze rate of convergence of proposed strategy.

MacDonald et al.[122] presented numerical solution of non-linear singularly perturbed BVP arising from 1-dimensional Q-tensor model of liquid crystals using adaptive FEM. The concept of spatial rescaling is introduced to study singularly perturbed behavior of considered problem. Further, the asymptotic behavior of solution in boundary layer region is discussed. The concept of mesh equidistribution, arc-length (AL) and Beckett-Mackenzie (BM) monitor function is also introduced. Since AL monitor function are less effective for exponential-like boundary layers, therefore the alternative monitor function

$$M(S_n(Z)) = \alpha + \left( \frac{|dS_n|}{|dz|} \right)^{1/m},$$

$$\text{where } \alpha = \int_0^1 \left( \frac{|dS_N|}{|dz|} \right)^{1/m} dz,$$

with  $m$  as constant is discussed. It is observed that these BM monitor functions are more useful as they involve lesser user defined parameters. An adaptive strategy is discussed. The authors showed numerically that adaptive meshes obtained by equidistribution of BM monitor functions are quite effective, as they results in optimal rate of convergence of computed numerical solution. In the end, it is shown that the computed solution is robust with respect to the perturbation parameter.

Mohite and Upadhyay [135] gave numerical solution of three-dimensional laminated plates using adaptive FEM. Following a posteriori error estimates based on patch recovery are derived to control discretization error:

$$\psi_w = \sqrt{\sum_{\tau=1}^{N_{EL,w}} \eta_{\tau}^2},$$

and

$$\eta_\tau^2 = \int_{V_\tau^l} \{\sigma(u^{M,*}) - \sigma(u^{M,h})\}^T \{\epsilon(u^{M,*}) - \epsilon(u^{M,h})\} dv,$$

where  $V_\tau^l$  is the volume enclosed by the  $\tau$ -th element in  $l$ th layer,  $\{\sigma(u^{M,*})\}$  is the engineering stress,  $\{\epsilon(u^{M,*})\}$  is the strain vector and  $u^{M,*}$  is the recovered displacement field. Further, an explicit indicator is proposed to approximate the modeling error. The effectiveness of computed adaptive solution is tested on problems of damaged laminated plates. It is shown that the proposed adaptive strategy is effective in achieving optimal solution.

Rossi et al. [171] presented an adaptive refinement strategy for incompressible flow problems. With the aim to obtain conformant refined mesh, an adaptive strategy is proposed based on three basic components. The first component involves construction of element-driven global splitting algorithm. The second component involves error estimation strategy that helps to identify the regions where mesh resolution is not sufficient and to decide the elements that must be splitted and to communicate this information to other processes. The third component involves local refinement strategy. The reliability and effectiveness of proposed adaptive algorithm is observed for flow problems.

Shi et al.[182] studied the following Cahn-Hilliard Navier-Stokes equation together with generalized Navier boundary condition (GNBC) modelling moving contact line problems in three dimensions

$$\begin{aligned} \frac{\partial \phi}{\partial t} + \mathbf{u} \cdot \nabla \phi &= M \Delta \mu && \text{in } \Omega, \\ \mu &= -\varepsilon \Delta \phi - \frac{1}{\varepsilon} (\phi - \phi^3) && \text{in } \Omega, \\ Re \left( \frac{\partial \mathbf{u}}{\partial t} + (\mathbf{u} \cdot \nabla) \mathbf{u} \right) + \nabla p &= \Delta \mathbf{u} + \lambda \mu \nabla \phi + f && \text{in } \Omega, \\ \nabla \cdot \mathbf{u} &= 0 && \text{in } \Omega, \end{aligned}$$

together with boundary conditions

$$\begin{aligned}\phi_t + u_r \partial_r \phi &= -\Gamma \left( \varepsilon \partial_{\mathbf{n}} \phi - \frac{\sqrt{2}}{6} \pi \cos \theta_s \cos\left(\frac{\pi \phi}{2}\right) \right) \text{ on } \partial\Omega, \text{ (relaxational boundary condition)} \\ \frac{u_r^{slip}}{L_s} &= -(\partial_{\mathbf{n}} u_r + \partial_r u_{\mathbf{n}}) + \lambda \left( \varepsilon \partial_{\mathbf{n}} \phi - \frac{\sqrt{2}}{6} \pi \cos(\theta_s) \cos\left(\frac{\pi \phi}{2}\right) \right) \partial_r \phi \text{ on } \partial\Omega, \text{ (GNBC)} \\ u_{\mathbf{n}} &= 0, \partial_{\mathbf{n}} \mu = 0 \text{ on } \partial\Omega, \text{ (non-penetration boundary condition)}\end{aligned}$$

and initial conditions

$$u(0) = u_0, \phi(0) = \phi_0,$$

where parameters are defined in the above cited paper. In order to perform time discretization, decoupling of Cahn-Hilliard and Navier-Stokes equation has been done. Finite element discretization of Cahn-Hilliard equation over tetrahedron mesh has been carried out. Further, Navier-Stokes equation has been discretized under finite element framework. To avoid nonlinear iterations, semi-implicit convex splitting scheme for Cahn-Hilliard equation and linearized semi-implicit scheme for Navier-Stokes equation has been used. Mesh adaptation strategy based on a posteriori error indicator

$$\begin{aligned}\eta_T(\phi_h) &= \left( \sum_{e \in \partial T} \int_e h^3 \left[ \frac{\partial \phi_h}{\partial n_e} \right]^2 de \right)^{1/2} \\ \text{and } \eta_T(u_h) &= \left( \sum_{e \in \partial T} \int_e h^3 \left[ \frac{\partial u_h}{\partial n_e} \right] \cdot \left[ \frac{\partial u_h}{\partial n_e} \right] de \right)^{1/2},\end{aligned}$$

is proposed. Here  $[ ]$  represents the jump on the element boundary and  $h$  is the length of edge  $e$ . Validation of adaptive algorithm has been done using numerical tests and it has been shown that the proposed scheme is reliable and efficient.

Hoffman et al.[86] analyzed different mathematical models of continuum mechanics e.g. incompressible flow, compressible flow and fluid-structure interaction. Authors developed a parallel adaptive FEM for approximating the solution of considered models. For compressible flow, explicit third order Runge-Kutta scheme is used for time

discretization. A posteriori error estimates

$$\epsilon_K \equiv \sum_{n=1}^N \left[ \int_{I_n} \int_K \sum_i |R_i(\hat{U})|_K \cdot w_i dxdt + \int_{I_n} |SD_\delta^n(\hat{U}; \hat{\phi})_K| dt \right],$$

based on solution of corresponding dual problem are proposed. Here  $R_i(\hat{U})$  is the residuals of the equations,  $\hat{u}$  represents a weak solution of the equations,  $\hat{U}$  is the finite element approximation,  $\hat{\phi}$  is the solution of dual problem,  $K \in \Gamma_n$ ,  $SD_\delta^n(\cdot; \cdot)_K$  represents stabilization over element  $K$  and  $w_i$  are stability weights. An adaptive mesh refinement strategy is discussed. The algorithm developed is suitable for problems with complex geometries and deforming domains. Different solvers such as UNICORN and DOLFIN are considered for implementation of the proposed adaptive algorithm. Efficiency of proposed adaptive strategy is proved for different problems of aerodynamics, biomedicine, etc.

Coupez and Hachem [50] proved that anisotropic adaptive meshes with highly stretched elements can be used to study high Reynolds number flow problems. A posteriori estimates based on length distribution tensor approach and associated edge based error analysis is presented. Further, variational multiscale finite element solver (VMS) is used for simulating flow at high Reynolds number which helps to decompose velocity and pressure into different scales. At the end, numerical experiments for driven flow cavity problem (2D) are carried out and it is shown that proposed solver provides stable and accurate results on anisotropic meshes.

Solin et al. [185] proposed an adaptive numerical solution of three benchmark problems i.e. Poisson equation, singularly Perturbed elliptic equation and Fitzhugh-Nagumo equation using adaptive FEM codes designed to tackle anisotropic refinements available at open source library HERMES.

Jasinski and Zboinski [92] considered the following small oscillation eigen problem representing linear isotropic elastic body:

Find  $w$  and  $u$  such that

$$\begin{aligned} w^2 \rho u + \nabla \cdot \sigma &= 0 \quad \text{in } \Omega, \\ \sigma \cdot \mathbf{n} &= 0 \quad \text{at } \Gamma_t, \\ u &= 0 \quad \text{at } \Gamma_u, \\ \epsilon &:= ((\nabla u)^T + \nabla u)/2, \\ \sigma &= D\epsilon, \end{aligned}$$

where  $\Omega \subset \mathbb{R}^3$  is elastic undeformed domain with  $\partial\Omega = \overline{\Gamma_t \cup \Gamma_u}$ . It is assumed that  $\Gamma_t \cap \Gamma_u = \emptyset$  where  $\Gamma_t$  and  $\Gamma_u$  are boundary parts describing tractions and displacements. The authors proposed  $h-p$ -adaptive technique based on Texas 3-step adaptive strategy[149]. A posteriori error estimates

$$\eta_{ERM} := \left( \sum_K A_K(\phi_K^{S^+}, \phi_K^{S^+}) \right)^{1/2},$$

using equilibrated residual method are developed to decrease the discretization error. Here  $\phi_K^{S^+} \in S_K^+$ ,  $\phi_K \in V_K$  and  $S_K^+ : S_K^+ \supseteq S_K$ . Numerically, it is shown that the developed adaptive strategy is very effective in computing approximate solution.

Mitchell [129] proposed an adaptive grid refinement algorithm to solve two dimensional elliptic partial differential equations exhibiting singularities such as point singularity, line singularity, boundary layers, sharp peaks and wave fronts.

Bao et al.[18] presented an adaptive mesh redistribution technique for finding solution of Kohn-Sham equation involving minimization of the total energy of a many-electron system

$$(\hat{T} + v_{eff}(x))\Psi_i(x) = \epsilon_i \Psi_i(x),$$

$$\text{where } \hat{T} = -\frac{1}{2}\nabla^2$$

represents kinetic energy,  $\epsilon_i$  are eigen values,  $\Psi_i$  are wave functions and  $v_{eff}$  is effective potential. The authors used standard finite element method involving self-consistent field iteration to obtain self-consistent electron density followed by adaptive

optimizing mesh grid distribution based on harmonic mapping. Since the variation of the wavefunction in the vicinity of nucleus and between atoms of chemical bonds is very large as compared to other regions, therefore, the following monitor function

$$M = \left( \sqrt{\epsilon + \sum_i^{occ} |\nabla \psi_i(x)|^2} \right) I,$$

has been considered. Here  $I$  represents identity matrix and  $\epsilon$  is parameter. Further, moving mesh method[186] is used to improve the quality of mesh obtained using finite element solver. At the end, convergence of adaptive technique is analyzed using numerical experiments.

Li and Yang [118] considered the second order self-adjoint elliptic eigenvalue problem

$$Lu \equiv - \sum_{i,j=1}^d \partial_j (a_{ij} \partial_i u) + cu = \lambda \beta u \text{ in } \Omega,$$

$$u = 0 \quad \text{on } \partial\Omega,$$

where  $\Omega \subset \mathbb{R}^d$  ( $d = 1,2,3,\dots$ ) is a polyhedral bounded domain,  $A = (a_{ij})_{d \times d}$  is symmetric, positive definite matrix,  $\lambda \in \mathbb{R}$  and  $c, \beta$  are real functions. The authors presented finite element formulation of the considered eigenvalue problem. Some multi-scale discretization schemes based on Rayleigh quotient iteration [200] is used. The authors established

$$\|u - u^{h_l}\|_a \leq (\tilde{C}_1 + \delta) \eta_{h_l}(u^{h_l}, \Omega),$$

$$(\tilde{C}_2 + \delta)^2 \eta_{h_l}^2(u^{h_l}, \Omega) - (\tilde{C}_3 + \delta)^2 \text{osc}(L(u^{h_l}), \pi_{h_l})^2 \leq \|u - u^{h_l}\|_a^2,$$

where  $V_{h_l}$  is a finite element space,  $\delta$  is a positive constant independent of  $h_l$  and  $\eta_{h_l}(u^{h_l}, \Omega)$  is error estimate. Reliability and efficiency of residual type a posteriori error estimates[10, 125, 181, 193, 60] are discussed. An adaptive algorithm based on derived a posteriori error estimates are proposed. At the end, efficiency of proposed adaptive algorithm is verified numerically using Harmonic oscillator equation and Schrodinger equation for hydrogen atoms.

Deolmi et al. [57] analyzed inverse convection problem whose direct model is represented by the following parabolic convection-diffusion-reaction equation

$$\begin{aligned} \frac{\partial c}{\partial t} - \nabla \cdot (\mu \nabla c) + u \cdot \nabla c + \sigma c &= 0 \quad \text{in } (0, t_f) \times \Omega, \\ c &= c_0 \quad \text{on } \{0\} \times \Omega, \\ c &= c_{in} \quad \text{on } (0, t_f) \times \Gamma_{in}, \\ c &= c_{up} \quad \text{on } (0, t_f) \times \Gamma_{up}, \\ \nu \frac{\partial c}{\partial \mathbf{n}} &= 0 \quad \text{on } (0, t_f) \times \Gamma_{down}, \\ c &= 0 \quad \text{on } (0, t_f) \times \Gamma_r, \end{aligned}$$

on a fixed domain with space-varying inlet lateral boundary conditions. Here  $\Omega \subseteq \mathbb{R}^2$  is open, continuous and Lipschitz domain with boundary  $\partial\Omega$ ,  $c: [0, t_f] \rightarrow \mathbb{R}$ ,  $c = c(t, x)$  is unknown,  $\partial\Omega = \Gamma_{in} \cup \Gamma_{up} \cup \Gamma_r \cup \Gamma_{down}$  where  $\Gamma_{in}$ ,  $\Gamma_{up}$ ,  $\Gamma_{down}$ ,  $\Gamma_r$  are disjoint sets. We assume  $c_{in} \in H^{\frac{1}{2}}(\Gamma_{in})$ ,  $c_{up} \in H^{\frac{1}{2}}(\Gamma_{up})$ ,  $c_0 \in L^2(\Omega)$ ,  $\mu \in L^\infty(\Omega)$ ,  $\sigma \in L^\infty(\Omega)$ ,  $\sigma(x) \geq 0$  a.e. in  $\Omega$ ,  $u \in [L^\infty(\Omega)]^2$  and  $\mu(x) > 0 \forall x \in \Omega$ . The authors predicted intensity and location of air and water pollution. In this paper, the inverse convection problem with boundary control, where sources are along the boundary of domain is studied. Firstly, the problem with known source location is studied with Projected Damped Gauss Newton (Gauss-Newton method with truncated singular value decomposition) method. Then, the problem with unknown source location is analyzed using adaptive parametrization with space-time localization. At the end, authors proved numerically that proposed adaptive parametrization with space-time localization is reliable and effective for parameter estimation.

Murotani et al. [141] considered two-dimensional elasticity problems to develop an adaptive FEM using hierarchical mesh and level-of-detail (LOD) approximation on the basis of adaptivity analysis given in [117, 198, 213]. Firstly, Delaunay triangulation is used for fine mesh generation followed by progressive meshing to obtain hierarchical mesh. A posteriori error estimation is carried out using Zienkiewicz-Zhu's

method [198]. Further, remeshing is performed based on error estimates. Lastly, new proposed adaptive technique is tested on different problems based on fracture mechanics e.g. crack propagation analysis, etc.

Porta et al. [158] developed space-time adaptive scheme for numerical simulation of unsteady shallow water equation (SWE)

$$\frac{\partial \mathbf{U}}{\partial t} + A_1 \frac{\partial \mathbf{U}}{\partial x} + A_2 \frac{\partial \mathbf{U}}{\partial y} = S \text{ in } \Omega,$$

defined over polygonal domain  $\Omega$  in  $\mathbb{R}^2$  where  $U = (u, v, c)^T$  is unknown,  $c = 2\sqrt{gh}$ ,  $h$  is total water depth with respect to bottom profile,  $c$  depends on water depth and  $S$  represents all sources and sinks of the momentum. Here symmetric matrices  $A_1$  and  $A_2$  are given by

$$A_1 = \begin{pmatrix} u & 0 & \frac{c}{2} \\ 0 & u & 0 \\ \frac{c}{2} & 0 & u \end{pmatrix}, A_2 = \begin{pmatrix} v & 0 & 0 \\ 0 & v & \frac{c}{2} \\ 0 & \frac{c}{2} & v \end{pmatrix}$$

Finite element discretization is performed using streamline-diffusion shock-capturing finite element method (SDSCFEM). In order to control discretization error, recovery based error estimator in space as well as in time is proposed. Based on error estimates, space-time adaptive strategy is proposed. The robustness of the proposed adaptive scheme is tested by applying it to various hydraulic applications.

Further, Lin et al. [119] studied Laplace eigenvalue problem defined as:

$$\begin{aligned} -\Delta u &= \lambda u \text{ in } \Omega, \\ u &= 0 \text{ on } \partial\Omega, \\ \int_{\Omega} u^2 d\Omega &= 1, \end{aligned}$$

where  $\Omega$  is bounded Lipschitz polygonal domain in  $\mathbb{R}^2$ . Nonconforming discretization of considered problem is presented. Following reliable and efficient residual based a posteriori estimates using extended Crouziex-Raviart element (ECR) are developed:

### Reliability

$$|||\nabla_h e_h||| \leq C(\eta_h(\lambda_h, u_h) + \|\lambda_h u_h - \lambda u\|_{0,h}),$$

where  $C$  is a constant depending upon minimum angle of  $\Gamma_h$ ,  $(\lambda_h, u_h)$  is nonconforming finite element approximation,  $(\lambda, u)$  is exact solution and  $e_h = u - u_h$  is corresponding error.

### Efficiency

$$\eta_K \leq C(\|\nabla_h e_h\|_{0,w_K} + (\sum_{K \in w_K} h_K^2 \|\lambda_h u_h - \lambda u\|_{0,K}^2)^{1/2}),$$

where  $w_K$  represents the set of elements that share a common vertex with  $K$  and  $C$  is a constant. Based on these derived estimates, an adaptive algorithm is developed. Analysis of lower bounds for ECR element on adaptive meshes is discussed. At the end, reliability of proposed adaptive strategy is tested using numerical experiments. Kou and Sun [108] formulated an adaptive FEM to approximate the surface tension based on gradient theory of fluid interfaces. Finite element approximation of nonlinear Euler-Lagrange equation is presented. Newton method is used to solve system of nonlinear discrete equations arising from FE approximations of the considered problem. Some error estimates of the type

$$0 \leq \sigma_H - \sigma_h \leq CH^\gamma,$$

are derived where  $V \supset V_h \supseteq V_H$ ,  $H > h$ ,  $C$  depends on exact solution and  $\sigma_h$  is the discrete surface tension. For the numerical validity of proposed adaptive scheme, hydrocarbon fluid system is considered to predict surface tension at different temperatures. It has been shown that the proposed method is very much effective in computing optimal numerical solution.

Canuto et al. [30] proposed an adaptive Legendre-Galerkin method for elliptic boundary-value problem given as

$$\begin{aligned} Lu &:= -D \cdot (\vartheta Du) + \sigma u = f \text{ in } (-1, 1), \\ u(-1) &= u(1) = 0, \end{aligned}$$

where  $\vartheta$  and  $\sigma$  are sufficiently smooth real coefficients satisfying  $0 < \vartheta(x) < \infty$  and  $0 \leq \sigma(x) < \infty$  in  $I=(-1,1)$ . Similar type of analysis has been done to study contraction

and optimality of adaptive Fourier-Galerkin method[29] for periodic box in dimension  $d \geq 1$ . Some error estimator is proposed. Using the error estimator, an adaptive algorithm is developed. Dörfler marking strategy is used for mesh refinement. At each step of adaptive algorithm, the optimality of computed numerical solution is enhanced using coarsening.

Gittelsohn et al. [78] considered the following parametric parabolic partial differential equation

$$\begin{aligned}\partial_t u(t, y) + A(t, y)u(t, y) &= g(t, y), \quad t \in I, \\ u(0, y) &= h(y),\end{aligned}$$

where  $I = [0, T]$ ,  $A(t, y; \cdot, \cdot)$  is sesquilinear form on  $V \times V$  and  $y \in \Gamma = [-1, 1]^N$ . Weak formulation in space-time domain and parameter domain is presented. Further, the need of Riesz bases in the parameter domain and multiresolution (wavelet) Riesz bases [177] in space-time domain is discussed. An adaptive Galerkin method which is simultaneously adaptive in space-time and in parameter space is developed. At the end, optimality of the proposed adaptive method is discussed.

Hu et al. [89] proposed an adaptive non-conforming FEM using Wilson element on 1-irregular mesh for solving second order two-dimensional Poisson problem. Following a priori error estimates have been proposed:

$$\|\nabla_h(u - u_h)\| \leq h_{\Gamma_h} \|D^2 u\|,$$

where  $h_{\Gamma_h} := \max_{K \in \Gamma_h} h_K$  and  $u \in H^2(\Omega) \cap H_0^1(\Omega)$ . In order to study the optimal behavior of proposed adaptive strategy, discrete reliability and efficiency of proposed error estimator

$$\|\nabla_h(u - u_h)\|^2 \leq C_{Rel} \eta^2(u_h, \Gamma_h) \leq C_{Eff} (\|\nabla_h(u - u_h)\|)^2 + osc^2(f, \Gamma_h),$$

is discussed. Here  $u$  and  $u_h$  are the exact and approximate solutions respectively. Discrete reliability of the estimator  $\eta$  based on Scott-Zhang interpolation has been

discussed. Numerical tests have been performed to study the effectiveness of developed algorithm.

Feischl et al. [65] proposed an adaptive lowest-order finite element method for second order elliptic partial differential equation

$$\begin{aligned} -\Delta u &= f \text{ in } \Omega, \\ u &= g \text{ on } \Gamma_D, \\ \partial_{\mathbf{n}} u &= \phi \text{ on } \Gamma_N, \end{aligned}$$

subjected to mixed Dirichlet-Neumann boundary conditions,  $\Omega \subset \mathbb{R}^2$  is bounded Lipschitz domain with polygonal boundary  $\Gamma = \partial\Omega$ ,  $\Gamma = \overline{\Gamma_D} \cup \overline{\Gamma_N}$  and  $\Gamma_D \cap \Gamma_N = \emptyset$ . Element based and edge based residual error estimators are developed. For both of these estimators, the following reliability and efficiency estimates are obtained:

#### **Reliability and efficiency of element-based residual error estimator**

$$\begin{aligned} \|u - U_l\|_{H^1(\Omega)} &\leq C_2 \varrho_l, \\ C_3^{-1} \varrho_l &\leq (\|\nabla(u - U_l)\|_{L^2(\Omega)}^2 + \text{osc}_{\rho,l}^2 + \text{osc}_{N,l}^2 + \text{osc}_{D,l}^2), \end{aligned}$$

#### **Reliability and efficiency of edge-based residual error estimator**

$$\begin{aligned} \|u - U_l\|_{H^1(\Omega)} &\leq C_{rel} \varrho_l, \\ C_{eff}^{-1} \varrho_l &\leq (\|\nabla(u - U_l)\|_{L^2(\Omega)}^2 + \text{osc}_{\rho,l}^2 + \text{osc}_{N,l}^2 + \text{osc}_{D,l}^2). \end{aligned}$$

Here  $C_2$ ,  $C_3$ ,  $C_{rel}$  and  $C_{eff}$  are positive constants. An adaptive algorithm, based on proposed error estimates, is developed. Dörfler marking strategy and newest vertex bisection is considered for mesh refinement. Convergence analysis for adaptive FEM in two-and three-dimensions is presented. Effectiveness of proposed adaptive strategy is tested numerically.

Hecht and Kuate [84] developed an anisotropic mesh adaptation strategy based on Lagrange finite element approximation of degree  $k$ ,  $k > 1$ , for approximation of metrics.

Numerical tests based on mesh adaptation are performed to validate the theoretical findings.

Quan et al. in their paper [161] developed an adaptive approach for modeling embedded surfaces. The authors considered a two-dimensional Laplace problem with Dirichlet and Neumann boundary conditions. The need of faster local refinement to remove large error that occurs on the embedded interface is discussed. Appropriate amount of local isotropic refinements based on body-fitted meshes is discussed. Optimal convergence rate for finite elements of order  $p$  is proved. At the end, it is shown through numerical experiments that the use of anisotropically refined meshes results in decrease in geometrical error.

Mostaghimi et al.[138] developed an adaptive numerical scheme to study unsaturated incompressible flow in porous media subjected to heap leaching. The governing equation representing Darcy's law and conservation of mass is given by

$$\frac{\partial}{\partial t}(\phi\rho_l S_l) + \nabla \cdot (\rho_l \underline{\mathbf{u}}_l) = 0,$$

where  $\underline{\mathbf{u}}_l = \frac{-K_l}{\mu_l}(\nabla p_l - \rho_l \underline{\mathbf{g}})$ ,  $\phi$  is porosity of porous media,  $\rho_l$  is density,  $u_l$  is superficial velocity of phase  $l$ ,  $S_l$  is saturation,  $\mu_l$  is viscosity of phase  $l$ ,  $\underline{\mathbf{g}}$  is acceleration due to gravity,  $p_l$  is pressure and  $K_l$  is permeability. Implicit pressure explicit saturation (IMPES) method is used to obtain pressure and saturation equation. For spatial discretization, pressure is approximated using finite element method and saturation using node centered control volume method. An adaptive algorithm based on anisotropic mesh adaptation is proposed. Order of convergence of the proposed scheme is discussed based on prediction of saturation using

$$E_s = \|S - S_A\|_1 = \int_0^1 |S - S_A| dx,$$

where  $E_s$  is the  $L_1$ -norm of error for saturation and  $S_A$  is the quasi-analytical solution. Buckley Leverett problem is considered for numerical validation of the algorithm. Open source package Fluidity is used for numerical simulation.

Branco et al.[26] presented review of different three-dimensional adaptive remeshing techniques based on finite element method for fatigue crack growth model problem. Roberts et al.[168] considered the following incompressible Navier-Stokes equation

$$\begin{aligned} -\nabla p + \mu \Delta \mathbf{u} &= f, \\ \nabla \cdot \mathbf{u} &= 0, \end{aligned}$$

defined over domain  $\Omega$  with boundary  $\partial\Omega$ . Here  $\mathbf{u}$  represents velocity,  $p$  is pressure and  $f$  is vector-valued forcing function. Dirichlet boundary conditions  $\mathbf{u} = g$  on  $\partial\Omega$  have been considered. Authors proposed an adaptive strategy based on discontinuous Petrov-Galerkin method for numerical simulation of considered model problem. The proposed strategy is based on discontinuous Petrov-Galerkin method given by Demkowicz et al.[56]. Various numerical experiments on problems such as lid-driven cavity problem, backward-facing step problem, flow past a cylinder problem, etc., are performed to study the convergence rate of the proposed adaptive algorithm.

Carstensen et al.[33] proposed an adaptive FEM for affine obstacle problem. Lowest order conforming finite element approximation of considered problem is presented. The authors proposed side oriented error estimator. An adaptive algorithm is presented. Newest vertex bisection method is used for refinement. Further, discrete reliability and efficiency of a posteriori error estimator is discussed. At the end, convergence analysis of proposed adaptive algorithm is presented.

Later on, the authors [34] also considered nonconvex variational problem based on relaxation of two-well problem arising as a result of solid-solid phase transitions with dependence on linear strains in two dimensions and incompatible walls. Finite element space with Courant elements is taken into consideration. Based on derived a priori error estimates, an adaptive algorithm is proposed. Dörfler marking strategy is used in the adaptive algorithm. Newest vertex bisection method is used for mesh refinement. The following global convergence result for the proposed adaptive

algorithm is established:

$$\lim_{l \rightarrow \infty} I^{qc}(u_l) = I^{qc}(u) = \min_{v \in u_D + H_0^1(\Omega; \mathbb{R}^2)} I^{qc}(v),$$

where  $u_l \in u_D + V_0^l, l \in \mathbb{N}_0$  is approximate solution obtained using adaptive algorithm and  $u$  is minimizer of the variational integral  $I^{qc}$ . Verfurth [190] proposed robust a posteriori error estimates for different stabilized finite element methods applied on stationary and non-stationary convection-diffusion problems. The authors considered the following non-stationary convection-diffusion problem:

$$\begin{aligned} \partial_t u - \epsilon \Delta u + \mathbf{a} \cdot \nabla u + bu &= f && \text{in } \Omega \times (0, T], \\ u &= 0 && \text{on } (0, T] \times \Gamma_D, \\ \epsilon \frac{\partial u}{\partial \mathbf{n}} &= g && \text{on } (0, T] \times \Gamma_N, \\ u(0, \cdot) &= u_o && \text{in } \Omega, \end{aligned}$$

defined in bounded space-time cylinder where  $\Omega \subset \mathbb{R}^2$  is a polygonal domain and  $0 < \epsilon \ll 1$ . It is shown that all the stabilized finite element methods such as streamline diffusion method, local projection schemes, etc., results in a posteriori error estimates in which the multiplicative constants in the lower and upper bounds are independent of size of reaction or convection term. The author established the following lower and upper error bounds

### Upper error bound

$$|||u - u_h||| + |||\mathbf{a} \cdot \nabla(u - u_h)|||_* \leq \tilde{C}^* \left\{ \sum_{K \in \Gamma_h} [\eta_{N,K}^2 + \theta_K^2] \right\}^{1/2},$$

### Lower error bound

$$\left\{ \sum_{K \in \Gamma_h} \eta_{N,K}^2 \right\}^{1/2} \leq \tilde{C}_* \left[ |||u - u_h||| + |||\mathbf{a} \cdot \nabla(u - u_h)|||_* + \left\{ \sum_{K \in \Gamma_h} \theta_K^2 \right\}^{1/2} \right],$$

where  $|||v||| = \{\epsilon \|\nabla u\|_0^2 + \beta \|u\|_0^2\}^{1/2}$ . Here the constants  $\tilde{C}_*, \tilde{C}^*$  depend only on the polynomial degree  $k$  and on ratios  $\frac{h_K}{\rho_K}$ .

Carstensen et al.[37] studied the following linear elasticity problem:

Find displacement  $u$  and stress tensor  $\sigma$  such that

$$\begin{aligned} -\mathbf{div}\sigma &= f, & \sigma &= C\epsilon(u) \text{ in } \Omega, \\ u &= u_D \text{ on } \Gamma_D, & \sigma\nu &= g \text{ on } \Gamma_N, \end{aligned}$$

where  $\Omega \subseteq \mathbb{R}^2$  with boundary  $\partial\Omega = \Gamma_D \cup \Gamma_N$ . Here  $f : \Omega \rightarrow \mathbb{R}^2$  is volume force,  $u_D : \Gamma_D \rightarrow \mathbb{R}^2$  is displacement,  $g : \Gamma_N \rightarrow \mathbb{R}^2$  is a traction and  $u : \Omega \rightarrow \mathbb{R}^2$ . Arnold-Winther finite element space is considered for domain discretization. The authors developed the following residual based a posteriori error estimator:

$$\begin{aligned} \eta_l^2 &= \text{osc}^2(f, \mathbf{T}) + \text{osc}^2(g, \epsilon(\Gamma_N)) + \sum_{T \in \mathbf{T}} h_T^2 \|\text{curl}(c^{-1}\sigma_{AW} + \nu_h)\|_{L^2(T)}^2 \\ &+ \sum_{E \in \epsilon(\Omega)} \|[c^{-1}\sigma_{AW} + \nu_h]_{E\tau_E}\|_{L^2(E)}^2 \\ &+ \sum_{E \in \epsilon(\Gamma_D)} h_E \|(C^{-1}\sigma_{AW} + \nu_h - Du_D)\tau\|_{L^2(E)}^2, \end{aligned}$$

where  $\eta_l$  is proposed error estimator,  $\nu_h$  represents arbitrary asymmetric approximation,  $\sigma_{AW}$  be the Arnold-Winther finite element solution and  $\sigma$  is the exact solution. The reliability and efficiency of the proposed estimator is discussed using

$$\begin{aligned} \|\sigma - \sigma_{AW}\|_{C^{-1}} &\leq C_{rel}\eta_l, \\ \eta_l &\leq C_{eff}(\|\sigma - \sigma_{AW}\|_{C^{-1}} + \|\text{skew}(Du) - \nu_h\|_{L^2(\Omega)}), \end{aligned}$$

where  $C_{rel}, C_{eff}$  are  $\lambda$ -independent constants. Based on the error estimates, an adaptive algorithm is proposed. Numerical tests are performed to validate the theoretical findings.

Later on, Carstensen alongwith other authors [36] also proposed an adaptive finite element method for discretization of variational inequality in elastoplasticity. In the beginning, discretization is performed using low-order finite element method based on triangulation of the domain. Residual based explicit error estimates are derived.

Discrete reliability of the proposed error estimates is proved using

$$E(w_l) - E(w_{l+m}) \lesssim \|\sigma_{l+m} - \sigma_l\|_{L^2(\Omega; \mathbb{R}^{d \times d})}^2 \lesssim \eta_l^2(\Gamma_l \setminus \Gamma_{l+m}),$$

where  $\Gamma_l \setminus \Gamma_{l+m} := \{T \in \Gamma_l | T \notin \Gamma_{l+m}\}$ ,  $\sigma_l := \sigma(u_l, p_l)$ ,  $E$  is the functional,  $w_l = (u_l, p_l, \alpha_l) \in W_l$  and  $\eta^2(T) := |T| \|f\|_{L^2(T; \mathbb{R}^d)}^2 + |T|^{1/2} \sum_{E \in \epsilon(T)} R_E^2$  for  $T \in \Gamma_l$ . Dörfler marking strategy is used. Newest vertex bisection method is used for mesh refinement. The optimal convergence of developed adaptive algorithm in terms of degrees of freedom is proved. At the end, influence of the hardening and bulk parameters on convergence of proposed adaptive algorithm is tested numerically.

Zhao et al.[209] considered the following fractional differential equation

$$\begin{aligned} D_x^\alpha u(x) &= f(x) \quad x \in (b, c), 1 < \alpha < 2, \\ u(b) &= 0, u(c) = 0, \end{aligned}$$

having Reisz fractional derivative where  $f \in L^2([b, c])$ . FE discretization of considered problem is discussed. To reduce computational complexity,  $H$ - matrix representation is adapted to approximate dense matrices, resulted from finite element discretization. Further, to solve linear system of equations involving  $H$ -matrices, geometric multigrid (GMG) method is used. Based on gradient recovery approach, following a posteriori error estimator is developed:

$$\eta_l(\bar{u}_l, \tau) : \|\nabla \bar{u}_l - G\bar{u}_l\|_\tau \quad \tau \in \Gamma_l,$$

where  $G\bar{u}_l \in V_l = \text{span}\{\phi_1^l, \dots, \phi_{N_l}^l\}$ ,  $G\bar{u}_l := \sum_i^{N_l} (G\bar{u}_l)_i \phi_i^l$ ,  $(G\bar{u}_l)_i := \frac{h_i^l \nabla \bar{u}_l|_{[x_{i-1}^l, x_i^l]} + h_{i+1}^l \nabla \bar{u}_l|_{[x_i^l, x_{i+1}^l]}}{h_i^l + h_{i+1}^l}$

and  $G\bar{u}_l$  is recovery gradient. Using these estimates, an adaptive algorithm is developed. Dörfler marking strategy is used for marking the elements to be refined. Bisection method is used for mesh refinement. Numerical tests are carried out to validate the reliability and efficiency of proposed strategy despite of presence of singularities. The proposed adaptive strategy results in optimal second order accuracy.

Kreuzer et al.[109] proposed an adaptive linear FEM for approximating numerical solution of Poisson equation

$$\begin{aligned} -\Delta u &= f \text{ in } \Omega \subset \mathbb{R}^d, \\ u &= 0 \text{ on } \partial\Omega. \end{aligned}$$

Conforming linear finite elements are considered for mesh discretization. A posteriori error bounds

$$\begin{aligned} \|\nabla(u - U_\tau)\|_\Omega^2 &\lesssim \sum_{z \in \nu_\tau} \|P_\tau f + \Delta U_\tau\|_{-1;w_{\tau,z}}^2 + \|f - P_\tau f\|_{-1;w_{\tau,z}}^2, \\ \|P_\tau f + \Delta U_\tau\|_{-1;w_{\tau,z}}^2 + \|f - P_\tau f\|_{-1;w_{\tau,z}}^2 &\lesssim \|\nabla(u - U_\tau)\|_{w_{\tau,z}}^2, \end{aligned}$$

with error-dominated oscillation are derived. Here  $z \in \vartheta_\tau$ ,  $U_\tau$  is Galerkin approximation,  $P : H^{-1} \rightarrow \mathbb{D}(\tau)$  is projection operator and  $u$  is the exact solution. An adaptive algorithm is proposed. Further, on the basis of marking strategy necessary and sufficient condition for convergence of adaptive FE procedure is provided in the form i.e.

$$\forall T \in \mathbf{T}^*, \delta(T) = 0 \text{ and } \lim_{k \rightarrow \infty} \varepsilon_k(T) = 0,$$

where  $\varepsilon_{\mathbf{T}}(T)$ ,  $T \in \mathbf{T}$  are element indicators,  $\mathbf{T}^* := \{T | \exists m \in \mathbb{N}_0 \forall k \geq m T \in T_k\} \neq \emptyset$  and  $\delta(T)$  is the oscillation.

## 1.5 Conclusion

In this Chapter, need of adaptive finite element strategies for numerical approximation of the solution of singularly perturbed problems have been focussed. Basic concepts and some definitions involved in the thesis work have been discussed. Survey on different adaptive techniques, like  $h$ -adaptivity,  $h-p$ -adaptivity,  $p$ -adaptivity,  $h-p-q$ -adaptivity,  $r$ -adaptivity,  $r-h$ -adaptivity, etc., mostly based on a posteriori error estimates, have been presented. Various models governing real life phenomenon have

also been presented. Based on the extensive survey, gaps in the literature have been pointed out and consequently, objectives of the thesis have been framed. These objectives have been achieved via the work which has been categorized in four different Chapters to follow.

# Adaptive finite element scheme for one-dimensional singularly perturbed parabolic problems

---

## 2.1 Introduction

Partial differential equations are used to model wide variety of phenomena such as diffusion[160, 172], heat, sound, etc. Singularly perturbed parabolic differential equations occur frequently during the analysis of biological systems, heat transfer process, mass transfer process, etc. From literature, it can be easily seen that the classical discretization methods fail to give good approximations to exact solutions for problems exhibiting sharp boundary layers until very large number of mesh points are considered in the domain. Various numerical methods have been proposed for solving singularly perturbed parabolic differential equations on layer adapted meshes e.g. Bakhlov mesh, Shishkin mesh, Logarithmic mesh, etc. Ramos et al. [163] developed a third-order convergent numerical strategy for solving non-linear singularly perturbed problems using non-standard algorithm on adaptive Shishkin mesh and through numerical tests shown that the proposed scheme is very efficient in capturing sharp boundary layers. Natesan et al.[142] proposed parameter uniform convergent numerical technique for approximating singularly perturbed turning point problems

on piecewise uniform Shishkin mesh and discussed the error estimates, efficiency and accuracy of the proposed scheme. Kaushik et al.[101] gave a parameter uniform finite element numerical scheme for singularly perturbed problems on modified graded mesh. The authors derived some error estimates and compared their numerical results with those existing in the literature. Clavero et al.[43] proposed uniform convergent numerical scheme for convection-diffusion parabolic problems on nonuniform mesh. Ramos[162] developed exponentially fitted numerical scheme for singularly perturbed linear parabolic convection-diffusion-reaction problems on uniform mesh.

In [94], Jiwari et al. developed two numerical schemes i.e. based on cubic trigonometric B-splines functions and modified cubic trigonometric B-splines functions for approximating non-linear parabolic problems.

In this Chapter, firstly a singularly perturbed parabolic differential equation in 1D, representing a linear model in fluid mechanics, has been considered. Implicit Euler scheme has been used for time semi-discretization. Spatial discretization has been carried out using finite element technique and Streamline upwind/Petrov-Galerkin (SUPG) method on layer adapted Shishkin mesh. Exponentially fitted splines have been considered to obtain uniform convergent scheme. Numerical tests have been carried out and it has been shown that the proposed adaptive schemes are efficient in capturing sharp boundary layers arising in the solution as the singular perturbation parameter  $\epsilon$  becomes small. Further, one-dimensional non-linear singularly perturbed parabolic differential equation has been taken into consideration. Quasilinearization process has been used to deal with the nonlinearity occurring in the problem. Time semi-discretization has been done using implicit Euler method. Further, spatial discretization has been carried out using finite element method and SUPG technique. An adaptive numerical schemes have been obtained using layer adapted Shishkin mesh based on exponentially fitted splines. The region of absolute stability has been discussed. At the end, numerical tests have been carried out and it has been shown

that the proposed adaptive schemes works efficiently for solving SPP.

The Chapter is organized as follows: In Section 2.2, a singularly perturbed linear parabolic differential equation in one-dimension has been presented. Section 2.3 deals with the construction of numerical scheme using temporal and spatial discretization. Streamline upwind/Petrov-Galerkin (SUPG) stabilization technique has been discussed for the considered problem. In Section 2.4, effectivity of proposed adaptive numerical scheme has been tested using various numerical examples. It has been shown that sharp boundary layers appear in the solution as  $\epsilon \rightarrow 0$ . In Section 2.5, one-dimensional non-linear singularly perturbed parabolic differential equation has been discussed. In Section 2.6, adaptive numerical scheme has been proposed using finite element method and SUPG technique. Section 2.7 deals with the stability analysis. Section 2.8 includes numerical tests which have been performed to test the effectivity of proposed adaptive numerical scheme. In the last, conclusion has been presented.

## 2.2 Singularly perturbed linear parabolic partial differential equation

Consider the time dependent singularly perturbed linear parabolic partial differential equation

$$\frac{\partial w}{\partial t} - \epsilon \frac{\partial^2 w}{\partial x^2} + a(x, t)w_x + b(x, t)w = f(x, t), \quad 0 < x < 1, 0 < t \leq 1, \quad (2.2.1)$$

with boundary conditions

$$w(0, t) = f_1(t) \text{ for } 0 < t \leq 1,$$

$$w(1, t) = f_2(t) \text{ for } 0 < t \leq 1,$$

and initial condition as

$$w(x, 0) = w_0(x) \text{ for } 0 \leq x \leq 1,$$

whose solution domain is  $D = [0 \leq x \leq 1] \times [0 \leq t \leq 1]$ .  $\epsilon$  is singular perturbation parameter ( $0 < \epsilon \ll 1$ ). Take  $\Omega = (0 < x < 1)$ . Assume that  $a(x, t)$ ,  $b(x, t)$  and  $f(x, t)$  are continuous functions satisfying  $a(x, t) > \alpha > 0$  and  $b(x, t) \geq b \geq 0$ .

## 2.3 Construction of adaptive numerical scheme

### 2.3.1 Temporal discretization

To find the weak formulation of Eq.(2.2.1), first we will discretize the equation w.r.t. time. Temporal semi-discretization has been performed using implicit Euler method with uniform step size  $\Delta t$ . After performing semi-discretization with respect to time, the above equation reduces to

$$w^{j+1} = \Delta t [\epsilon(w_{xx})^{j+1} - a(x, t)(w_x)^{j+1} - b(x, t)w^{j+1} + f(x, t)^{j+1}] + w^j, j \geq 0, x \in \Omega, \quad (2.3.1.1)$$

with boundary conditions

$$\begin{aligned} w^{j+1}(0) &= f_1(t_{j+1}), \\ w^{j+1}(1) &= f_2(t_{j+1}), \quad j \geq 0, \end{aligned}$$

where  $\Delta t = \frac{1}{M}$ ,  $M$  is the no. of time-steps and  $w^{j+1}$  is solution of the above equation at  $(j + 1)$ -th time level i.e.  $t_{j+1} = (j + 1)\Delta t$ .

### 2.3.2 Shishkin mesh methodology

Static grid refinement techniques result in generation of mesh where in grid is more finely spaced in some regions as compared to other regions but the shape is maintained over the time. Static adaptation results in improving the accuracy and efficiency of the approximations on a discrete mesh. Since the solutions to the considered singularly perturbed problems exhibit sharp boundary layers as  $\epsilon$  approaches 0, therefore, in the present work, static grid adaption approach has been considered for grid refinement under SUPG framework while approximating the solutions of linear and non-linear

singularly perturbed partial differential equation. From asymptotic analysis available in literature, it has been observed that the problem under consideration displays sharp boundary layers near  $x = 1$  as  $\epsilon \rightarrow 0$ . In order to resolve these sharp boundary layers, a piecewise uniform mesh, called Shishkin mesh, has been considered so that more mesh points can be generated in the boundary layer region as  $\epsilon \rightarrow 0$ . Suppose that number of mesh elements be  $N$  where  $N \geq 4$  is a positive even integer. Shishkin mesh is obtained by dividing spatial domain  $\Omega$  into two subintervals  $[0, 1-\tau]$  and  $[1-\tau, 1]$ , where  $\tau$  is transition parameter defined as

$$\tau = \min\left\{\frac{1}{2}, C\epsilon \log N\right\},$$

where  $C$  is a constant chosen appropriately.

We discretize each of the two subintervals  $[0, 1-\tau]$  and  $[1-\tau, 1]$  into  $\frac{N}{2}$  equal mesh elements with mesh spacing defined by

$$h = \begin{cases} h_1 = 2\frac{(1-\tau)}{N}, & \text{if } i = 1, 2, \dots, \frac{N}{2}, \\ h_2 = 2\frac{\tau}{N}, & \text{if } i = \frac{N}{2} + 1, \dots, N. \end{cases}$$

Therefore, mesh points  $\{x_i\}_{i=1}^N$  are given by

$$x_i = \begin{cases} h_1 i, & i = 0, 1, 2, \dots, \frac{N}{2}, \\ (1-\tau) + h_2(i - \frac{N}{2}), & i = \frac{N}{2} + 1, \dots, N. \end{cases}.$$

Hence, the piecewise uniform discretization of the spatial domain  $\bar{\Omega}$  is defined as:

$$\bar{\Omega}_h = \bigcup_{e=1}^N \Omega_e^h,$$

where  $\Omega_e^h$  represents linear element  $[x_e, x_{e+1}]$  and  $N$  is the number of elements.

### 2.3.3 Exponentially fitted finite element method

Assume that

$$S = \{w \in (H^1(\Omega); L^2(T)): w(x, 0) = w_0(x), w(0, t) = f_1(t), w(1, t) = f_2(t)\},$$

and

$$V = \{v \in (H^1(\Omega); L^2(T)): v(0, t) = 0, v(1, t) = 0\},$$

be solution space and test space.

The variational formulation of Eq.(2.3.1.1) is defined as follows: Find  $w \in S$  such that

$$\begin{aligned} \int_{\Omega} w^{j+1} v dx &= \Delta t \left[ \int_{\Omega} \epsilon(w_{xx})|^{j+1} - a(x, t)w_x|^{j+1} - b(x, t)w|^{j+1} + f(x, t)|^{j+1} \right] v dx \\ &+ \int_{\Omega} w^j v dx, \quad \forall v \in V. \end{aligned} \tag{2.3.3.1}$$

Assume that  $S_h$  and  $V_h$  be finite dimensional subspaces of  $S$  and  $V$ . In the literature, it has been shown that classical methods fail to give satisfactory results for singularly perturbed problems as singular perturbation parameter  $\epsilon$  tends to zero, unless large number of mesh points are to be chosen or some other special treatment has to be incorporated. In order to overcome this difficulty and to produce uniform convergent scheme, exponentially fitted splines have been used as test functions satisfying the condition

$$\epsilon(\psi_i^e)_{xx}(x, t_{j+1}) + \alpha(\psi_i^e)_x(x, t_{j+1}) = 0.$$

Spatial discretization of Eq.(2.3.3.1) has been done using standard Galerkin FEM. Let  $\{\phi_i^e(x)\}_{i=1}^N$  be standard basis of  $S_h$  comprising of standard linear interpolation functions defined on each element  $\Omega_e^h$ . Therefore, discrete approximation to exact solution  $w(x, t)$  is given as:

$$w_h(t) = \sum_{i=1}^N w_i(t) \phi_i(x).$$

By substituting the above finite element discretization into the element-level finite dimensional discrete version of Eq.(2.3.3.1) we get element-level linear system of equations. After assembly of element-level matrices and on solving the global system we get

$$[A]\{w\} = \{f\},$$

where  $w = w^{j+1}$  is finite element solution at  $(j + 1)$ th-time level.

### 2.3.4 Streamline upwind/Petrov-Galerkin (SUPG) method

Since the classical Galerkin formulation fails to give satisfactory results for singularly perturbed problems. To enhance the precision and stability of the Galerkin discretization, SUPG technique proposed by Brooks and Hughes[96] has been preferred by many researchers for convection dominated problems. For approximating the sols. of SPP, we have also considered the SUPG technique. The SUPG technique eliminates unwanted oscillations in the region of boundary layer. The weak formulation of Eq.(2.2.1) is defined as:

Find  $w \in H^1(D)$

$$a(w, v) = (F, v) \quad \forall v \in H_0^1(D).$$

Here  $a(w, v) = \epsilon(\nabla w, \nabla v) + (\mathbf{a}\nabla w, v)$  and  $F = f - bw$ .

The SUPG technique is defined as:

Find  $w_h \in L^2(D)$  such that

$$a_h(w_h, v_h) + (R_h(w_h), \tau \mathbf{a}\nabla_h v_h) = (F, v_h) \quad \forall v_h \in V_h,$$

where  $R_h(w) = -\epsilon\Delta_h w + \mathbf{a}\nabla_h w - F$ ,  $\tau$  is the nonnegative stabilization parameter and  $V_h$  is the finite dimensional solution subspace. We choose

$$\tau|_K \equiv \tau_K = \begin{cases} \tau_0 h_K, & \text{if } Pe_K > 1, \\ \tau_1 h_K^2 / \epsilon, & \text{if } Pe_K \leq 1, \end{cases}$$

as proposed by Roos[169] where  $Pe_K = \frac{|\mathbf{a}|h_K}{2\epsilon}$ ,  $K$  is the element of the mesh,  $h_K$  is the characteristic dimension of  $K$ ,  $\tau_0$  and  $\tau_1$  are positive constants.

## 2.4 Numerical results

In this Section, some numerical results have been presented to test the efficiency of proposed adaptive numerical scheme.

**Example 1.** Consider Eq. (2.2.1) for the specific values of  $a(x, t) = 1$  and  $b(x, t) = 0$  subject to initial condition

$$w(x, 0) = \exp(-0)(C_1 + C_2x - \exp(-(1 - x)/\epsilon)), \quad 0 < x < 1,$$

and boundary conditions

$$w(0, t) = \exp(-t)(C_1 + C_2 \cdot 0 - \exp(-(1 - 0)/\epsilon)), \quad t > 0,$$

$$w(1, t) = \exp(-t)(C_1 + C_2 \cdot 1 - \exp(-(1 - 1)/\epsilon)), \quad t > 0.$$

The source function  $f(x, t)$  is so chosen to satisfy the analytical solution given by

$$w(x, t) = \exp(-t)(C_1 + C_2x - \exp(-(1 - x)/\epsilon)),$$

where  $C_1 = \exp(-1/\epsilon)$  and  $C_2 = 1 - C_1$ . Since for the present problem the analytical solution is known, some error estimates have been presented in  $L_\infty$ -norm defined by

$$\| w(x, t) - w_h(x, t) \|_{L_\infty} = \max_{1 \leq i \leq N} | w(x_i, t) - w_h(x_i, t) |,$$

$$E_\epsilon^{N, \delta t} = \max_{0 \leq i \leq N, 0 \leq j \leq M} | w(x_i, t_j) - w_h(x_i, t_j) |,$$

where  $N$  represents the number of mesh points in the spatial direction. In Table 2.1 and 2.2, maximum absolute errors have been tabulated at time level  $t = 1$  and have been compared with uniform convergent scheme proposed by Clavero et al.[43] for different values of  $\epsilon$ . In Fig. 2.1, comparison of numerical solution has been done for the Example 1 using FEM and SUPG method on piecewise uniform Shishkin mesh. From the solution plot, it can be verified that the both SUPG method and FEM works efficiently for very small values of  $\epsilon$ . For the other solution plots, FEM has been taken into consideration. In Fig. 2.2, grid validation of the code has been tested for different values of singular perturbation parameter  $\epsilon = 2^{-8}$  and  $2^{-18}$  at time level  $t = 1$ . From solution plots, it can be seen that a grid of 64 elements is sufficient enough to capture the boundary layers even for very small values of  $\epsilon$  like  $\epsilon = 2^{-18}$ . From grid validation tests, we analyze that as we move from grid of 16 elements to grid

Table 2.1: Maximum pointwise errors  $E_\epsilon^{N,\Delta t}$  for Example 1 on piecewise uniform Shishkin mesh

|            | Proposed Sch | Clavero [43] | Proposed Sch | Clavero[43] | Proposed Sch | Clavero[43] |
|------------|--------------|--------------|--------------|-------------|--------------|-------------|
| $\epsilon$ | N=16         | N=16         | N=32         | N=32        | N=64         | N=64        |
| $2^{-0}$   | 2.132E-5     | 1.307E-3     | 1.755E-5     | 7.907E-4    | 1.662E-5     | 3.698E-4    |
| $2^{-2}$   | 1.000E-3     | 1.739E-2     | 4.733E-4     | 9.684E-3    | 3.523E-4     | 5.105E-3    |
| $2^{-4}$   | 6.700E-3     | 4.013E-2     | 3.000E-3     | 2.555E-2    | 1.500E-3     | 1.586E-2    |
| $2^{-6}$   | 6.700E-3     | 5.966E-2     | 3.100E-3     | 3.737E-2    | 1.700E-3     | 2.179E-2    |
| $2^{-8}$   | 6.700E-3     | 6.879E-2     | 3.100E-3     | 4.540E-2    | 1.700E-3     | 2.711E-2    |
| $2^{-10}$  | 6.700E-3     | 7.147E-2     | 3.100E-3     | 4.833E-2    | 1.700E-3     | 2.963E-2    |
| $2^{-12}$  | 6.700E-3     | 7.217E-2     | 3.100E-3     | 4.912E-2    | 1.700E-3     | 3.038E-2    |
| $2^{-14}$  | 6.700E-3     | 7.235E-2     | 3.100E-3     | 4.932E-2    | 1.700E-3     | 3.055E-2    |
| $2^{-16}$  | 6.700E-3     | 7.239E-2     | 3.100E-3     | 4.937E-2    | 1.700E-3     | 3.063E-2    |
| $2^{-18}$  | 6.700E-3     | 7.240E-2     | 3.100E-3     | 4.939E-2    | 1.700E-3     | 3.064E-2    |
| $2^{-20}$  | 6.700E-3     | 7.241E-2     | 3.100E-3     | 4.939E-2    | 1.700E-3     | 3.064E-2    |
| $2^{-22}$  | 6.700E-3     | 7.241E-2     | 3.100E-3     | 4.939E-2    | 1.700E-3     | 3.064E-2    |
| $2^{-24}$  | 6.700E-3     | 7.241E-2     | 3.100E-3     | 4.939E-2    | 1.700E-3     | 3.064E-2    |
| $2^{-26}$  | 6.700E-3     | 7.241E-2     | 3.100E-3     | 4.939E-2    | 1.700E-3     | 3.064E-2    |

Table 2.2: Maximum pointwise errors  $E_\epsilon^{N,\Delta t}$  for Example 1 on piecewise uniform Shishkin mesh

|            | Proposed Scheme | Clavero [43] | Proposed Scheme | Clavero[43] |
|------------|-----------------|--------------|-----------------|-------------|
| $\epsilon$ | N=128           | N=128        | N=256           | N=256       |
| $2^{-0}$   | 1.639E-5        | 1.889E-4     | 1.633E-5        | 9.551E-5    |
| $2^{-2}$   | 3.226E-4        | 2.622E-3     | 3.152E-4        | 1.328E-3    |
| $2^{-4}$   | 1.000E-3        | 9.560E-3     | 9.000E-4        | 5.599E-3    |
| $2^{-6}$   | 1.300E-3        | 1.238E-2     | 1.200E-3        | 6.970E-3    |
| $2^{-8}$   | 1.300E-3        | 1.527E-2     | 1.300E-3        | 8.339E-3    |
| $2^{-10}$  | 1.400E-3        | 1.708E-2     | 1.300E-3        | 9.466E-2    |
| $2^{-12}$  | 1.400E-3        | 1.772E-2     | 1.300E-3        | 9.976E-3    |
| $2^{-14}$  | 1.400E-3        | 1.789E-2     | 1.300E-3        | 1.013E-2    |
| $2^{-16}$  | 1.400E-3        | 1.793E-2     | 1.300E-3        | 1.013E-2    |
| $2^{-18}$  | 1.400E-3        | 1.794E-2     | 1.300E-3        | 1.017E-2    |
| $2^{-20}$  | 1.400E-3        | 1.795E-2     | 1.300E-3        | 1.018E-2    |
| $2^{-22}$  | 1.400E-3        | 1.795E-2     | 1.300E-3        | 1.018E-2    |
| $2^{-24}$  | 1.400E-3        | 1.795E-2     | 1.300E-3        | 1.018E-2    |
| $2^{-26}$  | 1.400E-3        | 1.795E-2     | 1.300E-3        | 1.018E-2    |

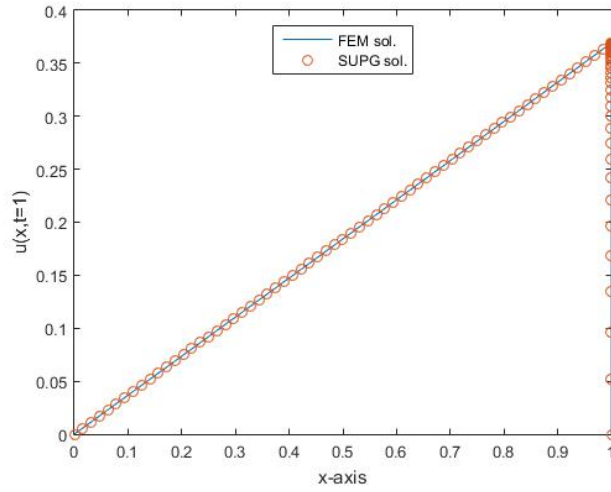
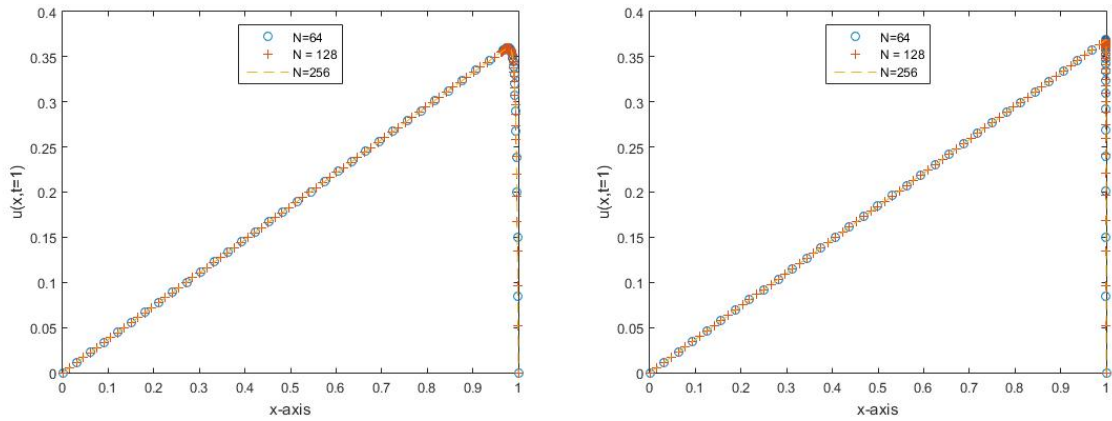


Figure 2.1: Comparison of numerical solution profile for  $\epsilon = 2^{-16}$  using FEM and SUPG method

of 256 elements, the boundary layers are captured very nicely. For further numerical results to follow, grid of 128 elements has been considered. In Fig. 2.3, the effect of



(a)  $\epsilon = 2^{-8}$

(b)  $\epsilon = 2^{-18}$

Figure 2.2: Grid validation test for  $\epsilon = 2^{-8}, 2^{-18}$

singular perturbation parameter  $\epsilon$  on the solution has been depicted as  $\epsilon \rightarrow 0$ . The solution plots have been drawn for various values of  $\epsilon$  at time levels  $t = 0.5$  and  $t = 1$ . In both the plots, it is very clear that as singular perturbation parameter becomes smaller and smaller, sharper boundary layers appear in the solution and the proposed numerical scheme is efficient enough to capture these boundary layers.

In Fig. 2.4(a), finite element solution of singularly perturbed problem has been

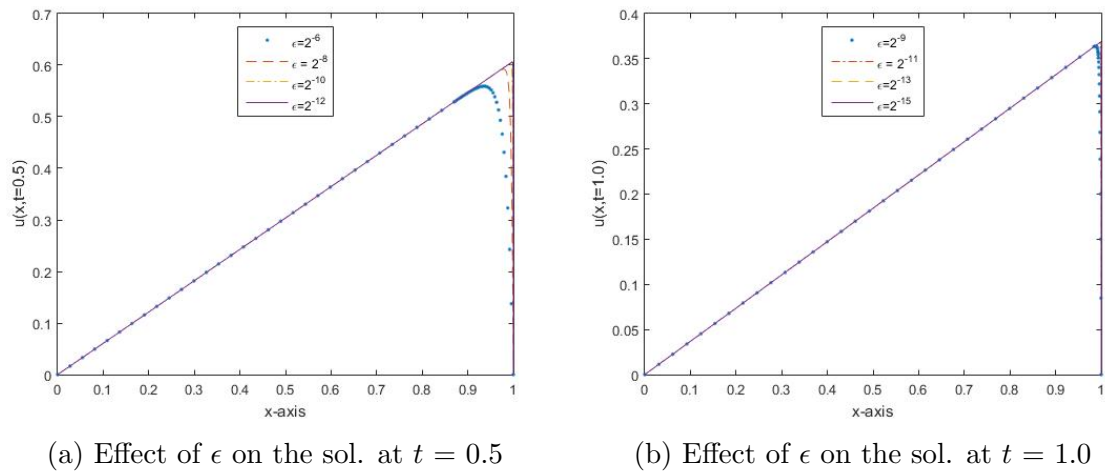


Figure 2.3:  $\epsilon$  - effect at different time levels

plotted for  $\epsilon = 2^{-12}$  at different time levels  $t = 0.2, 0.4, 0.6, 0.8$  and  $1$ . Further, the solution has been plotted for  $\epsilon = 2^{-16}$  at various time levels  $t = 0.1, 0.3, 0.5, 0.7$  and  $0.9$  in Fig. 2.4(b). Both the plots depict the efficiency and robustness of the proposed method in capturing very sharp boundary layers. Fig. 2.5 presents numerical solution

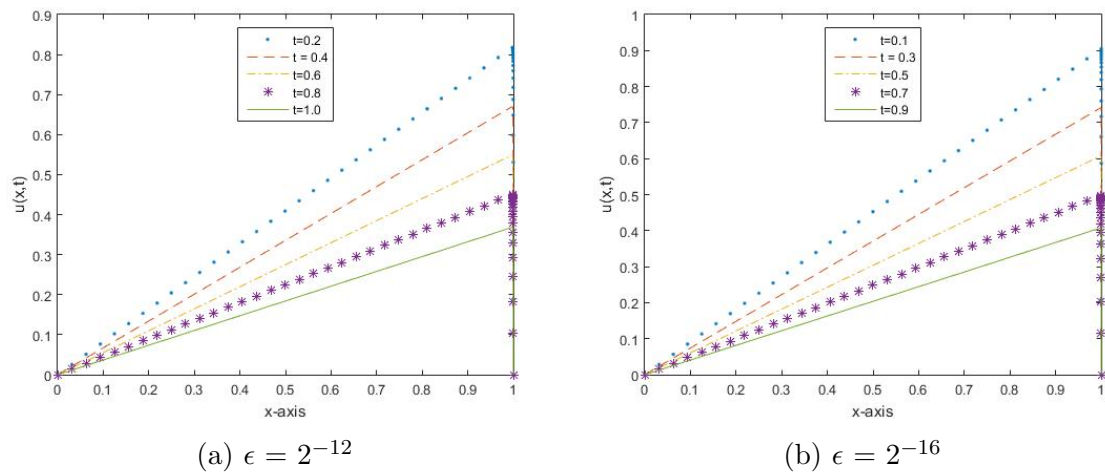


Figure 2.4: Time-effect for  $\epsilon = 2^{-12}, 2^{-16}$

profile of Example 1. for  $\epsilon = 2^{-26}$  over the whole time domain  $[0, 1]$ .

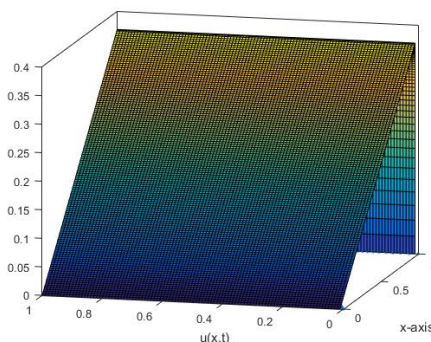


Figure 2.5: The numerical solution profile for  $\epsilon = 2^{-26}$

## 2.5 Non-linear singularly perturbed parabolic partial differential equation

Consider time dependent singularly perturbed non-linear parabolic partial differential equation in one-dimension

$$\frac{\partial u}{\partial t} - \epsilon \frac{\partial^2 u}{\partial x^2} + a(x, t, u)u_x = f(x, t, u), \quad 0 < x < 1, t > 0, \quad (2.5.1)$$

with boundary conditions

$$u(0, t) = f(t), \quad t \geq 0,$$

$$u(1, t) = g(t), \quad t \geq 0,$$

and initial condition as

$$u(x, 0) = u_0(x) \text{ for } 0 \leq x \leq 1,$$

over the domain  $D = [0 \leq x \leq 1] \times [t \geq 0]$ , where  $\epsilon$  is small singular perturbation parameter ( $0 < \epsilon \ll 1$ ) and  $\Omega = [0 < x < 1]$ . Assuming  $a(x, t, u)$  and  $f(x, t, u)$  as continuous functions.

## 2.6 Proposed numerical strategy

### 2.6.1 Time semi-discretization

In the first step, we discretize the time derivative using implicit Euler method with constant step size  $\Delta t$ . Using time-discretization, we get the following semi-discretized

non-linear differential problem:

$$\frac{(u^{j+1} - u^j)}{\Delta t} = \epsilon u_{xx}^{j+1} - a(x, t, u)u_x|^{j+1} + f(x, t, u)|^{j+1}, \quad (2.6.1.1)$$

$$u^0 = u(x, 0) = u_0(x), \quad 0 < x < 1, \quad (2.6.1.2)$$

together with the boundary conditions

$$u(0, t_{j+1}) = u^{j+1}(0) = f(t_{j+1}), \quad u(1, t_{j+1}) = u^{j+1}(1) = g(t_{j+1}), \quad j > 0, \quad (2.6.1.3)$$

where  $u^{j+1}$  denote the solution of the above differential equation at  $(j + 1)$ -th time level. Next, before proceeding to spatial discretization of Eq. (2.6.1.1), we will use quasilinearization process to linearize the equation.

## 2.6.2 Quasilinearization process and its convergence

Quasilinearization is a very well known and established process used for approximating and obtaining the solutions of nonlinear problems. Lot of researchers have used different quasilinearization techniques. For instance, Yakar and Koksal [199] proposed quasilinearization strategy for approximating non-linear problems using casual operators. Motsa et al. [139] proposed successive linearization technique for approximating non-linear problems and then the obtained reduced system of equations have been solved using Chebyshev spectral collocation method. Mittal and Jiwari[130]developed numerical scheme based on differential quadrature method for solving nonlinear generalizations of Fisher and Burgers' equation using quasilinearization technique proposed by Bellman and Kalaba[22].

In the present work, we have used the quasilinearization technique proposed by Bellman and Kalaba [22] to obtain linear approximates of the non-linear differential equations. It has been shown that the sequence of approximate solutions of these linearized problems converges monotonically and quadratically to the solution of the non-linear

equation (2.5.1). The semi-discretized equation (2.6.1.1) is linearized around a nominal solution satisfying the given boundary conditions. Let  $u_r(x)$  be nominal solution of the above problem (2.6.1.1-2.6.1.3). Applying quasilinearization process for a fixed time level  $t_{j+1}$ , we get a sequence of solutions  $\{u_r^{j+1}(x)\}_{r=0}^{\infty}$  of linear equations given by the following recurrence relation:

$$u_{r+1}^0 = u_0(x). \quad (2.6.2.1)$$

We write the Eq.(2.6.1.1) as

$$\frac{u^{j+1} - u^j}{\Delta t} = \epsilon u_{xx}^{j+1} - a(x, t, u)u_x|^{j+1} + f(x, t, u)|^{j+1} = \epsilon u_{xx}^{j+1} + G(u, u_x, x, t)|^{j+1}. \quad (2.6.2.2)$$

Applying quasilinearization technique [22], we get

$$\begin{aligned} \frac{u_{r+1}^{j+1} - u_r^j}{\Delta t} &= \epsilon (u_{xx})_{r+1}^{j+1} + G(u, u_x, x, t)|_r^{j+1} + (u_{r+1}^{j+1} - u_r^{j+1}) \left( \frac{\partial G(u, u_x, x, t)}{\partial u} \right) \Big|_r^{j+1} \\ &+ ((u_x)_{r+1}^{j+1} - (u_x)_r^{j+1}) \left( \frac{\partial G(u, u_x, x, t)}{\partial u_x} \right) \Big|_r^{j+1}. \end{aligned} \quad (2.6.2.3)$$

Also, the boundary conditions reduce to

$$u_{r+1}^{j+1}(0) = f((j+1)\Delta t), \quad u_{r+1}^{j+1}(1) = g((j+1)\Delta t), \quad j \geq 0, \quad (2.6.2.4)$$

where  $r = 0, 1, 2, \dots$  is iteration index and  $u_0^{j+1}(x)$  is initial guess. Further, in order to prove the convergence of the quasilinearization process, for the sake of convenience, we consider

$$\epsilon u_{xx}^{j+1} = H(u^{j+1}), \quad 0 < x < 1,$$

$$u^{j+1}(0) = f(t_{j+1}), \quad u^{j+1}(1) = g(t_{j+1}).$$

Using quasilinearization process, we obtain a sequence of linear differential equations determined by the following recurrence relation:

$$\epsilon (u_{xx})_{r+1}^{j+1} = H(u_r^{j+1}) + (u_{r+1}^{j+1} - u_r^{j+1}) \frac{\partial H(u_r^{j+1})}{\partial u}, \quad 0 < x < 1, \quad (2.6.2.5)$$

$$u_{r+1}^{j+1}(0) = f(t_{j+1}) \text{ and } u_{r+1}^{j+1}(1) = g(t_{j+1}),$$

where we assume that  $u_{r=0}^{j+1}$  is the initial guess which satisfy the boundary conditions also. Rewriting the above relation at previous iteration step, we get

$$\epsilon(u_{xx})_r^{j+1} = H(u_{r-1}^{j+1}) + (u_r^{j+1} - u_{r-1}^{j+1}) \frac{\partial H(u_{r-1}^{j+1})}{\partial u}, \quad 0 < x < 1. \quad (2.6.2.6)$$

Subtracting Eq.(2.6.2.6) from Eq.(2.6.2.5), we get

$$\begin{aligned} \epsilon((u_{xx})_{r+1}^{j+1} - (u_{xx})_r^{j+1}) &= H(u_r^{j+1}) - H(u_{r-1}^{j+1}) + (u_{r+1}^{j+1} - u_r^{j+1}) \frac{\partial H(u_r^{j+1})}{\partial u} \\ &\quad - (u_r^{j+1} - u_{r-1}^{j+1}) \frac{\partial H(u_{r-1}^{j+1})}{\partial u}, \quad 0 < x < 1. \end{aligned}$$

The above differential equation is of second order in  $(u_{r+1}^{j+1} - u_r^{j+1})$ . Converting it into integral equation by using Green's function, we obtain

$$\begin{aligned} \epsilon(u_{r+1}^{j+1} - u_r^{j+1}) &= \int_0^1 G(x, s) [H(u_r^{j+1}) - H(u_{r-1}^{j+1}) + (u_{r+1}^{j+1} - u_r^{j+1}) \frac{\partial H(u_r^{j+1})}{\partial u} \\ &\quad - (u_r^{j+1} - u_{r-1}^{j+1}) \frac{\partial H(u_{r-1}^{j+1})}{\partial u}] ds, \quad 0 < x < 1, \end{aligned} \quad (2.6.2.7)$$

where Green's function  $G(x, s)$  is given by

$$G(x, s) = \begin{cases} x(s-1), & 0 \leq x \leq s \leq 1, \\ (x-1)s, & 0 \leq s \leq x \leq 1, \end{cases}$$

and

$$\max_{x,s} G(x, s) = \frac{1}{4}. \quad (2.6.2.8)$$

Using Mean Value Theorem,

$$H(u_r^{j+1}) - H(u_{r-1}^{j+1}) = (u_r^{j+1} - u_{r-1}^{j+1}) \frac{\partial H(u_{r-1}^{j+1})}{\partial u} + \frac{(u_r^{j+1} - u_{r-1}^{j+1})^2}{2} \frac{\partial^2 H(\theta)}{\partial u^2}, \quad (2.6.2.9)$$

where  $u_{r-1}^{j+1} \leq \theta \leq u_r^{j+1}$ .

Using Eq.(2.6.2.9), Eq.(2.6.2.7) becomes

$$\epsilon(u_{r+1}^{j+1} - u_r^{j+1}) = \int_0^1 G(x, s) \left[ \frac{(u_r^{j+1} - u_{r-1}^{j+1})^2}{2} \frac{\partial^2 H(\theta)}{\partial u^2} + (u_{r+1}^{j+1} - u_r^{j+1}) \frac{\partial H(u_r^{j+1})}{\partial u} \right] ds,$$

$$0 < x < 1. \quad (2.6.2.10)$$

Taking

$$\max_{|u_r^{j+1}| \leq 1} \left| \frac{\partial^2 H(\theta)}{\partial u^2} \right| = P, \quad \max_{|u_r^{j+1}| \leq 1} \left| \frac{\partial H(u_r^{j+1})}{\partial u} \right| = Q. \quad (2.6.2.11)$$

Taking maximum norm over the spatial domain and using equations (2.6.2.8) and (2.6.2.11) in (2.6.2.10), we get

$$\left\| (u_{r+1}^{j+1} - u_r^{j+1}) \right\| \leq \frac{1}{4\epsilon} \int_0^1 \left[ \frac{P}{2} (u_r^{j+1} - u_{r-1}^{j+1})^2 + Q \left\| (u_{r+1}^{j+1} - u_r^{j+1}) \right\| \right] ds. \quad (2.6.2.12)$$

Simplifying this inequality, we get

$$\begin{aligned} \left\| (u_{r+1}^{j+1} - u_r^{j+1}) \right\|_{\Omega} &\leq \frac{P}{8\epsilon - 2Q} \left\| (u_r^{j+1} - u_{r-1}^{j+1}) \right\|_{\Omega}^2, \\ &\leq C \left\| (u_r^{j+1} - u_{r-1}^{j+1}) \right\|_{\Omega}^2, \end{aligned} \quad (2.6.2.13)$$

where  $C = \frac{P}{8\epsilon - 2Q}$ .

Thus, with appropriate choice of initial iterative approximation  $u_0^{j+1}$ , the quasilinearization process converges quadratically.

Therefore, in order to approximate the sol. of the problem (2.6.1.1-2.6.1.3), it is sufficient to approximate the sol. of its linearized version (2.6.2.3-2.6.2.4). The finite element formulation and SUPG formulation of the linearized problem (2.6.2.3-2.6.2.4) can be carried out on Shishkin mesh in similar way as discussed in Subsections 2.3.3 and 2.3.4 respectively.

## 2.7 Absolute stability

Consider the problem given by (2.5.1). Its approximate linear differential equation is given by equation (2.6.2.3). Applying Galerkin finite element or SUPG technique to

the linearized version in the spatial direction and using boundary conditions, we get a system of first order differential equations in time variable and can be written as

$$[A_1] \left\{ \frac{\partial \tilde{U}}{\partial t} \right\} = [B_1] \{ \tilde{U} \} + S, \quad (2.7.1)$$

with initial condition

$$\tilde{U}(0) = [\phi_2, \phi_3, \dots, \phi_N]^T, \quad (2.7.2)$$

where  $[A_1]$ ,  $[B_1]$  are  $(N-1) \times (N-1)$  tridiagonal matrices,  $\tilde{U} = \{u_2^{r+1}, u_3^{r+1}, \dots, u_N^{r+1}\}$  and  $S$  are column vectors of order  $(N-1)$ .

On simplifying the system (2.7.1), we get

$$\left\{ \frac{\partial \tilde{U}}{\partial t} \right\} = [C] \{ \tilde{U} \} + S_1, \quad (2.7.3)$$

where  $C = [A_1]^{-1}[B_1]$  and  $S_1 = [A_1]^{-1}S$ .

Let  $\{\lambda_s, s = 1, 2, \dots, N-1\}$  be eigen values of the matrix  $C$  where  $\lambda_s = \lambda_{sR} + i\lambda_{sI}$ .

The proposed numerical scheme will be stable if all the eigenvalues of matrix  $C$  lie outside the unit circle

$$(1 - \Delta t \lambda_{sR})^2 + (\Delta t \lambda_{sI})^2 = 1.$$

## 2.8 Numerical results

In this Section, we have presented some numerical results to check the efficiency and robustness of the developed adaptive schemes.

**Example 2.** Consider Eq. (2.5.1) for  $a(x, t, u) = 0$ ,  $f(x, t, u) = (-bu^2 - cu)$  together with the initial condition

$$u(x, 0) = (d.x + 1)^{-1}, \quad 0 < x < 1,$$

and boundary conditions

$$\begin{aligned} u(0, t) &= (c.t + 1)^{-1}, & t > 0, \\ u(1, t) &= (c.t + d.1 + 1)^{-1}, & t > 0. \end{aligned}$$

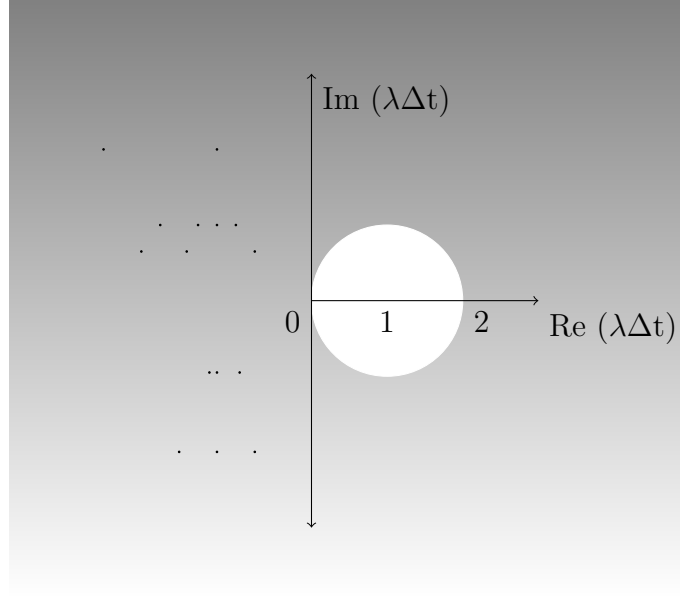


Figure 2.6: Stability region for non-linear singularly perturbed problem

The analytic solution of the above problem is given by

$$u(x, t) = (c.t + d.x + 1)^{-1},$$

where  $d = \sqrt{b/2\epsilon}$ ,  $b = 0.01$  and  $c = 0.01$ . The errors have been presented in the  $L_\infty$ -norm defined by

$$\| u(x, t) - u_h(x, t) \|_\infty = \max_{1 \leq i \leq N, 1 \leq j \leq M} | u(x_i, t_j) - u_h(x_i, t_j) |,$$

where  $M$  is the number of time-steps.

The problem has been solved using both the proposed numerical schemes FEM i.e. finite element method and stabilized SUPG technique. Since the solution obtained using both the schemes differs minutely, therefore, the results have been presented for stabilized SUPG technique. The region of absolute stability, which is outside the above mentioned unit circle, for the problem under consideration is shown in Fig. 2.6. From Fig. 2.6, it can easily be seen that all eigenvalues of matrix  $[C]$  lie in the region of absolute stability which proves the stability of the proposed numerical scheme. In Table 2.3, maximum absolute errors have been tabulated using SUPG method for

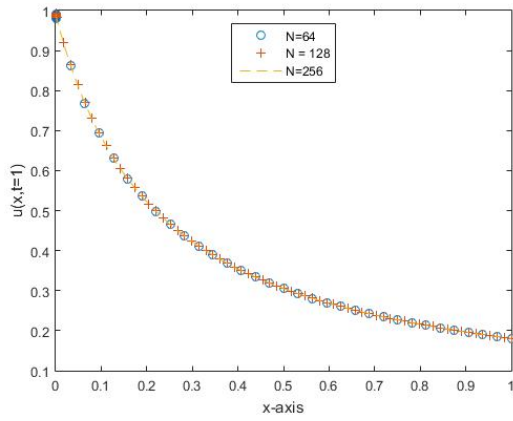
different values of  $\epsilon$  at time level  $t = 1$ .

In Fig. 2.7, grid validation of the code has been done for different values of singu-

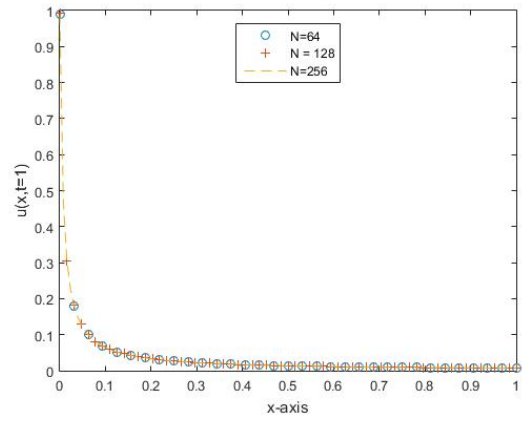
Table 2.3: Maximum SUPG pointwise errors  $E_\epsilon^{N,\Delta t}$  for the Example 2 on piecewise uniform Shishkin mesh

|            | Proposed Sch. | Proposed Sch. | Proposed Sch. | Proposed Sch. | Proposed Sch. |
|------------|---------------|---------------|---------------|---------------|---------------|
| $\epsilon$ | N=16          | N=32          | N=64          | N=128         | N=256         |
| $2^{-0}$   | 1.416E-5      | 1.415E-5      | 1.415E-5      | 1.415E-5      | 1.415E-5      |
| $2^{-2}$   | 3.473E-5      | 3.475E-5      | 3.472E-5      | 3.472E-5      | 3.471E-5      |
| $2^{-4}$   | 4.634E-5      | 4.502E-5      | 4.485E-5      | 4.483E-5      | 4.482E-5      |
| $2^{-6}$   | 5.533E-5      | 4.782E-5      | 4.571E-5      | 4.522E-5      | 4.509E-5      |
| $2^{-8}$   | 7.726E-5      | 5.704E-5      | 4.796E-5      | 4.574E-5      | 4.524E-5      |
| $2^{-10}$  | 1.254E-4      | 8.090E-5      | 5.679E-5      | 4.785E-5      | 4.571E-5      |
| $2^{-12}$  | 2.232E-4      | 1.354E-4      | 8.373E-5      | 5.578E-5      | 4.719E-5      |
| $2^{-14}$  | 3.950E-4      | 2.048E-4      | 1.420E-4      | 8.615E-5      | 5.477E-5      |
| $2^{-16}$  | 6.071E-4      | 2.518E-4      | 2.197E-4      | 1.456E-4      | 8.664E-5      |
| $2^{-18}$  | 8.025E-4      | 3.849E-4      | 2.535E-4      | 2.288E-4      | 1.475E-4      |
| $2^{-20}$  | 9.444E-4      | 5.075E-4      | 2.319E-4      | 2.704E-4      | 2.339E-4      |
| $2^{-22}$  | 1.000E-3      | 5.965E-4      | 3.054E-4      | 1.850E-4      | 2.804E-4      |
| $2^{-24}$  | 1.100E-3      | 6.515E-4      | 3.588E-4      | 1.783E-4      | 2.005E-4      |

lar perturbation parameter  $\epsilon = 2^{-12}, 2^{-22}$  at time level  $t=1$ . From solution plots, it can be seen that for very small values of  $\epsilon$  like  $2^{-22}$ , grid of 64 elements is sufficient enough to capture the boundary layers. From grid validation tests, we analyze that as we move from grid of 16 elements to grid of 256 elements, the boundary layers are captured very nicely. For further numerical results to follow, grid of 256 elements has been considered. In Fig. 2.8, the behavior of singular perturbation parameter  $\epsilon$  has been depicted as  $\epsilon \rightarrow 0$ . The solution plots have been drawn for various values of  $\epsilon$  at time levels  $t = 0.5$  and  $t = 1$ . In both the plots, it is very clear that as singular perturbation parameter gets smaller and smaller, sharper boundary layers appear in the solution and the proposed numerical scheme is efficient enough to capture these boundary layers. In Fig. 2.9(a), finite element solution of singularly perturbed problem has been plotted for  $\epsilon = 2^{-20}$  at different time levels  $t = 0.2, 0.4, 0.6$  and  $0.8$ . Further, the solution has been plotted for  $\epsilon = 2^{-16}$  at various time levels  $t = 0.1, 0.3, 0.5$  and  $0.7$  in Fig. 2.9(b). In Fig. 2.10, finite element solution profile of Example

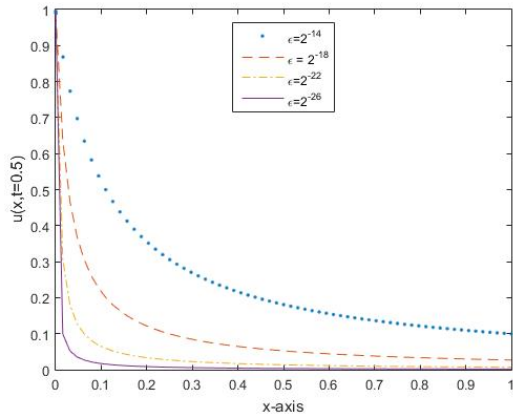


(a)  $\epsilon = 2^{-12}$

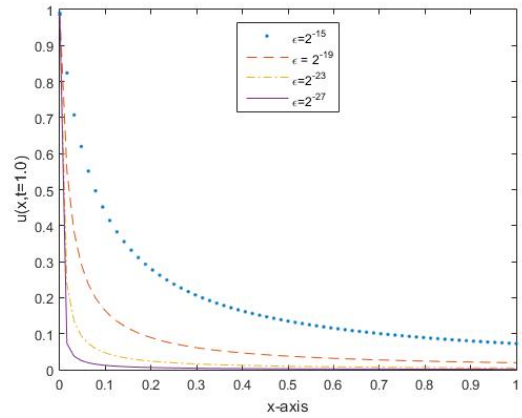


(b)  $\epsilon = 2^{-22}$

Figure 2.7: Grid validation test for  $\epsilon = 2^{-12}, 2^{-22}$



(a)  $t = 0.5$



(b)  $t = 1.0$

Figure 2.8:  $\epsilon$  - effect at  $t = 0.5, 1$

2 is shown for  $\epsilon = 2^{-25}$  over the continuous time-domain  $[0,1]$ . Further, the SUPG solution has been plotted on piecewise uniform Shishkin mesh for different values of  $\epsilon$  in Fig. 2.11.

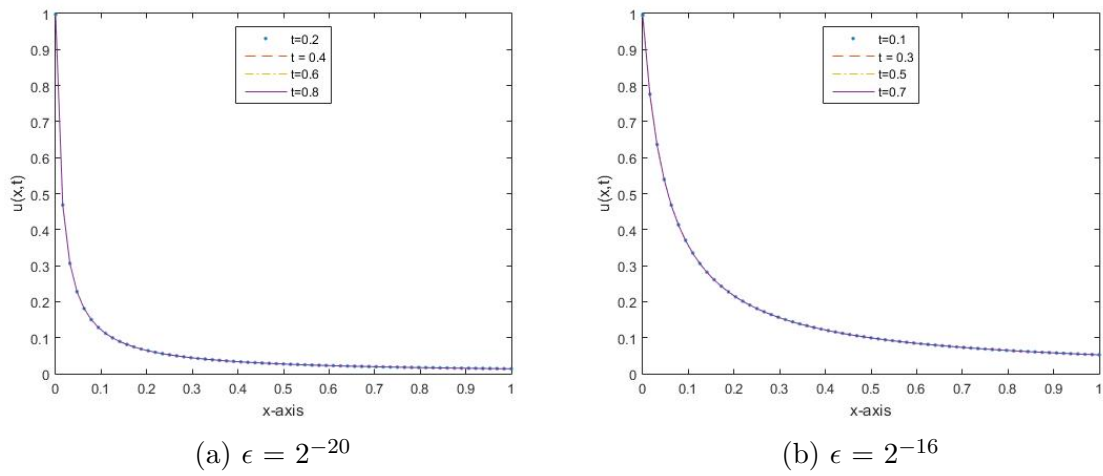


Figure 2.9: Temporal-effect on the FEM sol.

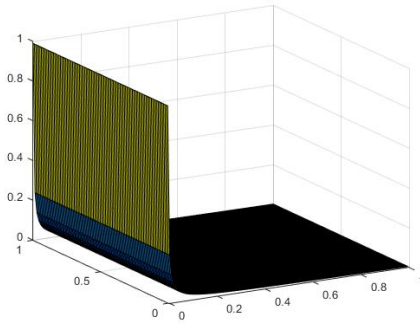


Figure 2.10: FEM solution profile for  $\epsilon = 2^{-25}$  over the time-domain  $[0,1]$

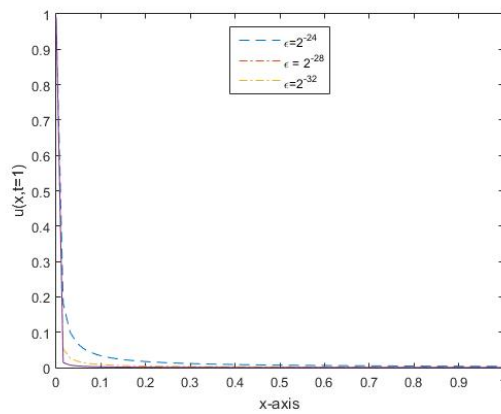


Figure 2.11: SUPG solution at  $t=1$  for different values of  $\epsilon$

**Example 3.** Consider the following singularly perturbed non-linear partial differential equation defined by

$$u_t - \epsilon u_{xx} = ku(1 - u), \quad 0 < x < 1.$$

The exact solution of the considered problem for  $\epsilon = 1$  is given by

$$u(x, t) = \frac{1}{\left(1 + \exp\left(\sqrt{\frac{k}{6}}x - \frac{5kt}{6}\right)\right)^2}.$$

In Table 2.4, numerical results obtained using the proposed scheme have been compared with those cited in [38] for  $\epsilon = 1$ . For the case  $\epsilon \ll 1$ , numerical results could not

Table 2.4: Numerical results for Example 3 for  $k = 6$ ,  $\epsilon = 1$  and  $\Delta t = 0.001$ ,  $T = 0.01$

| x    | Proposed Scheme | Semi-implicit method | Exact sol |
|------|-----------------|----------------------|-----------|
| 0.25 | 0.2027          | 0.2027               | 0.2026    |
| 0.50 | 0.1516          | 0.1516               | 0.1516    |
| 0.75 | 0.1101          | 0.1101               | 0.1101    |

be found. In order to test the effectivity of the proposed adaptive numerical scheme, the considered problem has been solved subject to the initial condition

$$u(x, 0) = 1 - \cos(x), \quad 0 \leq x \leq 1,$$

and boundary conditions

$$u(0, t) = 0, \quad t > 0,$$

$$u(1, t) = 0, \quad t > 0.$$

In Fig. 2.12(a) and (b),  $\epsilon$ -effect has been shown on the numerical solution at time  $t = 0.5$  and  $t = 1$ . From the solution plots, it can be noticed that the proposed scheme is efficient enough in capturing sudden sharp changes in the solution. Further, in Fig. 2.13(a) and (b), numerical solution has been plotted for  $\epsilon = 2^{-12}$  and  $2^{-15}$  at different time levels. It can be observed from the solution plots that the sharp boundary layers

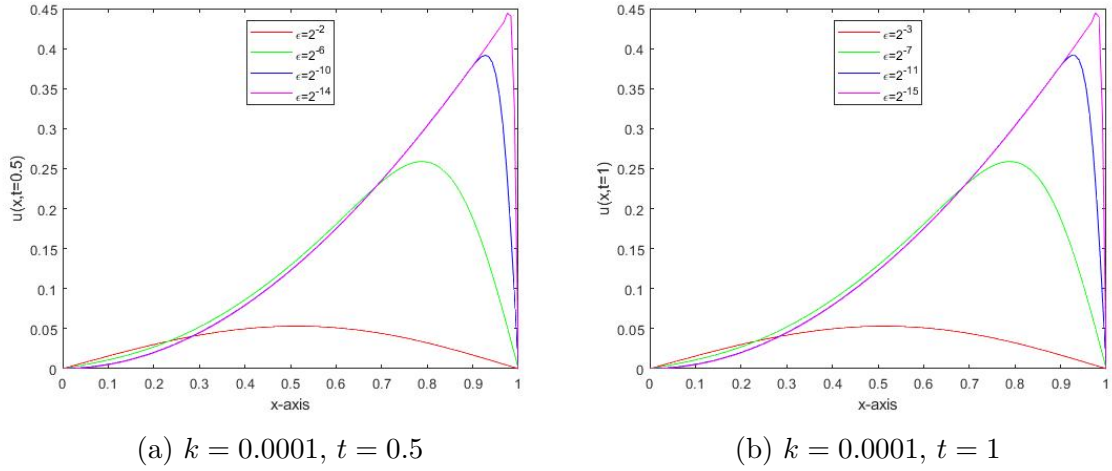


Figure 2.12:  $\epsilon$ -effect on the FEM sol.

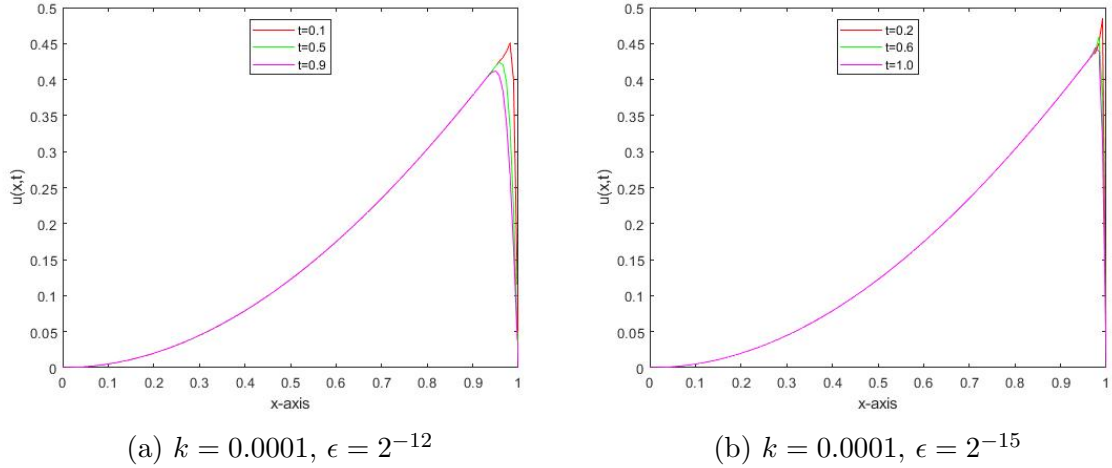


Figure 2.13: Time-effect on the sol. for  $\epsilon = 2^{-12}$  and  $2^{-15}$

appear near the boundary  $x = 1$  as singular perturbation parameter  $\epsilon$  becomes small. In Fig. 2.14, behavior of the numerical solution has been shown for  $\epsilon = 2^{-14}$  over the time-domain  $[0,1]$ .

## 2.9 Conclusion

In this Chapter, two numerical techniques, i.e. finite element technique and stabilized SUPG technique, on adaptive piecewise uniform Shishkin mesh have been proposed for approximating one-dimensional singularly perturbed problems. The considered

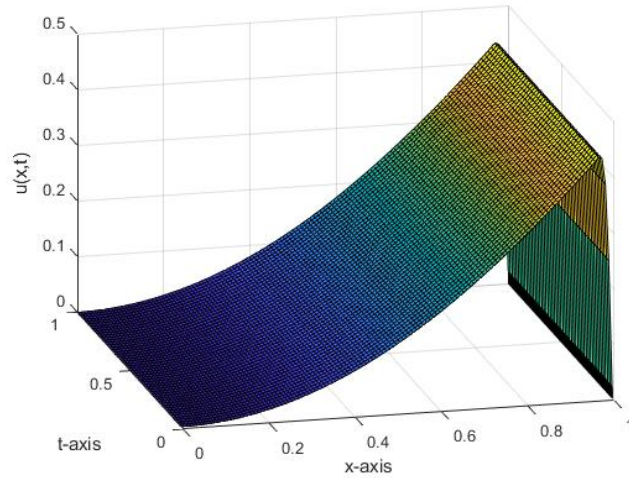


Figure 2.14: FEM solution profile for  $k = 0.0001$ ,  $\epsilon = 2^{-14}$  over the time-domain  $[0,1]$

problems are time-dependent. Time semi-discretization has been performed using implicit Euler's method. Piecewise uniform Shishkin mesh has been considered for spatial discretization. Spatial discretization has been carried out using both the proposed finite element and stabilized SUPG methods. Exponentially fitted splines have been considered as a basis for the test spaces. Streamline upwind/Petrov-Galerkin (SUPG) stabilization strategy removes the unwanted oscillations in the boundary layer region. For non-linear singularly perturbed problems, quasilinearization strategy has been invoked to handle the non-linear terms. Stability of the proposed schemes have also been discussed. Numerical experiments have been performed and it has been shown that the proposed schemes approximates the solution very effectively on adaptive Shishkin grids. It has been observed that both the schemes works very well for solving the singularly perturbed problems and the numerical solutions obtained by using both the proposed schemes agree with the exact solutions for both linear and non-linear problems. In the next Chapter, two-dimensional singularly perturbed convection-diffusion problem has been analyzed based on Hughes stabilized SUPG method. An adaptive anisotropic mesh refinement technique based on the a posteriori error estimates has been developed to capture the abrupt changes in the solution

as  $\epsilon \rightarrow 0$ .

# A posteriori error estimates for Hughes stabilized SUPG technique and adaptive refinement strategy for two-dimensional singularly perturbed problems

---

## 3.1 Introduction

Singularly perturbed problems occur frequently during the analysis of biological systems, heat transfer processes, etc. In general, it has been observed that singularly perturbed problems display singularities for sufficiently small values of  $\epsilon \rightarrow 0$ . Therefore, it becomes essential to implement some robust numerical technique to capture these singularities. Sharma et al.[180] presented a review on asymptotic and numerical analysis for solving singularly perturbed problems. From the literature review, it is clear that there exist various robust numerical strategies to handle these singularities. Adaptive mesh refinement techniques based on error estimates are among such techniques which are widely used to capture the layer behavior of SPPs. Broadly, we can categorize the error estimates into two categories, namely, a priori error es-

---

This Chapter has been published in *Advances in Mathematical Physics (2020)*

timates and a posteriori error estimates. Various researchers have derived error estimates for different type of problems. Nicaise and Repin[146] derived a posteriori error estimates for reaction-convection-diffusion problems based on purely functional arguments. Further, Zhao et al.[208] proposed adaptive numerical strategy for convection-diffusion problem based on semi-robust residual a posteriori error estimates for lower order nonconforming finite element approximations of streamline diffusion method. González et al.[79] developed residual type a posteriori error estimates for the linear convection-diffusion problem based on dual-mixed finite element method. Lin et.al[120] proposed a weak Galerkin FEM for SPP. Kopteva[107] developed a posteriori error estimates in maximum norm and shown second-order uniform convergence for the proposed method for solving singularly perturbed semilinear reaction-diffusion problems. Aguiar and Natesan[3] proposed two numerical schemes for two-point singularly perturbed problems. The first scheme is based on combination of classical finite difference scheme and exponentially fitted difference scheme and the second scheme is based on numerical scheme proposed by Aguiar and Ferrándiz[2]. Error estimates have been derived and the theoretical findings have been validated via numerical results.

From literature, we know that the classical finite element methods fail to provide satisfactory results for small values of singular perturbation parameter, i.e., when  $\epsilon \rightarrow 0$ . Since, the Streamline upwind/Petrov-Galerkin (SUPG) method results in good approximation in the region where there is no abrupt change in the solution but fails drastically in the subregions of boundary layers. It has been observed that the SUPG method is not monotonicity preserving in nature, therefore, oscillations appear in the approximate solution of SUPG technique. In order to overcome this problem, in the present work, we have used Hughes stabilization technique[90] alongwith the Streamline upwind/Petrov-Galerkin (SUPG) method. This results into addition of one more term in the SUPG discretization of convection-diffusion problem. Further,

error estimates have been derived for the proposed scheme. An anisotropic mesh refinement technique have been proposed for two-dimensional singularly perturbed problems based on the derived error estimates.

The Chapter is organised as follows:

In Section 3.2, the problem under consideration and its Hughes stabilized stream-line upwind finite element approximation have been discussed. In order to obtain reliable error bounds, some important tools have been discussed in Section 3.3. In Section 3.4, residual based a posteriori error estimates have been derived. Further, an adaptive refinement algorithm based on the derived a posteriori error estimates has been proposed in Section 3.5. Section 3.6 includes some numerical experiments which have been performed to analyze the robustness and efficiency of proposed adaptive refinement strategy. In the last, conclusion has been presented.

## 3.2 Continuous problem

Consider the following convection-diffusion equation in two-dimensions

$$-\nabla \cdot \epsilon \nabla u + \mathbf{a} \cdot \nabla u + bu = f \quad \text{in } \Omega, \quad (3.2.1)$$

$$u = 0 \quad \text{on } \partial\Omega_D, \quad (3.2.2)$$

$$\epsilon \frac{\partial u}{\partial n} = g \quad \text{on } \partial\Omega_N, \quad (3.2.3)$$

where  $\Omega \subset \mathbb{R}^2$  is a bounded domain and  $\partial\Omega = \partial\Omega_D \cup \partial\Omega_N$  is the Lipschitz-continuous boundary,  $\epsilon$  is singular perturbation parameter ( $0 < \epsilon \ll 1$ ),  $\mathbf{a}$ ,  $b$  and  $f$  are sufficiently smooth. Here  $\partial\Omega_D$  and  $\partial\Omega_N$  denote the Dirichlet and Neumann boundaries of the domain respectively.

$W^{1,\infty}(\Omega)$  and  $L^\infty(\Omega)$  represent the usual Sobolev and Lebesgue space. We will use the notation  $(\cdot, \cdot)$  for inner product  $(\cdot, \cdot)_\Omega$ .

Through out the Chapter, we assume that  $-\frac{1}{2}\nabla \cdot \mathbf{a} + b \geq b_0 > 0$  on  $\overline{\Omega}$ .

For any open bounded subset  $K \subseteq \bar{\Omega}$ , let  $H^1(K)$  be the standard Sobolev space.

Further, we define

$$V_0 = \{v \in H^1(\Omega), v = 0 \text{ on } \partial\Omega_D\}.$$

Let

$$|||v|||_K^2 = \epsilon ||\nabla v||_K^2 + b_0 ||v||_K^2, \quad (3.2.4)$$

be energy norm on bounded subset  $K \subset \bar{\Omega}$ . The weak formulation of Eq.(3.2.1) is given by

Find  $u \in H^1(\Omega)$

$$\mathbf{B}(u, v) = \langle F, v \rangle, \quad (3.2.5)$$

where

$$\mathbf{B}(u, v) = \epsilon(\nabla u, \nabla v) + (\mathbf{a} \cdot \nabla u, v) + (bu, v) \quad (3.2.6)$$

$$\text{and } \langle F, v \rangle = (f, v) + (g, v)_{\partial\Omega_N} \quad \forall v \in V_0.$$

The solution of weak formulation (3.2.5) is confirmed using Lax Milgram Lemma along with the condition (3.2.3). Let  $F = \{\Gamma_h\}$  be family of triangulations where  $\Gamma_h$  be the admissible and shape-regular triangulation of domain  $\bar{\Omega}$  consisting of triangles. Let  $L$  be any two-dimensional triangular element with edge  $E$ . Define  $n_{L,E} = (n_x, n_y)$  to be unit outward normal vector to  $L$  along  $E$  see Fig. 3.1. Fixing one of the two normal vectors, let  $n_E$  be the normal vector for each edge  $E$ . It has been observed that the convection dominated problems exhibit non-physical oscillations in the layer region i.e. if Peclet number (as discussed below) is large, the solution of singularly perturbed problem exhibits abrupt changes in the solution. Define local mesh Peclet number for any element  $K$  as

$$Pe_K = \frac{\|\mathbf{a}\|_{\infty, K} h_{\min}^K}{2\epsilon}, \quad (3.2.7)$$

where  $h_{\min}^K$  is the minimal length of element  $K$  defined in the next Section. Further, we define  $V^h = \{v_h \in H^1 : v_h|_K \in P_1(K)\}$ , where  $P_1(K)$  is the space of linear

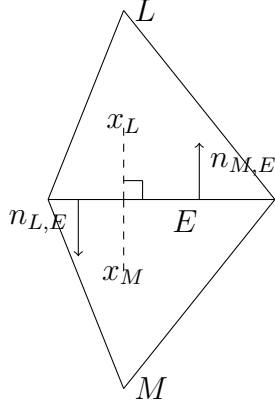


Figure 3.1: Orthogonality condition

polynomials over element  $K$  and  $V_0^h = \{v_h \in V^h : v_h|_{\partial\Omega_D} = 0\}$ . Since the standard FEM and SUPG methods results in unsatisfactory results for ( $\epsilon \ll 1$ )[169], in the present work, SUPG method together with the Hughes stabilization technique has been proposed for approximating the solution of the problem (3.2.1). The SUPG method[27] for problem (3.2.1) is defined as follows:

Find  $u_h \in V^h$  such that

$$\mathbf{B}_\rho(u_h, v_h) = \langle F, v_h \rangle \quad \forall \quad v_h \in V_0^h, \quad (3.2.8)$$

where

$$\mathbf{B}_\rho(u_h, v_h) = \mathbf{B}(u_h, v_h) + \langle R_h(u_h), \rho \mathbf{a} \cdot \nabla_h v_h \rangle,$$

$R_h(u) = -\epsilon \Delta_h u + \mathbf{a} \cdot \nabla_h u + bu - f$ ,  $\rho$  is non-negative stabilization parameter,  $\mathbf{B}(u, v)$  and  $\langle F, v \rangle$  are discussed in (3.2.6).

### 3.2.1 Hughes stabilization strategy

Since Streamline upwind/Petrov-Galerkin (SUPG) method results in good approximate solution in the region where there is no abrupt change in the solution but fails drastically in the boundary layer region. In order to deal with this hurdle, Hughes stabilization technique [96] together with SUPG method has been considered. It results in addition of term  $\langle R_h(u_h), \sigma \mathbf{a}_h \cdot \nabla_h v_h \rangle$  in the SUPG finite element discretization

of convection-diffusion equation where

$$\mathbf{a}_h = \begin{cases} \frac{(\mathbf{a} \cdot \nabla u_h) \nabla u_h}{|\nabla u_h|^2}, & \text{if } |\nabla u_h| \neq 0, \\ 0, & \text{if } |\nabla u_h| = 0, \end{cases} \quad (3.2.1.1)$$

and  $\sigma$  is nonnegative stabilization parameter. This additional term increases the robustness of SUPG method in the boundary layer region by controlling oscillations. Using Hughes stabilization technique along with SUPG finite element method, Eq.(3.2.1) is discretized as:

Find  $u_h \in V^h$  such that

$$\mathbf{B}_{\rho,\sigma}(u_h, v_h) = \langle F, v_h \rangle \quad \forall v_h \in V_0^h, \quad (3.2.1.2)$$

where  $\mathbf{B}_{\rho,\sigma}(u_h, v_h) = \mathbf{B}(u_h, v_h) + \langle R_h(u_h), \rho \mathbf{a} \cdot \nabla_h v_h \rangle + \langle R_h(u_h), \sigma \mathbf{a}_h \cdot \nabla_h v_h \rangle$  and  $R_h(u) = -\epsilon \Delta_h u + \mathbf{a} \cdot \nabla_h u + bu - f$ .

Let  $\rho_K$  be stabilization parameter over each element  $K$ . The existence and uniqueness of the finite element solution  $u_h$  derived using SUPG finite element discretization technique has been proved by Roos et al.[169]. It has been shown that the stabilization parameter  $\rho_K$  satisfies

$$0 \leq \rho_K \leq \frac{1}{2} \min\{b_0 \|b\|_{\infty, K}^{-2}, (h_{\min}^K)^2 \epsilon^{-1} \nu^{-2}\},$$

where  $h_{\min}^K$  is minimal length of element  $K$  and the constant  $\nu$  satisfies the inequality

$$\|\nabla \cdot \nabla v_h\|_K \leq \nu (h_{\min}^K)^{-1} \|\nabla v_h\|_K \quad \forall v_h \in V_0^h. \quad (3.2.1.3)$$

From inequality (3.2.1.3), it can easily be observed that  $\nu = 0$  for piecewise linear functions in  $V_0^h$ . Therefore, the above bounds reduces to  $0 \leq \rho_K \leq \frac{b_0}{2} \|b\|_{\infty, K}^{-2}$ . For simplicity, we introduce the notation  $c \lesssim d$  which means that there exists a positive constant  $A$  independent of  $c, d, \Gamma_h$  and  $\epsilon$  such that  $c \leq Ad$ . Further, we assume that

$$\rho_K \lesssim h_{\min}^K \|\mathbf{a}\|_{\infty, K}^{-1} \quad \forall K \in \Gamma_h. \quad (3.2.1.4)$$

Also, for any mesh function  $v_h \in V_0^h$ , using (3.2.1.3) and scaling arguments, we can get

$$\|\nabla v_h\|_K \lesssim (h_{\min}^K)^{-1} \|v_h\|_K.$$

Using energy norm def.(3.2.4),  $\|v_h\|_K \leq b_0^{-1/2} \|\|v_h\|\|_K$ . Thus we have,

$$\|\nabla v_h\|_K \lesssim (h_{\min}^K)^{-1} b_0^{-1/2} \|\|v_h\|\|_K. \quad (3.2.1.5)$$

Again, from energy norm, we have

$$\|\nabla v_h\|_K \leq \epsilon^{-1/2} \|\|v_h\|\|_K. \quad (3.2.1.6)$$

Using (3.2.1.5) and (3.2.1.6), we get

$$\|\nabla v_h\|_K \lesssim \min\{(h_{\min}^K)^{-1} b_0^{-1/2}, \epsilon^{-1/2}\} \|\|v_h\|\|_K. \quad (3.2.1.7)$$

### 3.3 Some important notations and tools

Since the considered singularly perturbed convection-diffusion problems displays abrupt change in the solution when Peclet number becomes large, in such cases, elements with large aspect ratio (anisotropic meshes) are preferred. Therefore, in the present work, anisotropic mesh has been considered for domain discretization. In the present Section, some important results on anisotropic meshes has been discussed.

#### 3.3.1 Notations

Consider a triangle  $K \in \Gamma_h$  with  $Q_0Q_1$  as longest edge (see Fig. 3.2). Represent two orthogonal vectors  $q_{i,K}$  with length  $h_{i,K} = |q_{i,K}|, i = 1, 2$ , where  $q_{1,K}$  is chosen along the the largest edge  $Q_0Q_1$ . From Fig. 3.2, it can be be confirmed that  $h_{1,K} \geq h_{2,K}$ . Define  $h_{\min}^K = h_{2,K}$ . These  $q_{i,K}$ 's correspond to two anisotropic directions. Further, define an orthogonal matrix  $C_K = (q_{1,K}, q_{2,K}) \in \mathbb{R}^{2 \times 2}$ . Let  $\alpha_K$  be scaling factor defined as

$$\alpha_K = \min\{b_0^{-1/2}, \epsilon^{-1/2} \cdot h_{\min}^K\}. \quad (3.3.1.1)$$

We represent triangles by  $K$  or  $K'$  or  $K_i$ , and its edges by  $E$ . Further, define its height over edge  $E$  as

$$h_{E,K} = 2 \frac{|K|}{|E|},$$

where  $|K|$  represents area of triangle  $K$ . Let  $w_E$  be the bounded domain formed by using two triangles having common edge  $E$  and  $w_K$  to be the domain consisting of triangle  $K$  and its edge neighboring triangles. Let

$$Pe_{w_K} = \max_{K' \subset w_K} Pe_{K'},$$

be mesh Peclet number defined on the domain  $w_K$  where  $Pe_K$  is discussed in (3.2.7).

For an interior edge  $E = K_1 \cap K_2$ , define parameters  $h_E = (h_{E,K_1} + h_{E,K_2})/2$ ,  $h_{\min}^E = (h_{\min}^{K_1} + h_{\min}^{K_2})/2$  and  $\alpha_E = (\alpha_{K_1} + \alpha_{K_2})/2$ .

For boundary edge  $E \subset \partial K \cap \partial \Omega$ , we define  $h_E = h_{E,K}$ ,  $h_{\min}^E = h_{\min}^K$  and  $\alpha_E = \alpha_K$ .

Since the mesh considered is assumed to be shape-regular and admissible, along with these requirements, we take

$$h_{i,K} \sim h_{i,K'} \quad \forall K, K' \text{ with } K \cap K' \neq \emptyset, i=1,2.$$

and number of triangles with node  $y_j$  is bounded uniformly.

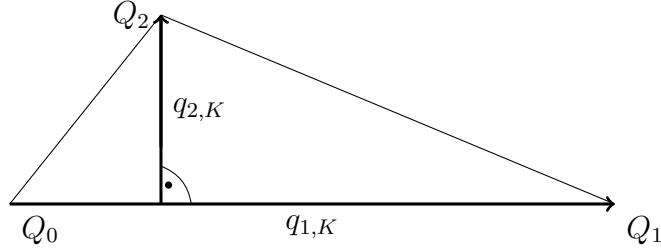


Figure 3.2: Triangle K

### 3.3.2 Interpolation

To derive reliable error upper bounds, we discuss a suitable matching function[111, 113] to estimate alignment of anisotropic mesh  $\Gamma_h$  and anisotropic function.

**Definition 1: (Matching function)** Let  $u \in H^1(\Omega)$  and  $\Gamma_h \in F$  be triangulation of

$\Omega$ . Here  $M_1: H^1(\Omega) \times F \rightarrow \mathbb{R}$  is defined as

$$M_1(u, \Gamma_h) := \left( \sum_{K \in \Gamma_h} (h_{\min}^K)^{-2} \cdot \|C_K^T \nabla u\|_K^2 \right)^{1/2} / \|\nabla u\|, \quad (3.3.2.1)$$

where  $C_K \in \mathbb{R}^{2 \times 2}$  has been defined previously.

We can easily verify that  $M_1(u, \Gamma_h) \sim 1$  for anisotropic meshes suitably aligned with anisotropic function  $u$ .

In order to derive reliable error estimates in energy norm, Clément interpolation operator [44]  $R_C: H_0^1(\Omega) \mapsto V_0^h$  has been considered which is defined as

$$R_C v := \sum_{a_j \in N_I} (P_j v)(a_j) \cdot \phi_j,$$

where  $N_I$  represents set of all inner nodes of the considered triangulation.

**Lemma 1:** Let  $u \in H_0^1(\Omega)$  and  $\alpha_K$  be the scaling factor as discussed in (3.3.1.1).

Then the Clément interpolation operator  $R_C: H_0^1(\Omega) \mapsto V_0^h$  satisfies

$$\sum_{K \in \Gamma_h} \alpha_K^{-2} \cdot \|u - R_C u\|_K^2 \lesssim M_1(u, \Gamma_h)^2 \cdot \|u\|^2, \quad (3.3.2.2)$$

$$\epsilon^{1/2} \sum_{E \subset \Omega \setminus \partial \Omega_D} \alpha_E^{-1} \cdot \|u - R_C u\|_E^2 \lesssim M_1(u, \Gamma_h)^2 \cdot \|u\|^2. \quad (3.3.2.3)$$

**Proof:** The proof of the Lemma has been discussed in [112].

### 3.4 Residual error estimates

In this Section, firstly we discuss exact and approximate residuals. Further, we will develop reliable error upper bounds for Hughes stabilized SUPG finite element solution on anisotropic meshes. It is shown that the error bounds obtained depend on anisotropic interpolation.

**Exact residuals:** We define exact element residual  $R_K$  and exact edge residual  $R_E$  as:

$$R_K = f - (-\epsilon \Delta u_h + \mathbf{a} \cdot \nabla u_h + b u_h) \quad \text{on} \quad K.$$

$$R_E(x) = \begin{cases} \epsilon \cdot \lim_{s \rightarrow +0} [\partial_{n_E} u_h(x + sn_E) - \partial_{n_E} u_h(x - sn_E)] & \text{if } E \subset \Omega \setminus \partial\Omega, \\ g - \epsilon \partial_n u_h & \text{if } E \subset \partial\Omega_N, \\ 0 & \text{if } E \subset \partial\Omega_D, \end{cases}$$

where  $n_E \perp E \subset \Omega \setminus \partial\Omega$  is unitary normal vector and  $n \perp E \subset \partial\Omega_N$  is outer unitary normal vector.

**Approximate residuals:** Let  $Q$  be approximation operator used to approximate the element residuals and the face residuals i.e.

$$\begin{aligned} r_K &= Q(R_K) \in P^0(K) \quad \forall K \in \Gamma_h, \\ r_E &= Q(R_E) \in P^0(E) \quad \forall E, \end{aligned}$$

where we have denoted approximate element residual by  $r_K$  and the (approximate) face residual by  $r_E$ . Since the numerical solution  $u_h$  is linear, thus

$$r_E = R_E \quad \forall E \subset \Omega \setminus \partial\Omega_N.$$

**Definition 2: (Residual error estimator):** Residual error estimator  $\eta_K$  and the approximation term  $\zeta_K$  over triangle  $K$  are defined as

$$\begin{aligned} \eta_K^2 &= a_K^2 \cdot \|r_K\|_K^2 + \epsilon^{-1/2} \cdot \alpha_K \cdot \sum_{E \subset \partial K \setminus \partial\Omega_D} \|r_E\|_E^2, \\ \zeta_K^2 &= a_K^2 \cdot \|r_K - R_K\|_{w_K}^2 + \epsilon^{-1/2} \cdot \alpha_K \cdot \sum_{E \subset \partial K \cap \partial\Omega_N} \|r_E - R_E\|_E^2, \end{aligned}$$

where  $\alpha_K$  be scaling factor and  $a_K = 3\alpha_K$ . Global error estimators are defined as

$$\eta^2 = \sum_{K \in \Gamma_h} \eta_K^2 \quad \text{and} \quad \zeta^2 = \sum_{K \in \Gamma_h} \zeta_K^2.$$

**Theorem (Residual error estimation):** Let  $v \in H_0^1(\Omega)$  be exact solution and  $v_h \in V_0^h$  be Hughes stabilized SUPG solution. Then the global error in energy norm is bounded above by

$$\begin{aligned} |||v - v_h||| &\lesssim C \left[ \left( \sum_{K \in \Gamma_h} a_K^2 (\|r_K - R_K\|_K^2 + \|r_K\|_K^2) \right)^{1/2} \right. \\ &\quad \left. + \left( \sum_{E \subset \partial K \setminus \partial\Omega_D} \epsilon^{-1/2} \alpha_E (\|r_E - R_E\|_E^2 + \|r_E\|_E^2) \right)^{1/2} \right]. \end{aligned}$$

**Proof:** We know that  $\mathbf{B}(v, v) \geq |||v|||^2 \quad \forall v \in H_0^1(\Omega)$ .

Using the above result, we get

$$|||v - v_h||| \leq \frac{\mathbf{B}_{\rho, \sigma}(v - v_h, v - v_h)}{|||v - v_h|||} = \frac{\mathbf{B}_{\rho, \sigma}(v - v_h, u)}{|||u|||}.$$

where  $u = v - v_h$ . Introducing *Clément* interpolation operator  $R_C$ , we can write the bilinear form  $B_{\rho, \sigma}(\cdot, \cdot)$  as

$$\mathbf{B}_{\rho, \sigma}(v - v_h, u) = \mathbf{B}_{\rho, \sigma}(v - v_h, u - R_C u) + \mathbf{B}_{\rho, \sigma}(v - v_h, R_C u). \quad (3.4.1)$$

Now, using the error equation and integration by parts, we have

$$\mathbf{B}_{\rho, \sigma}(v - v_h, w) = \sum_{K \in \Gamma_h} (R_K, w)_K + \sum_{E \subset \Omega \setminus \partial \Omega_D} (R_E, w)_E \quad \forall w \in H_0^1(\Omega). \quad (3.4.2)$$

Using Eq. (3.4.2), the middle term of Eq. (3.4.1) can be written as

$$\mathbf{B}_{\rho, \sigma}(v - v_h, u - R_C u) = \sum_{K \in \Gamma_h} (R_K, u - R_C u)_K + \sum_{E \subset \Omega \setminus \partial \Omega_D} (R_E, u - R_C u)_E. \quad (3.4.3)$$

Using Cauchy Schwarz inequality, we get

$$\begin{aligned} \sum_{K \in \Gamma_h} (R_K, u - R_C u)_K &\leq \left( \sum_{K \in \Gamma_h} \alpha_K^2 \|R_K\|_K^2 \right)^{1/2} \cdot \left( \sum_{K \in \Gamma_h} \alpha_K^{-2} \|u - R_C u\|_K^2 \right)^{1/2}, \\ \sum_{E \subset \Omega \setminus \partial \Omega_D} (R_E, u - R_C u)_E &\leq \left( \sum_{E \subset \Omega \setminus \partial \Omega_D} \epsilon^{-1/2} \alpha_E \|R_E\|_E^2 \right)^{1/2} \cdot \left( \sum_{E \subset \Omega \setminus \partial \Omega_D} \epsilon^{1/2} \alpha_E^{-1} \|u - R_C u\|_E^2 \right)^{1/2}. \end{aligned}$$

Further, using Lemma 1, we get

$$\begin{aligned} \sum_{K \in \Gamma_h} (R_K, u - R_C u)_K &\lesssim \left( \sum_{K \in \Gamma_h} \alpha_K^2 \|R_K\|_K^2 \right)^{1/2} C |||u|||, \\ \sum_{E \subset \Omega \setminus \partial \Omega_D} (R_E, u - R_C u)_E &\lesssim \left( \sum_{E \subset \Omega \setminus \partial \Omega_D} \epsilon^{-1/2} \alpha_E \|R_E\|_E^2 \right)^{1/2} C |||u|||. \end{aligned}$$

Therefore, the term  $\mathbf{B}_{\rho, \sigma}(v - v_h, u - R_C u)$  is bounded above by

$$\mathbf{B}_{\rho, \sigma}(v - v_h, u - R_C u) \lesssim \left[ \left( \sum_{K \in \Gamma_h} \alpha_K^2 \|R_K\|_K^2 \right)^{1/2} + \left( \sum_{E \subset \Omega \setminus \partial \Omega_D} \epsilon^{-1/2} \alpha_E \|R_E\|_E^2 \right)^{1/2} \right] C |||u|||. \quad (3.4.4)$$

From Eq.(3.2.1.7) and Eq.(3.3.1.1), we have

$$\|\nabla u_h\|_K \lesssim \min\{(h_{\min}^K)^{-1}b_0^{-1/2}, \epsilon^{-1/2}\} \|u_h\|_K = (h_{\min}^K)^{-1}\alpha_K \|u_h\|_K \text{ for } u_h \in V_0^h.$$

Next, we will find the bounds on the second term  $\mathbf{B}_{\rho,\sigma}(v - v_h, R_C u)$  of Eq. (3.4.1).

$$\begin{aligned} \mathbf{B}_{\rho,\sigma}(v - v_h, R_C u) &= \langle \epsilon \nabla v, \nabla R_C u \rangle + \langle \mathbf{a} \cdot \nabla v, R_C u \rangle + \langle bv, R_C u \rangle \\ &\quad - [\langle \epsilon \nabla v_h, \nabla R_C u \rangle + \langle \mathbf{a} \cdot \nabla v_h, R_C u \rangle + \langle bv_h, R_C u \rangle \\ &\quad + \sum_K \rho_K(R_K, \mathbf{a} \cdot \nabla R_C u) + \sum_K \sigma_K(R_K, \mathbf{a}_h \cdot \nabla R_C u)]. \end{aligned}$$

Using the standard scaling results and Galerkin orthogonality property, the above equation can be written as

$$\begin{aligned} \mathbf{B}_{\rho,\sigma}(v - v_h, R_C u) &= - \sum_K \rho_K(R_K, \mathbf{a} \cdot \nabla R_C u) - \sum_K \sigma_K(R_K, \mathbf{a}_h \cdot \nabla R_C u) \\ &\leq \sum_{K \in \Gamma_h} \rho_K \|R_K\|_K \|\mathbf{a}\|_{\infty, K} \|\nabla R_C u\|_K \\ &\quad + \sum_{K \in \Gamma_h} \sigma_K \|R_K\|_K \|\mathbf{a}_h\|_{\infty, K} \|\nabla R_C u\|_K \\ &\leq \sum_{K \in \Gamma_h} \rho_K \|R_K\|_K \|\mathbf{a}\|_{\infty, K} (h_{\min}^K)^{-1} \alpha_K \|R_C u\|_K \\ &\quad + \sum_{K \in \Gamma_h} \sigma_K \|R_K\|_K \|\mathbf{a}_h\|_{\infty, K} (h_{\min}^K)^{-1} \alpha_K \|R_C u\|_K. \end{aligned}$$

We know that for *Clément* operator [111],

$$\|R_C u\| \lesssim C \|u\| \quad \forall u \in H_0^1(\Omega).$$

Thus, we have

$$\begin{aligned} \mathbf{B}_{\rho,\sigma}(v - v_h, R_C u) &\leq \left( \sum_{K \in \Gamma_h} \rho_K^2 \|R_K\|_K^2 \|\mathbf{a}\|_{\infty, K}^2 (h_{\min}^K)^{-2} \alpha_K^2 \right)^{1/2} C \|u\| \\ &\quad + \left( \sum_{K \in \Gamma_h} \sigma_K^2 \|R_K\|_K^2 \|\mathbf{a}_h\|_{\infty, K}^2 (h_{\min}^K)^{-2} \alpha_K^2 \right)^{1/2} C \|u\|. \end{aligned}$$

It may be noted that the effect of nonlinear term in the  $L_\infty$  norm will be bounded by that of the term  $\|\mathbf{a}\|_\infty$  as shown below i.e.

$$\begin{aligned}\mathbf{a}_h &= \frac{(\mathbf{a} \cdot \nabla \mathbf{u}_h) \nabla \mathbf{u}_h}{|\nabla \mathbf{u}_h|^2}, \quad |\nabla \mathbf{u}_h| \neq 0 \\ \mathbf{a}_h &\leq \frac{\|\mathbf{a}\| \cdot \|\nabla \mathbf{u}_h\| \|\nabla \mathbf{u}_h\|}{|\nabla \mathbf{u}_h|^2} \quad (\text{Using Cauchy - Schwarz inequality}) \\ \|\mathbf{a}_h\| &\leq \frac{\|\mathbf{a}\| \cdot \|\nabla \mathbf{u}_h\| \|\nabla \mathbf{u}_h\|}{|\nabla \mathbf{u}_h|^2} \\ &\preceq \|\mathbf{a}\|\end{aligned}$$

Since,  $\mathbf{a}$ , the convection coefficient, is assumed to be smooth in the domain under consideration, it is bounded above. Hence, the nonlinear term  $\|\mathbf{a}_h\|_{\infty, K}$  is taken as bounded above by some constant and is absorbed in the constant term.

We know that

$$\begin{aligned}\rho_K &\lesssim h_{min}^K / \|\mathbf{a}\|_{\infty, K} \quad \forall K \in \Gamma_h, \\ \sigma_K &\lesssim h_{min}^K / \|\mathbf{a}_h\|_{\infty, K} \quad \forall K \in \Gamma_h.\end{aligned}$$

Therefore,

$$\begin{aligned}\mathbf{B}_{\rho, \sigma}(v - v_h, R_C u) &\lesssim \left[ \left( \sum_{K \in \Gamma_h} \alpha_K^2 \|R_K\|_K^2 \right)^{1/2} + \left( \sum_{K \in \Gamma_h} \alpha_K^2 \|R_K\|_K^2 \right)^{1/2} \right] C \|u\|. \\ &\quad (M_1(u, \Gamma_h) \approx C) \quad (3.4.5) \\ &\lesssim 2 \left( \sum_{K \in \Gamma_h} \alpha_K^2 \|R_K\|_K^2 \right)^{1/2} C \|u\|.\end{aligned}$$

Since

$$\|v - v_h\| \leq \frac{\mathbf{B}_{\rho, \sigma}(v - v_h, u)}{\|u\|},$$

using Eq. (3.4.4) and Eq. (3.4.5) in Eq. (3.4.1), we get

$$\|v - v_h\| \lesssim \left[ 3 \left( \sum_{K \in \Gamma_h} \alpha_K^2 \|R_K\|_K^2 \right)^{1/2} + \left( \sum_{E \subset \Omega \setminus \partial \Omega_D} \epsilon^{-1/2} \alpha_E \|R_E\|_E^2 \right)^{1/2} \right] C. \quad (3.4.6)$$

Using triangle inequalities,

$$\| R_K \|_K^2 \leq \| r_K - R_K \|_K^2 + \| r_K \|_K^2,$$

and

$$\| R_E \|_E^2 \leq \| r_E - R_E \|_E^2 + \| r_E \|_E^2,$$

we get

$$\begin{aligned} \| \|v - v_h\| \| \lesssim C & \left[ \left( \sum_{K \in \Gamma_h} a_K^2 (\|r_K - R_K\|_K^2 + \|r_K\|_K^2) \right)^{1/2} \right. \\ & \left. + \left( \sum_{E \subset \partial K \setminus \partial \Omega_D} \epsilon^{-1/2} \alpha_E (\|r_E - R_E\|_E^2 + \|r_E\|_E^2) \right)^{1/2} \right]. \end{aligned}$$

### 3.5 Adaptive refinement strategy

In this Section, an adaptive refinement strategy has been developed based on the proposed a posteriori error estimates. The following adaptive refinement algorithm is proposed:

1. Firstly, the whole domain is discretized using triangular elements. Triangulation is done based on red refinement.
2. The problem is to be solved numerically using the proposed scheme discussed in Section 3.2.
3. In the third step, over each element  $K$ , the residual error estimates  $\eta_K$  are to be evaluated as defined in Section 3.4.
4. All those elements  $\{K_{e_i}\}_{e_i=1}^M$  satisfying  $\eta_{K_{e_i}} > C \max_{L'} \eta_{L'}$ , where  $C$  is a user chosen constant from  $(0,1)$ , are to be marked for refinement.
5. These marked elements are to be refined using green refinement procedure.
6. In the next step, all the elements having hanging nodes are also to be refined in order to obtain continuous solution.

7. The problem is again solved on the new refined mesh.
8. This process of grid refinement is to be repeated until the numerical solution is computed upto a given desired precision.

### 3.6 Numerical results and discussion

In the present Section, numerical tests have been performed to check the efficiency and robustness of the developed adaptive refinement strategy.

**Example 1:** Consider the following singularly perturbed convection-diffusion problem:

$$\begin{aligned} -\nabla \cdot \epsilon \nabla u + 2u_x + 3u_y + u &= f \quad \text{in } \Omega = (0, 1)^2, \\ u &= 0 \quad \text{on } \partial\Omega. \end{aligned}$$

The right-hand side function  $f$  is so chosen to satisfy the exact solution

$$u = \sin(x)(1 - e^{-2(1-x)/\epsilon})y^2(1 - e^{-3(1-y)/\epsilon}).$$

The solution of the above problem exhibits exponential boundary layers along the lines  $x = 1$  and  $y = 1$ . For adaptive refinement, anisotropic triangular mesh have been taken into consideration. In Fig. 3.3, we present portion of adaptive triangular mesh for  $\epsilon = 2^{-3}$  with different degrees of freedom. Fig. 3.4 presents adaptive refined meshes for  $\epsilon = 2^{-5}$  with different degrees of freedoms. In Figs. 3.5 and 3.6, numerical solutions obtained using the proposed refinement algorithm for different values of the singular perturbation parameter  $\epsilon = 2^{-3}$  and  $\epsilon = 2^{-5}$  have been plotted. It can be easily seen that even very sharp boundary layers have been efficiently captured using the proposed refinement algorithm and scheme. From the solution plots, it can also be observed that the problem is very sensitive to the singular perturbation parameter  $\epsilon$  i.e. even for  $\epsilon = 2^{-5}$ , very sharp boundary layers appear in the solution. Since the mesh refinement is carried out only in the part of the domain wherein it is required

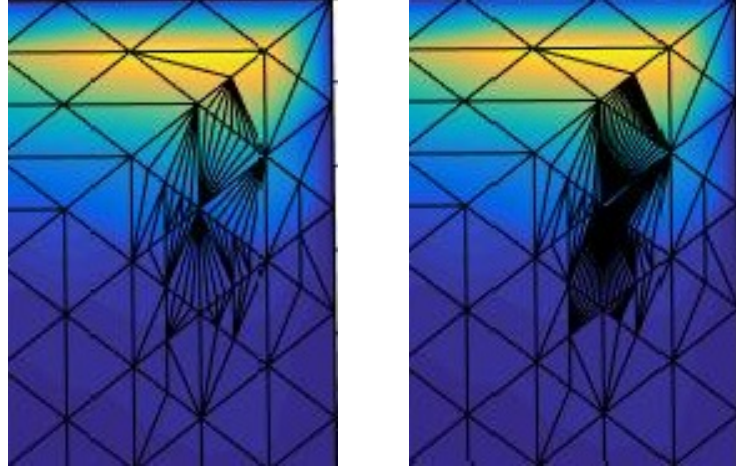


Figure 3.3: Portion of adaptive mesh for  $\epsilon = 2^{-3}$  with  $\text{DOF} = 187,224$

rather than refining the mesh throughout the domain as can be seen in Figs. 3.3 and 3.4, therefore, the same accuracy is attained with less number of degrees of freedoms making the proposed scheme computationally very effective. In Fig. 3.7, energy norm errors for  $\epsilon = 2^{-5}$  have been presented. The behavior of effectivity index  $\psi = \frac{\|v-v_h\|}{\text{ErrorEstimator}}$  is shown in Fig. 3.8.

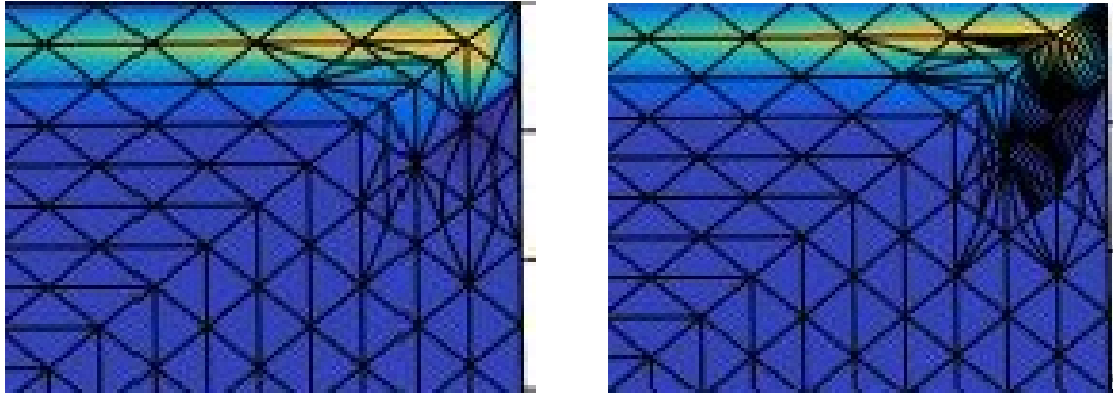


Figure 3.4: Portion of adaptive mesh for  $\epsilon = 2^{-5}$  with  $\text{DOF} = 559,587$

### 3.7 Conclusion

In this Chapter, an adaptive numerical strategy has been proposed for two-dimensional singularly perturbed convection-diffusion problem. The problem under consideration

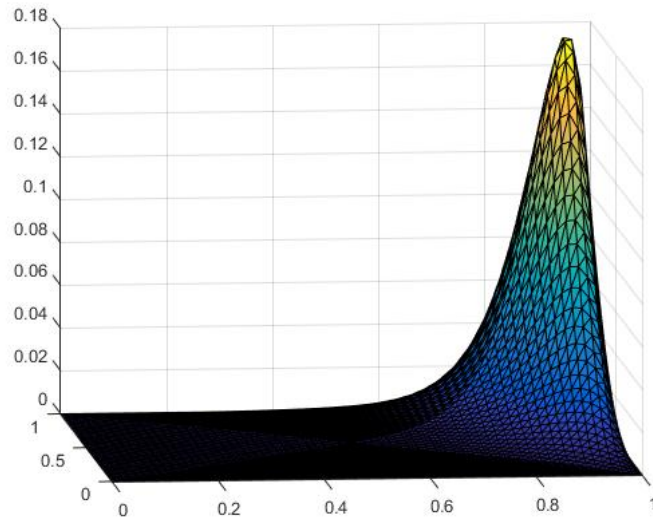


Figure 3.5: Numerical Solution Profile for  $\epsilon = 2^{-3}$

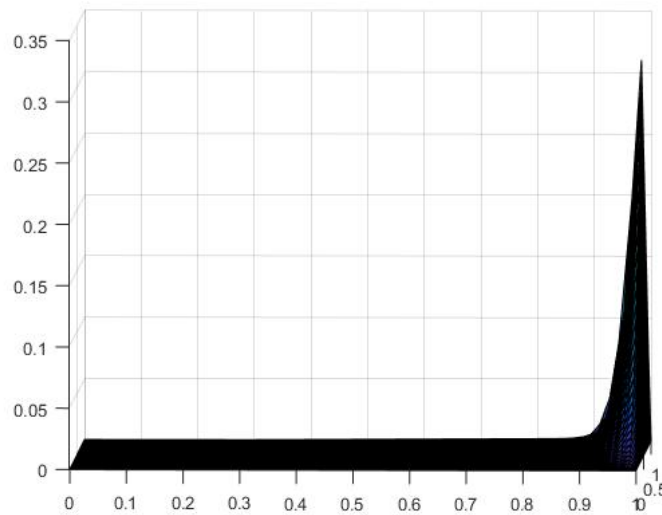


Figure 3.6: Numerical Solution Profile for  $\epsilon = 2^{-5}$

has been solved using Hughes stabilization technique together with SUPG finite element method. The domain discretization has been carried out based on anisotropic triangular meshes. Further, reliable a posteriori error estimates in energy norm have been developed. An adaptive mesh refinement strategy has been proposed based on derived error estimates. Numerical results validate the proposed adaptive refinement strategy in capturing the sharp boundary layers arising in the solution as  $\epsilon \rightarrow 0$ .

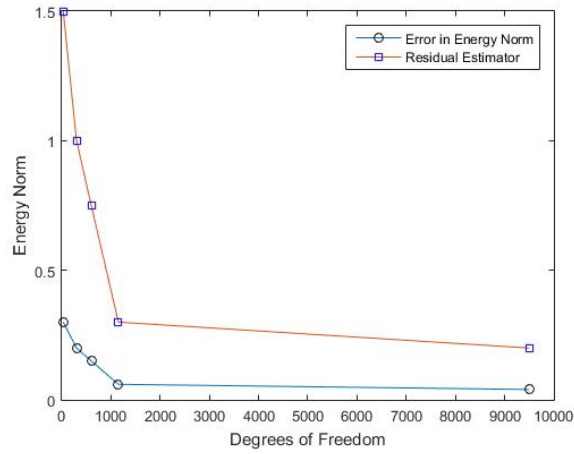


Figure 3.7: Error  $\|v - v_h\|$  and Error estimator for  $\epsilon = 2^{-5}$

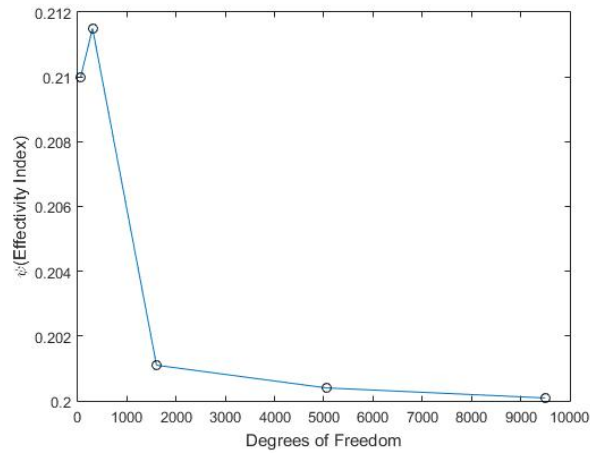


Figure 3.8:  $\psi$  (Effectivity Index) for  $\epsilon = 2^{-5}$

In the next Chapter, the proposed scheme has been extended for three-dimensional singularly perturbed convection-diffusion problems.

# A posteriori error estimates for Hughes stabilized SUPG method for three-dimensional singularly perturbed problems

---

## 4.1 Introduction

Many important mathematical models governing various physical phenomena occurring during the analysis of biological systems, heat transfer process, mass transfer process, etc., are represented by partial differential equations [160, 172]. Very few researchers have developed finite element strategies for simulating three-dimensional partial differential equations. To name a few, Branco et al.[25] proposed three-dimensional finite element technique to analyse the shape evolution of fatigue cracks. Numerical tests have been performed and it has been shown that the numerical results agree with the experimental findings. Mola et al.[136] developed Streamline upwind Petrov-Galerkin (SUPG) technique for approximating unsteady three-dimensional non-linear water waves arising due to ship hull advancing in water based on semi-Lagrangian framework. SUPG projection has been considered to recover accurate estimates of position vector and potential gradients on free surface. The proposed

technique results in stabilization of the transport dominated terms and robust adaptation of the spatial discretization on unstructured quadrilateral grids. Zhai et al.[203] analysed three-dimensional time fractional convection-diffusion equation by proposing an implicit compact finite difference scheme which uses fourth-order Padé approximation for spatial discretization and central difference scheme for time discretization. Mohanty and Setia[133] developed high order compact finite difference scheme for approximating three-dimensional quasi-linear elliptic partial differential equation. In the present Chapter, we will focus on proposing the Hughes stabilized SUPG finite element technique for solving the singularly perturbed problems.

Consider the three-dimensional SPP given by

$$-\nabla \cdot \epsilon \nabla u + \mathbf{b} \cdot \nabla u + cu = f \quad \text{in } \Gamma, \quad (4.1.1)$$

$$u = 0 \quad \text{on } \partial\Gamma_D, \quad (4.1.2)$$

$$\frac{\partial u}{\partial n} = g \quad \text{on } \partial\Gamma_N, \quad (4.1.3)$$

where  $\Gamma \subset \mathbb{R}^3$  is a bounded domain with Lipschitz-continuous boundary  $\partial\Gamma$  and  $\epsilon$  is singular perturbation parameter satisfying  $0 < \epsilon \ll 1$ . We assume that  $\partial\Gamma = \partial\Gamma_D \cup \partial\Gamma_N$  with  $\partial\Gamma_D \cap \partial\Gamma_N = \emptyset$ , and  $\mathbf{b}$ ,  $c$  and  $f$  are analytic.  $\partial\Gamma_D$  and  $\partial\Gamma_N$  represent the Dirichlet and Neumann boundaries of the domain respectively.

The considered problem is comprised of two basic phenomena-convection and diffusion. For the case when  $\epsilon \ll \|\mathbf{b}\|$ , the above problem becomes convection dominant in nature. This results in singularities, such as shocks, interior and boundary layers which deteriorate the accuracy of numerical solutions obtained by various numerical schemes. Therefore, it becomes essential to obtain some reliable and efficient error estimates for the computed numerical solution to rely on.

Broadly, error estimates are of two different types, namely, a priori error estimates

and a posteriori error estimates. It is seen that a priori error estimates provide crude information only about the asymptotic behavior of the solution and involves regularity conditions which are very difficult to achieve in case of singularities whereas a posteriori error estimates provide quantitative information of the computed numerical solution. Therefore, it is more expected to derive some reliable a posteriori error estimates based on the data of the problem and the computed numerical solution.

Stephansen[63] proposed robust a posteriori error estimates for convection-diffusion-reaction problems based on weighted interior-penalty discontinuous Galerkin methods. Lazarov[116] derived residual based a posteriori estimates for convection-diffusion-reaction equations using finite volume element approximations. Carstensen et al.[31] proposed residual-type explicit error estimators and averaging techniques for steady convection-diffusion-reaction problems using finite volume method. Further, the authors proposed adaptive mesh refining strategy and considered numerical examples to test the theoretical findings.

It has been seen that Streamline upwind/Petrov-Galerkin (SUPG) method provides good approximate solution in the region where there is no sharp change in the solution but fails badly in the small subregions of sharp boundary layers appearing in the sol. of singularly perturbed problems. It has been observed that occurrence of these nonphysical oscillations in the region of sharp boundary layers in discrete solution of SUPG method is based on the fact that this scheme is not monotonicity preserving. To overcome this hurdle, in the present work, an effort has been made by using Hughes stabilization strategy [90] alongwith Streamline upwind/Petrov-Galerkin (SUPG) method. This corresponds to addition of one more term in the SUPG discretization of the considered convection-diffusion problem. A posteriori error estimates have been obtained for the developed technique.

The Chapter is organised as follows:

In Section 4.2, some notations and standard norms have been discussed. Then the

variational formulation and Hughes stabilized Streamline upwind finite element approximation of the continuous problem have been discussed. Section 4.3 deals with some important tools which are essential for deriving reliable error estimates. In Section 4.4, residual based a posteriori error estimates have been derived on anisotropic meshes. In the last Section 4.5, concluding remarks have been made.

## 4.2 Hughes stabilized SUPG technique

Let  $W^{1,\infty}(\Gamma)$  and  $L^\infty(\Gamma)$  denote the usual Sobolev space and Lebesgue space respectively. We will use the notation  $(\cdot, \cdot)$  for inner product  $(\cdot, \cdot)_\Gamma$ .

We assume that  $-\frac{1}{2}\nabla \cdot \mathbf{b} + c \geq c_0 > 0$  on  $\bar{\Gamma}$ .

For any open and bounded subset  $T \subset \bar{\Gamma}$ , let  $H^1(T)$  be the standard Sobolev space.

Let

$$V_0 = \{w \in H^1(\Gamma), w = 0 \text{ on } \partial\Gamma_D\}.$$

Since, our objective is to bound the global error  $w - w_h$  in energy norm, so we define the energy norm on any bounded subset  $T \subset \bar{\Gamma}$  as

$$|||w|||_T^2 = \epsilon \cdot \|\nabla w\|_T^2 + c_0 \cdot \|w\|_T^2. \quad (4.2.1)$$

The finite element weak formulation of (4.1.1) is given as:

Find  $v \in H^1(\Gamma)$  such that

$$B(v, w) = \langle F, w \rangle, \quad (4.2.2)$$

where

$$\begin{aligned} B(v, w) &= \epsilon(\nabla v, \nabla w) + (\mathbf{b} \cdot \nabla v, w) + (cv, w) \\ \langle F, w \rangle &= (f, w) + (g, w)_{\partial\Omega_N}, \quad \forall w \in V_0. \end{aligned} \quad (4.2.3)$$

The existence and uniqueness of solution of above weak formulation (4.2.2) can be confirmed using the Lax Milgram lemma. Let  $F = \{\Gamma_h\}$  denote the family of triangulations of  $\Gamma$ . Let  $\Gamma_h$  be triangulation of domain  $\Gamma$  consisting of tetrahedrons in

three-dimensions, assuming only admissible and shape-regular triangulation in  $\Gamma_h$ . For any tetrahedron  $T$  with face  $E$ , we define  $n_{T,E} = (n_x, n_y, n_z)$  to be the unit outward normal vector for face  $E$  of the tetrahedron  $T$ . Let  $n_E$  be the normal vector for face  $E$  obtained from  $n_{T,E}$  by fixing any of two normal components.

### 4.2.1 SUPG method

We define  $V^h = \{w_h \in H^1 : w_h|_T \in P_1(T), \forall T \in \Gamma_h\}$ , where  $P_1(T)$  is the space of linear polynomials over tetrahedron  $T$  and  $V_0^h = \{w_h \in V^h : w_h|_{\partial\Gamma_D} = 0\}$ . The SUPG method[27] for problem (4.1.1) is given by

Find  $v_h \in V^h$  such that

$$\mathbf{B}_\rho(v_h, w_h) = \langle F, w_h \rangle \quad \forall w_h \in V_0^h, \quad (4.2.1.1)$$

where  $\mathbf{B}_\rho(v_h, w_h) = \mathbf{B}(v_h, w_h) + \langle R_h(v_h), \rho \mathbf{b} \cdot \nabla_h w_h \rangle$  and  $\langle R_h(v_h), \rho \mathbf{b} \cdot \nabla_h w_h \rangle = \sum_{T \in \Gamma_h} \rho_T (-\epsilon \Delta_h v_h + \mathbf{b} \cdot \nabla_h v_h + c v_h - f, \mathbf{b} \cdot \nabla_h w_h)_T$ ,  $\rho$  is nonnegative stabilization parameter,  $\mathbf{B}(v, w)$  and  $\langle F, w \rangle$  are defined in (4.2.3).

### 4.2.2 Hughes stabilized SUPG technique

As is well known that convection dominated problems exhibit nonphysical oscillations at layers as  $\epsilon$  decreases, the solution of singularly perturbed problem displays boundary layers. Since the Streamline upwind/Petrov-Galerkin (SUPG) method results in good approximate solution in the region where there is no sharp change in the solution but fails drastically in the subregions of sharp boundary layers, in the trial to overcome this hurdle, we propose Hughes stabilization technique [96] to SUPG method. It results in an addition of the term  $\langle R_h(v_h), \sigma \mathbf{b}_h \cdot \nabla_h w_h \rangle$  in the SUPG finite element discretization of the convection-diffusion equation where

$$\mathbf{b}_h = \begin{cases} \frac{(\mathbf{b} \cdot \nabla_h v_h) \nabla_h v_h}{|\nabla_h v_h|^2}, & \text{if } |\nabla_h v_h| \neq 0, \\ 0, & \text{if } |\nabla_h v_h| = 0, \end{cases} \quad (4.2.2.1)$$

and  $\sigma$  is nonnegative stabilization parameter. This additional term increases the robustness of SUPG method in the boundary layer region by controlling oscillations.

Using Hughes stabilization technique to SUPG finite element method, Eq.(4.1.1) is discretized as follows:

Find  $v_h \in V^h$  such that

$$B_{\rho,\sigma}(v_h, w_h) = \langle F, w_h \rangle \quad \forall w_h \in V_0^h. \quad (4.2.2.2)$$

Here  $B_{\rho,\sigma}(v_h, w_h) = \mathbf{B}(v_h, w_h) + \langle R_h(v_h), \rho \mathbf{b} \cdot \nabla_h w_h \rangle + \langle R_h(v_h), \sigma \mathbf{b}_h \cdot \nabla_h w_h \rangle$   
and  $\langle R_h(v_h), \sigma \mathbf{b}_h \cdot \nabla_h w_h \rangle = \sum_{T \in \Gamma_h} \sigma_T (-\epsilon \Delta_h v_h + \mathbf{b} \cdot \nabla_h v_h + c v_h - f, \mathbf{b}_h \cdot \nabla_h w_h)_T$ .

Let  $\rho_T$  and  $\sigma_T$  be stabilization parameters over each element  $T$ . The existence and uniqueness of the finite element solution  $v_h$  obtained using SUPG finite element discretization has been proved by Roos et al.[169]. The stabilization parameter  $\rho_T$  satisfies

$$0 \leq \rho_T \leq \frac{1}{2} \min\{c_0 \|c\|_{\infty, T}^{-2}, (h_{\min}^T)^2 \epsilon^{-1} \nu^{-2}\}, \quad (4.2.2.3)$$

where  $h_{\min}^T$  is minimal length of element  $T$  and the constant  $\nu$  satisfies the inequality

$$\|\nabla \cdot \nabla v_h\|_T \leq \nu (h_{\min}^T)^{-1} \|\nabla v_h\|_T \quad \forall v_h \in V_0^h. \quad (4.2.2.4)$$

It can be observed that  $\nu = 0$  for piecewise linear functions in  $V_0^h$ . Therefore, the above bounds reduces to  $0 \leq \rho_T \leq \frac{c_0}{2} \|c\|_{\infty, T}^{-2}$ . For easiness, we will use  $c \lesssim d$  to denote that there exists a positive constant  $A$  independent of  $c, d, \Gamma_h$  and  $\epsilon$  such that  $c \leq Ad$ . Further, we assume that

$$\rho_T \lesssim h_{\min}^T \|\mathbf{b}\|_{\infty, T}^{-1} \quad \forall T \in \Gamma_h. \quad (4.2.2.5)$$

### 4.3 Some auxiliary tools

Since the considered singularly perturbed problem displays abrupt changes in the solution when Peclet number becomes very large as clear from (4.3.2), in such situations, elements with large aspect ratio i.e. anisotropic meshes are preferred. Therefore, in the present work, anisotropic mesh has been considered for domain discretization. In the present Section, some notations on anisotropic meshes have been discussed which

will be used in later Sections.

**Notations:** Consider an arbitrary tetrahedron  $T \in \Gamma_h$  with  $Q_0Q_1$  as longest edge (see Fig. 4.1). Represent three orthogonal vectors by  $q_{i,T}$  with lengths  $h_{i,T} = |q_{i,T}|$ , where  $q_{1,T}$  is taken along the largest edge. From Fig. 4.1, it can be confirmed that  $h_{1,T} > h_{2,T} \geq h_{3,T}$ . Define  $h_{\min}^T = h_{3,T}$ . These  $q_{i,T}$ 's correspond to three anisotropic directions. Define an orthogonal matrix as  $C_T = (q_{1,T}, q_{2,T}, q_{3,T}) \in \mathbb{R}^{3 \times 3}$ . Let  $\alpha_T$  be scaling factor defined as

$$\alpha_T = \min\{c_0^{-1/2}, \epsilon^{-1/2} \cdot h_{\min}^T\}. \quad (4.3.1)$$

We denote tetrahedron by  $T$  or  $T'$  or  $T_i$ , and its faces by  $E$ . Denote its height over face  $E$  by

$$h_{E,T} = 3 \cdot \frac{|T|}{|E|},$$

where  $|T|$  represents the volume of the tetrahedron and  $|E|$  represents the area of the face  $E$ . Let  $w_E$  be the bounded domain formed by using two tetrahedrons with common face  $E$  and  $w_T$  to be the domain consisting of tetrahedron  $T$  and its face neighbouring tetrahedra. We denote the local mesh Peclet number as

$$Pe_T = \frac{\|\mathbf{b}\|_{\infty, T} h_{\min}^T}{2\epsilon}, \quad (4.3.2)$$

where  $h_{\min}^T$  is minimal length of element  $T$ . Let

$$Pe_{w_T} = \max_{T' \subset w_T} Pe_{T'},$$

be mesh Peclet number on the domain  $w_T$ . For an interior face  $E = T_1 \cap T_2$ , define face based parameters  $h_E = (h_{E,T_1} + h_{E,T_2})/2$ ,  $h_{\min}^E = (h_{\min}^{T_1} + h_{\min}^{T_2})/2$  and  $\alpha_E = (\alpha_{T_1} + \alpha_{T_2})/2$ .

For boundary face  $E \subset \partial T \cap \partial \Gamma$ , we define  $h_E = h_{E,T}$ ,  $h_{\min}^E = h_{\min}^T$  and  $\alpha_E = \alpha_T$ .

We assume

$$h_{i,T} \sim h_{i,T'} \quad \forall T, T' \text{ with } T \cap T' \neq \emptyset, i=1,2,3,$$

and number of tetrahedra with node  $y_j$  is bounded uniformly.

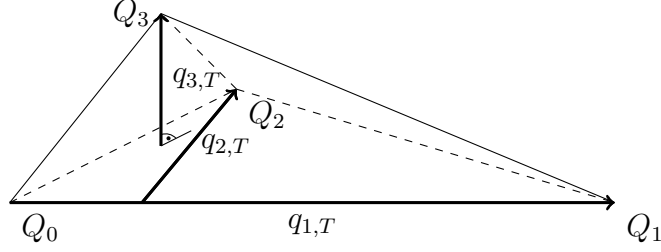


Figure 4.1: Tetrahedron  $T$

## 4.4 Interpolation

Till now, very few researchers have proposed different a posteriori error estimates on anisotropic meshes for three-dimensional singularly perturbed problems. Since the focus is to obtain reliable upper error bounds, therefore, a suitable estimate or function called matching function[111] has been defined to measure alignment of anisotropic mesh  $\Gamma_h$  and anisotropic function.

**Matching function:** Let  $v \in H^1(\Gamma)$  and  $\Gamma_h \in F$  be triangulation of  $\Gamma$ . Then  $M_1: H^1(\Gamma) \times F \rightarrow \mathbb{R}$  is defined as

$$M_1(v, \Gamma_h) := \left( \sum_{T \in \Gamma_h} (h_{\min}^T)^{-2} \cdot \|C_T^T \nabla v\|_T^2 \right)^{1/2} / \|\nabla v\|, \quad (4.4.1)$$

where  $C_T \in \mathbb{R}^{3 \times 3}$  has been defined earlier.

In order to derive reliable error estimates in energy norm, we define Clément interpolation operator  $I_c$ [44] for  $v \in H^1(\Gamma)$ .

**Lemma 1:** Let  $v \in H_0^1(\Gamma)$  and  $\alpha_T$  be the scaling factor defined by (4.3.1). Define Clément interpolation operator  $I_c : H_0^1(\Gamma) \mapsto V_0^h$  as defined in [44, 112]. Then it satisfies

$$\|I_c v\| \lesssim M_1(v, \Gamma_h) \cdot \|v\|, \quad (4.4.2)$$

$$\sum_{T \in \Gamma_h} \alpha_T^{-2} \cdot \|v - I_c v\|_T^2 \lesssim M_1(v, \Gamma_h)^2 \cdot \|v\|^2, \quad (4.4.3)$$

$$\epsilon^{1/2} \sum_{E \subset \Gamma \setminus \partial \Gamma_D} \alpha_E^{-1} \cdot \|v - I_c v\|_E^2 \lesssim M_1(v, \Gamma_h)^2 \cdot \|v\|^2. \quad (4.4.4)$$

**Proof:** The proof of the Lemma has been discussed in [112].

#### 4.4.1 Residual error estimates

In the present Section, first we will discuss exact and approximate residuals. Then, residual error estimator based on residuals has been defined to estimate error in energy norm. Further, reliable error bounds for the proposed scheme Hughes stabilized SUPG finite element method has been proposed on anisotropic meshes.

**Exact residuals:** Let  $R_T$  and  $R_E$  denote the exact element residual and exact face residual over a general tetrahedron element  $T$  respectively and are defined as

$$R_T = f - (-\epsilon \Delta u_h + \mathbf{b} \cdot \nabla u_h + c u_h) \quad \text{on} \quad T,$$

$$R_E(x) = \begin{cases} \lim_{s \rightarrow 0^+} [\partial_{n_E} u_h(x + s n_E) - \partial_{n_E} u_h(x - s n_E)] & \text{if } E \subset \Gamma \setminus \partial \Gamma, \\ g - \partial_n u_h & \text{if } E \subset \partial \Gamma_N, \\ 0 & \text{if } E \subset \partial \Gamma_D, \end{cases}$$

where  $n_E \perp E$  is unitary normal vector for face  $E \subset \Gamma - \Gamma_N$  and  $n \perp E \subset \partial \Gamma_N$  is outer unitary normal vector.

**Approximate residuals:** Let  $Q$  be approximation operator, used to approximate the element residuals and the face residuals i.e.

$$r_T = Q(R_T) \in P^0(T) \quad \forall T \in \Gamma_h,$$

$$r_E = Q(R_E) \in P^0(E) \quad \forall E.$$

where  $r_T$  denotes the approximate element residual and  $r_E$  denotes the approximate face residual. Since the numerical solution  $u_h$  is linear on  $E$ , therefore,

$$r_E = R_E \quad \forall E \subset \Gamma \setminus \partial \Gamma_N.$$

**Residual error estimator:** Residual error estimator  $\eta_T$  and the approximation term  $\zeta_T$  over any tetrahedron  $T$  are defined as

$$\eta_T^2 = a_T^2 \cdot \|r_T\|_T^2 + \epsilon^{-1/2} \cdot \alpha_T \cdot \sum_{E \subset \partial T \setminus \partial \Gamma_D} \|r_E\|_E^2,$$

$$\zeta_T^2 = a_T^2 \cdot \|r_T - R_T\|_{w_T}^2 + \epsilon^{-1/2} \cdot \alpha_T \cdot \sum_{E \subset \partial T \cap \partial \Gamma_N} \|r_E - R_E\|_E^2,$$

where  $\alpha_T$  be scaling factor and  $a_T = 3\alpha_T$ . Global error estimators are defined as

$$\eta^2 = \sum_{T \in \Gamma_h} \eta_T^2 \quad \text{and} \quad \zeta^2 = \sum_{T \in \Gamma_h} \zeta_T^2. \quad (4.4.1.1)$$

Before proposing reliable error upper bounds, we will prove the following two lemmas which will be used in the results to follow:

**Lemma 2:** Let  $v \in H_0^1(\Gamma)$  be exact solution and  $v_h \in V_0^h$  be numerical solution obtained by the proposed scheme. Then the bilinear form  $\mathbf{B}_{\rho,\sigma}(\cdot, \cdot)$  satisfies the bounds

$$\mathbf{B}_{\rho,\sigma}(v - v_h, w - I_c w) \lesssim \left[ \left( \sum_{T \in \Gamma_h} \alpha_T^2 \|R_T\|_T^2 \right)^{1/2} + \left( \sum_{E \subset \Gamma \setminus \partial \Gamma_D} \epsilon^{-1/2} \alpha_E \|R_E\|_E^2 \right)^{1/2} \right] \cdot M_1(w, \Gamma_h) \cdot \|w\|.$$

**Proof:** Using *Clément* interpolation operator  $I_c$ , we can write the bilinear form  $\mathbf{B}_{\rho,\sigma}(\cdot, \cdot)$  as

$$\mathbf{B}_{\rho,\sigma}(v - v_h, w) = \mathbf{B}_{\rho,\sigma}(v - v_h, w - I_c w) + \mathbf{B}_{\rho,\sigma}(v - v_h, I_c w). \quad (4.4.1.2)$$

Now, integrating by parts and using exact element residual  $R_T$  and face residual  $R_E$ , the bilinear form  $\mathbf{B}_{\rho,\sigma}(v - v_h, w)$  can be written as

$$\mathbf{B}_{\rho,\sigma}(v - v_h, w) = \sum_{T \in \Gamma_h} (R_T, w)_T + \sum_{E \subset \Gamma \setminus \partial \Gamma_D} (R_E, w)_E \quad \forall w \in H_0^1(\Gamma).$$

Using the above expression for bilinear form, the middle term of (4.4.1.2) can be expressed as

$$\mathbf{B}_{\rho,\sigma}(v - v_h, w - I_c w) = \sum_{T \in \Gamma_h} (R_T, w - I_c w)_T + \sum_{E \subset \Gamma \setminus \partial \Gamma_D} (R_E, w - I_c w)_E.$$

Using Cauchy Schwarz inequality, we get

$$\begin{aligned} \sum_{T \in \Gamma_h} (R_T, w - I_c w)_T &\leq \left( \left( \sum_{T \in \Gamma_h} \alpha_T^2 \|R_T\|_T^2 \right)^{1/2} \cdot \left( \sum_{T \in \Gamma_h} \alpha_T^{-2} \|w - I_c w\|_T^2 \right)^{1/2} \right), \\ \sum_{E \subset \Gamma \setminus \partial \Gamma_D} (R_E, w - I_c w)_E &\leq \left( \left( \sum_{E \subset \Gamma \setminus \partial \Gamma_D} \epsilon^{-1/2} \alpha_E \|R_E\|_E^2 \right)^{1/2} \cdot \left( \sum_{E \subset \Gamma \setminus \partial \Gamma_D} \epsilon^{1/2} \alpha_E^{-1} \|w - I_c w\|_E^2 \right)^{1/2} \right). \end{aligned}$$

Further, using Lemma 1, we get

$$\begin{aligned} \sum_{T \in \Gamma_h} (R_T, w - I_c w)_T &\lesssim \left( \left( \sum_{T \in \Gamma_h} \alpha_T^2 \|R_T\|_T^2 \right)^{1/2} \cdot M_1(w, \Gamma_h) \right) \cdot \|w\|, \\ \sum_{E \subset \Gamma \setminus \partial \Gamma_D} (R_E, w - I_c w)_E &\lesssim \left( \left( \sum_{E \subset \Gamma \setminus \partial \Gamma_D} \epsilon^{-1/2} \alpha_E \|R_E\|_E^2 \right)^{1/2} \cdot M_1(w, \Gamma_h) \right) \cdot \|w\|. \end{aligned}$$

Therefore, the term  $\mathbf{B}_{\rho, \sigma}(v - v_h, w - I_c w)$  is bounded above by

$$\mathbf{B}_{\rho, \sigma}(v - v_h, w - I_c w) \lesssim \left[ \left( \sum_{T \in \Gamma_h} \alpha_T^2 \|R_T\|_T^2 \right)^{1/2} + \left( \sum_{E \subset \Gamma \setminus \partial \Gamma_D} \epsilon^{-1/2} \alpha_E \|R_E\|_E^2 \right)^{1/2} \right] \cdot M_1(w, \Gamma_h) \cdot \|w\|.$$

**Lemma 3:** Let  $v \in H_0^1(\Gamma)$  be exact solution and  $v_h \in V_0^h$  be the approximate solution. Then the *Clément* interpolation operator  $I_c : H_0^1(\Gamma) \mapsto V_0^h$  satisfies the inequality

$$\mathbf{B}_{\rho, \sigma}(v - v_h, I_c w) \lesssim 2 \left( \sum_{T \in \Gamma_h} \alpha_T^2 \|R_T\|_T^2 \right)^{1/2} \cdot M_1(w, \Gamma_h) \|w\|.$$

**Proof:** For any mesh function  $v_h \in V_0^h$ , using (4.2.2.4) and scaling arguments, we can get

$$\|\nabla v_h\|_T \lesssim (h_{\min}^T)^{-1} \|v_h\|_T.$$

From energy norm def.(4.2.1), we have

$$\|v_h\|_T \leq c_0^{-1/2} \|\nabla v_h\|_T.$$

$$\Rightarrow \|\nabla v_h\|_T \lesssim (h_{\min}^T)^{-1} c_0^{-1/2} \|v_h\|_T. \quad (4.4.1.3)$$

Again, from energy norm, we get

$$\|\nabla v_h\|_T \leq \epsilon^{-1/2} \|v_h\|_T. \quad (4.4.1.4)$$

$$\Rightarrow \|\nabla v_h\|_T \lesssim \min\{(h_{\min}^T)^{-1} c_0^{-1/2}, \epsilon^{-1/2}\} \|v_h\|_T \quad (4.4.1.5)$$

On simplification, inequality (4.4.1.5) reduces to

$$\|\nabla v_h\|_T \lesssim \min\{(h_{\min}^T)^{-1}c_0^{-1/2}, \epsilon^{-1/2}\} \|v_h\|_T = (h_{\min}^T)^{-1}\alpha_T \|v_h\|_T \text{ for } v_h \in V_0^h.$$

(Using Eq.(4.3.1))

$$\begin{aligned} \mathbf{B}_{\rho,\sigma}(v - v_h, I_c w) &= \langle \epsilon \nabla v, \nabla I_c w \rangle + \langle \mathbf{b} \cdot \nabla v, I_c w \rangle + \langle cv, I_c w \rangle \\ &\quad - \{ \langle \epsilon \nabla v_h, \nabla I_c w \rangle + \langle \mathbf{b} \cdot \nabla v_h, I_c w \rangle + \langle cv_h, I_c w \rangle \\ &\quad + \sum_T \rho_T (R_T, \mathbf{b} \cdot \nabla I_c w) + \sum_T \sigma_T (R_T, \mathbf{b}_h \cdot \nabla I_c w) \}. \end{aligned}$$

Now based on the Galerkin orthogonal property and standard scaling results, the above equation can be rewritten as

$$\begin{aligned} \mathbf{B}_{\rho,\sigma}(v - v_h, I_c w) &= - \sum_T \rho_T (R_T, \mathbf{b} \cdot \nabla I_c w) - \sum_T \sigma_T (R_T, \mathbf{b}_h \cdot \nabla I_c w) \\ &\leq \sum_{T \in \Gamma_h} \rho_T \|R_T\|_T \|\mathbf{b}\|_{\infty, T} \|\nabla I_c w\|_T \\ &\quad + \sum_{T \in \Gamma_h} \sigma_T \|R_T\|_T \|\mathbf{b}_h\|_{\infty, T} \|\nabla I_c w\|_T \\ &\leq \sum_{T \in \Gamma_h} \rho_T \|R_T\|_T \|\mathbf{b}\|_{\infty, T} (h_{\min}^T)^{-1} \alpha_T \|I_c w\|_T \\ &\quad + \sum_{T \in \Gamma_h} \sigma_T \|R_T\|_T \|\mathbf{b}_h\|_{\infty, T} (h_{\min}^T)^{-1} \alpha_T \|I_c w\|_T. \end{aligned}$$

Using Lemma 1, we get

$$\|I_c w\| \lesssim M_1(w, \Gamma_h) \cdot \|w\| \quad \forall w \in H_0^1(\Gamma).$$

Thus, we have

$$\mathbf{B}_{\rho,\sigma}(v - v_h, I_c w) \leq \left( \sum_{T \in \Gamma_h} \rho_T^2 \|R_T\|_T^2 \|\mathbf{b}\|_{\infty, T}^2 (h_{\min}^T)^{-2} \alpha_T^2 \right)^{1/2} \cdot M_1(w, \Gamma_h) \cdot \|w\|$$

$$+ \left( \sum_{T \in \Gamma_h} \sigma_T^2 \|R_T\|_T^2 \|\mathbf{b}_h\|_{\infty, T}^2 (h_{\min}^T)^{-2} \alpha_T^2 \right)^{1/2} \cdot M_1(w, \Gamma_h) \cdot |||w|||.$$

It may be noted that the effect of nonlinear term  $\mathbf{b}_h$  in the  $L_\infty$  norm will be bounded by that of the term  $\|\mathbf{b}\|_\infty$  as shown below i.e.

$$\begin{aligned} \mathbf{b}_h &= \frac{(\mathbf{b} \cdot \nabla \mathbf{v}_h) \nabla \mathbf{v}_h}{|\nabla \mathbf{v}_h|^2}, \quad |\nabla \mathbf{v}_h| \neq 0 \\ \mathbf{b}_h &\leq \frac{\|\mathbf{b}\| \|\nabla \mathbf{v}_h\| |\nabla \mathbf{v}_h|}{|\nabla \mathbf{v}_h|^2} \quad \{\text{Using Cauchy-Schwarz inequality}\} \\ \|\mathbf{b}_h\| &\leq \frac{\|\mathbf{b}\| \|\nabla \mathbf{v}_h\| \|\nabla \mathbf{v}_h\|}{|\nabla \mathbf{v}_h|^2} \\ &\preceq \|\mathbf{b}\| \end{aligned}$$

From relation (4.2.2.5), we get

$$\begin{aligned} \rho_T &\lesssim h_{\min}^T / \|\mathbf{b}\|_{\infty, T} \quad \forall T \in \Gamma_h, \\ \sigma_T &\lesssim h_{\min}^T / \|\mathbf{b}_h\|_{\infty, T} \quad \forall T \in \Gamma_h. \end{aligned}$$

Therefore,

$$\begin{aligned} \mathbf{B}_{\rho, \sigma}(v - v_h, I_c w) &\lesssim \left[ \left( \sum_{T \in \Gamma_h} \alpha_T^2 \|R_T\|_T^2 \right)^{1/2} + \left( \sum_{T \in \Gamma_h} \alpha_T^2 \|R_T\|_T^2 \right)^{1/2} \right] \cdot M_1(w, \Gamma_h) \cdot |||w||| \\ &\lesssim 2 \left( \sum_{T \in \Gamma_h} \alpha_T^2 \|R_T\|_T^2 \right)^{1/2} \cdot M_1(w, \Gamma_h) \cdot |||w|||. \end{aligned}$$

**Theorem: (Residual error estimation)** Let  $v \in H_0^1(\Gamma)$  be the exact solution and  $v_h \in V_0^h$  be the Hughes stabilized SUPG finite element solution of (4.1.1)-(4.1.3).

Then the error in energy norm is bounded above globally by

$$|||v - v_h||| \lesssim M_1(v - v_h, \Gamma_h) \cdot [\eta + \zeta].$$

**Proof:** We know that  $\mathbf{B}_{\rho, \sigma}(v, v) \geq |||v|||^2 \quad \forall v \in H_0^1(\Gamma)$ . Using this result, we get

$$|||v - v_h||| \leq \frac{\mathbf{B}_{\rho, \sigma}(v - v_h, w)}{|||v - v_h|||}, \quad (4.4.1.6)$$

where  $w = v - v_h$ . Putting  $a_T = 3\alpha_T$  and using Lemma 2 and Lemma 3 in Eq.(4.4.1.2), the above equation reduces to

$$|||v - v_h||| \lesssim \left[ \left( \sum_{T \in \Gamma_h} a_T^2 \|R_T\|_T^2 \right)^{1/2} + \left( \sum_{E \subset \Gamma \setminus \partial \Gamma_D} \epsilon^{-1/2} \alpha_E \|R_E\|_E^2 \right)^{1/2} \right] \cdot M_1(w, \Gamma_h). \quad (4.4.1.7)$$

Using triangle inequalities

$$\begin{aligned} \|R_T\|_T^2 &\leq \|r_T - R_T\|_T^2 + \|r_T\|_T^2, \\ \|R_E\|_E^2 &\leq \|r_E - R_E\|_E^2 + \|r_E\|_E^2, \end{aligned}$$

Substituting these inequalities in Eq.(4.4.1.7), we get

$$|||v - v_h||| \lesssim M_1(v - v_h, \Gamma_h) \cdot [\eta + \zeta],$$

where  $\eta^2$  and  $\zeta^2$  are defined in Eq.(4.4.1.1).

**Remark:** The adaptive mesh refinement strategy which have been proposed for two-dimensional singularly perturbed problems in Chapter 3 can be extended for the three-dimensional problems in a similar way.

## 4.5 Conclusion

In this Chapter, Hughes stabilization strategy together with SUPG finite element method has been proposed to approximate the solutions of three-dimensional singularly perturbed convection-diffusion problems. The domain has been discretized using anisotropic meshes and residual based a posteriori error estimates in energy norm have been proposed for the proposed scheme. In the next Chapter, some applications of the singularly perturbed problems have been presented and have been solved using the adaptive strategy discussed in the second Chapter.

---

# Applications of singularly perturbed problems

---

## 5.1 Introduction

Singularly perturbed problems occur frequently during the analysis of the biological systems, mass transfer process, etc. In this Chapter, two real-life singularly perturbed model problems governing the travelling wave phenomenon have been considered. For the first problem, we have considered a particular case of the generalized singularly perturbed Burgers-Fisher equation given by

$$u_t + \alpha u^\delta u_x = \epsilon u_{xx} + \beta u(1 - u^\delta), \quad a < x < b, t > 0, \quad (5.1.1)$$

for  $\delta = 1$ , where  $u$  represents traveling wave phenomena,  $u_{xx}$  corresponds to diffusion term,  $\epsilon$  is the diffusion coefficient,  $\alpha$ ,  $\beta$  and  $\delta$  are parameters satisfying  $\alpha, \beta \geq 0$ ,  $\delta > 0$  and  $0 < \epsilon \ll 1$ . Keeping other parameters fixed, when  $\epsilon \rightarrow 0$ , the above equation becomes singularly perturbed problem.

Burger, in 1948, posed Burgers equation as a remarkable model of one-dimensional turbulence which describes weak nonlinear acoustics waves in gases. The Burgers equation is a particular case of Eq.(5.1.1) for  $\beta = 0$ ,  $\delta = 1$ , i.e.,

---

The part of this Chapter has been published in *International Journal of Computer Mathematics*, 96(7):1502-1513, 2019

$$u_t + \alpha uu_x = \epsilon u_{xx}, \quad a < x < b, t > 0.$$

A lot of researchers have worked on the Burgers problem. Mittal et al.[131] proposed differential quadrature method for solving the Burgers problem. The authors used quasilinearization process to deal with the nonlinearity arising in the problem and utilized RK fourth-order method for time discretization. Stability and convergence analysis of the proposed scheme has been discussed. Numerical experiments depict that the proposed scheme provides more accurate results as compared to some of the methods existing in the literature. Gowrisankar and Natesan [80] applied upwind finite difference scheme for approximating the solution of the singularly perturbed Burgers equation on a layer-adapted nonuniform mesh after linearizing the Burgers equation. Mohanty et al.[134] proposed compact operator method for approximating coupled viscous Burger's equation. Kadalbajoo et al.[97] developed a parameter uniform implicit upwind difference scheme for solving Burgers' equation on piecewise uniform Shishkin mesh. The authors utilized Bellman and Kalaba[22] quasilinearization strategy to linearize the considered problem and proved the uniform convergence of the proposed scheme.

For  $\alpha = 0$ ,  $\delta = 1$ , the above equation (5.1.1) reduces to classical Fishers equation, i.e.,

$$u_t = \epsilon u_{xx} + \beta u(1 - u), \quad a < x < b, t > 0.$$

Fisher, in 1937, proposed in his paper that the Fishers equation represents spatial spread of an advantageous allele.

The second model problem, singularly perturbed Burgers-Huxley problem

$$\frac{\partial v}{\partial t} + \alpha v \frac{\partial v}{\partial x} - \epsilon \frac{\partial^2 v}{\partial x^2} = \beta v(1 - v)(v - \gamma), \quad 0 < x < 1, t > 0,$$

has been considered. The considered equation represents interaction between convection, diffusion and reaction and governs the wave phenomenon. For  $\alpha = 0$ , the above

equation reduces to Hodgkin-Huxley equation given by

$$\frac{\partial v}{\partial t} - \epsilon \frac{\partial^2 v}{\partial x^2} = \beta v(1-v)(v-\gamma), \quad 0 < x < 1, t > 0,$$

which represents wall motion in liquid crystals. The problem is widely used in theoretical neuroscience[160] and represents the ionic processes at a real nerve membrane[160, 172]. The Hodgkin-Huxley model problem can provide approximate solutions of the nondimensional FitzHugh-Nagumo model problem via some appropriate affine transformations as shown by Postnikov [160].

Till date, very few researchers have proposed some numerical schemes to solve generalized Burgers-Fisher equation and that too for  $\epsilon = 1$ . But a very little effort has been made for solving the equation for small values of  $\epsilon \ll 1$ , though some researchers have developed some numerical schemes for Burgers-Huxley problem. Javidi[93] gave numerical solution of generalized Burgers-Fisher equation for the case  $\epsilon = 1$  using spectral collocation method. Sari et al.[175] proposed a compact finite difference scheme for solving generalized Burgers-Fisher equation for  $\epsilon = 1$ . Zhu and Kang[210] used cubic B-splines quasi-interpolation to solve Burgers-Fisher equation for the case  $\epsilon = 1$ . Zhang et al.[207] presented a numerical scheme for solving Burgers-Huxley and Burgers-Fisher equation using local discontinuous Galerkin method for  $\epsilon = 1$ . Mittal et al.[132] proposed a numerical scheme based on cubic splines for solving generalized Burgers-Fisher and Burgers-Huxley problems for the case  $\epsilon \ll 1$ . Pei et al.[206] proposed direct discontinuous Galerkin method to solve singularly perturbed generalized Burgers-Fisher (SPGBF) equation for  $\epsilon \ll 1$ . Wang et al.[196] analyzed the wave solutions of the generalized Burgers-Huxley problem. Kumar et al.[110] presented a robust and convergent three-step Taylor-Galerkin finite element numerical technique for approximating the solutions of singularly perturbed Burgers-Huxley problems as  $\epsilon \rightarrow 0$ . The authors carried out stability and convergence analysis. The efficiency of the proposed numerical scheme has been tested via numerical results. Motsa et al. [140] proposed spectral local linearization technique for approximating non-linear

boundary layer problems. The considered non-linear problem was linearized and the obtained reduced system has been solved using spectral collocation method. Numerical tests show that the proposed technique converges rapidly and produces accurate results. Kaushik[100] developed pointwise uniform convergent numerical scheme for the nonstationary Burgers-Huxley problem based on grid equidistribution for the case  $\epsilon \ll 1$ . Kaushik et al.[102] analysed singularly perturbed two-parameter problems using higher order finite element method. The authors proved that the proposed scheme is parameter uniform convergent.

Since both the problems under consideration are singularly perturbed in nature, traditional finite element methods cannot be relied to capture sharp boundary layers arising the solution. Therefore, we need some special treatment to capture these sharp boundary layers as  $\epsilon \rightarrow 0$ . In the present work, we propose exponentially fitted finite element method for capturing the boundary layers occurring in solution of singularly perturbed Burgers-Fisher (SPBF) equation and singularly perturbed Burgers-Huxley (SPBH) equation for the case  $\epsilon \ll 1$ . Shishkin mesh methodology has been used so as to refine the mesh in the boundary layer region. Also, for the method to be uniform convergent, exponentially fitted splines[170, 173] have been used as test functions in the proposed finite element scheme. Time discretization has been performed prior to spatial discretization and quasilinearization process proposed by Bellman and Kalaba[22] has been invoked to deal with the nonlinearity occurring in the problem. For the numerical scheme to be stable, time discretization has been performed using implicit Euler method. The proposed numerical scheme has already been discussed in Chapter 2.

The Chapter is divided into different Sections to follow:

In Section 5.2, the SPBF equation has been presented. The weak formulation of the proposed scheme has also been presented. Section 5.3 includes some numerical experiments which have been performed to test the efficiency and robustness of the nu-

merical scheme. In Section 5.4, the singularly perturbed generalized Burgers-Huxley equation and its weak formulation has been presented. Numerical tests have been carried out to test the effectivity of proposed adaptive numerical scheme in Section 5.5. At the end, conclusion has been presented.

## 5.2 Singularly perturbed generalized Burgers-Fisher equation

The time dependent singularly perturbed generalized Burgers-Fisher (SPGBF) initial-boundary value problem is given by

$$\frac{\partial u}{\partial t} = -\alpha u^\delta \frac{\partial u}{\partial x} + \epsilon \frac{\partial^2 u}{\partial x^2} + \beta u(1 - u^\delta), \quad 0 < x < 1, t > 0, \quad (5.2.1)$$

with initial condition

$$u(x, 0) = \phi(x), \quad x \in \Omega = (0, 1),$$

and boundary conditions as

$$\begin{aligned} u(0, t) &= f(t), & t > 0, \\ u(1, t) &= g(t), & t > 0, \end{aligned}$$

over a domain  $D = \Omega \times T = (0 < x < 1) \times (t > 0)$ , where  $\alpha$ ,  $\beta$  and  $\delta$  are parameters such that  $\alpha, \beta \geq 0$ ,  $\delta > 0$  and  $\epsilon$  is the singular perturbation parameter ( $0 < \epsilon \ll 1$ ). Here, we consider a particular case of Eq.(5.2.1) for  $\delta = 1$ , though the proposed scheme can be applied for other values of  $\delta$  in a similar way. For  $\delta = 1$ , the above equation reduces to

$$u_t = \epsilon u_{xx} - \alpha u u_x + \beta u(1 - u), \quad 0 < x < 1, t > 0. \quad (5.2.2)$$

The temporal and spatial discretization of Eq.(5.2.2) and quasilinearization can be carried out in a similar way as described in Chapter 2. Using implicit Euler scheme for temporal discretization and applying quasilinearization process for a fixed time

level  $t_{j+1}$ , we get a sequence of solutions  $\{u_r(x)\}_{r=0}^{r=\infty}$  of linear equations given by the following recurrence relation:

$$u_{r+1}^0 = u_0(x), \quad (5.2.3)$$

$$\begin{aligned} \frac{u_{r+1}^{j+1} - u_r^j}{\Delta t} = & \epsilon(u_{xx})_{r+1}^{j+1} - \alpha u_{r+1}^{j+1}(u_x)_r^{j+1} + \alpha u_r^{j+1}(u_x)_r^{j+1} - \alpha u_r^{j+1}(u_x)_{r+1}^{j+1} \\ & - 2\beta u_r^{j+1}u_{r+1}^{j+1} + \beta u_{r+1}^{j+1} + \beta(u_r^{j+1})^2. \end{aligned} \quad (5.2.4)$$

Also, the boundary conditions reduces to

$$u_{r+1}^{j+1}(0) = f((j+1)\Delta t), u_{r+1}^{j+1}(1) = g((j+1)\Delta t), \quad j \geq 0, \quad (5.2.5)$$

where  $r = 0, 1, 2, \dots$  is iteration index and  $u_0^{j+1}(x)$  is initial guess. The proof of convergence of quasilinearization process and Shishkin mesh methodology has been discussed in Chapter 2.

The finite element weak formulation of Eq.(5.2.4) is given by

Find  $u \in S_h$  such that

$$\begin{aligned} \int_{\Omega} u_{r+1}^{j+1} v dx = & \Delta t \left[ -\epsilon \int_{\Omega} (u_x)_{r+1}^{j+1} v_x - \alpha u_{r+1}^{j+1} (u_x)_r^{j+1} v + \alpha u_r^{j+1} (u_x)_r^{j+1} v - 2\beta u_r^{j+1} u_{r+1}^{j+1} v \right. \\ & \left. - \alpha u_r^{j+1} (u_x)_{r+1}^{j+1} v + \beta u_{r+1}^{j+1} v + \beta (u_r^{j+1})^2 v \right] dx + \int_{\Omega} u_{r+1}^j v dx, \forall v \in V. \end{aligned} \quad (5.2.6)$$

Exponentially fitted splines have been used as test functions satisfying

$$\epsilon(\phi_i^e)_{xx}(x, t_{j+1}) + \alpha u(x_e, t_{j+1})(\phi_i^e)_x(x, t_{j+1}) = 0.$$

Now the finite element sol. can be obtained by following the procedure mentioned in Section (2.3.3) of Chapter 2.

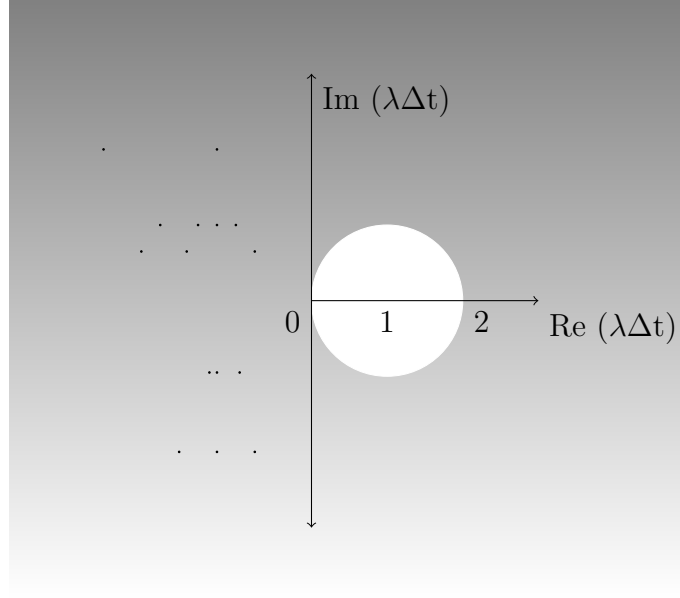


Figure 5.1: Stability region for singularly perturbed Burgers-Fisher equation

### 5.3 Numerical results

In this Section, some numerical results have been presented to demonstrate the efficiency and robustness of the proposed numerical scheme.

**Example 1.** Consider Eq.(5.2.2) for the specific parameter values of  $\alpha = 0.01$ ,  $\beta = 0.01$  together with the initial condition

$$u(x, 0) = \frac{1}{2} + \frac{1}{2} \tanh(\theta_1 x), \quad 0 < x < 1,$$

and boundary conditions

$$\begin{aligned} u(0, t) &= \frac{1}{2} + \frac{1}{2} \tanh(0 - \theta_1 \theta_2 t), & t > 0, \\ u(1, t) &= \frac{1}{2} + \frac{1}{2} \tanh(\theta_1 - \theta_1 \theta_2 t), & t > 0. \end{aligned}$$

The analytic solution of the problem is given by

$$u(x, t) = \frac{1}{2} + \frac{1}{2} \tanh(\theta_1 x - \theta_1 \theta_2 t),$$

where  $\theta_1 = \frac{-\alpha}{4\epsilon}$  and  $\theta_2 = \frac{\alpha}{2} + \frac{2\epsilon\beta}{\alpha}$ . The problem under consideration has not been solved so far for small values of  $\epsilon$ , hence numerical results are not available.

The stability analysis can be carried in the same way as described in Chapter 2. The region of absolute stability, which is outside the above mentioned unit circle, for the Burgers-Fisher problem is shown in Fig. 5.1. From Fig. 5.1, it can easily be seen that all eigenvalues of matrix [C] lie in the region of stability which proves the stability of the proposed numerical scheme.

Define the  $L_\infty$ -norm as

$$\| u(x, t) - u_h(x, t) \|_{L_\infty} = \max_{1 \leq i \leq N, 1 \leq j \leq M} | u(x_i, t_j) - u_h(x_i, t_j) |,$$

where  $N$  represents the number of mesh points in the spatial direction and  $t_j = j\Delta t$ ,  $\Delta t$  is the time step. In Table 5.1, maximum absolute errors have been tabulated at different time levels  $t = 1, 10, 50$  and have been compared with the variational iteration method(VIM), lattice Boltzmann method(LBM) and Adomian decomposition method(ADM) from [206] for  $\epsilon = 1$ . From this comparison table, it can

Table 5.1: Maximum absolute errors in Example 1 for  $\alpha = 0.01$ ,  $\beta = 0.01$ ,  $\epsilon = 1$  and  $\Delta t = 0.0002$

| t  | x   | Proposed Scheme         | LBM                    | VIM                    | ADM                    |
|----|-----|-------------------------|------------------------|------------------------|------------------------|
| 1  | 0.1 | $2.5982 \times 10^{-7}$ | $1.080 \times 10^{-4}$ | $1.780 \times 10^{-8}$ | $1.780 \times 10^{-8}$ |
|    | 0.5 | $7.0165 \times 10^{-7}$ | $0.325 \times 10^{-4}$ | $5.290 \times 10^{-9}$ | $5.290 \times 10^{-9}$ |
|    | 0.9 | $2.4219 \times 10^{-7}$ | $1.730 \times 10^{-4}$ | $7.280 \times 10^{-9}$ | $7.280 \times 10^{-9}$ |
| 10 | 0.1 | $2.9587 \times 10^{-6}$ | $1.080 \times 10^{-4}$ | $2.070 \times 10^{-5}$ | $2.070 \times 10^{-5}$ |
|    | 0.5 | $8.0982 \times 10^{-6}$ | $0.314 \times 10^{-4}$ | $1.940 \times 10^{-5}$ | $1.940 \times 10^{-5}$ |
|    | 0.9 | $2.7571 \times 10^{-6}$ | $1.720 \times 10^{-4}$ | $1.810 \times 10^{-5}$ | $1.810 \times 10^{-5}$ |
| 50 | 0.1 | $1.7174 \times 10^{-5}$ | $1.010 \times 10^{-4}$ | 0.002552               | 0.002552               |
|    | 0.5 | $4.7068 \times 10^{-5}$ | $0.306 \times 10^{-4}$ | 0.002552               | 0.002552               |
|    | 0.9 | $1.6010 \times 10^{-5}$ | $1.620 \times 10^{-4}$ | 0.002492               | 0.002492               |

be easily noticed that the proposed numerical scheme provides more accurate results. In order to check the robustness of the proposed numerical scheme for the solution of SPBF equation with respect to very small values of the singular perturbation parameter  $\epsilon$ , the  $L_\infty$ -error estimates and order of convergence(for different values of  $\epsilon$ ) have been presented in Table 5.2. For calculating order of convergence, we define

$$E_\epsilon^{N,\Delta t} = \max_{0 \leq i \leq N, 0 \leq j \leq M} |u(x_i, t_j) - u_h(x_i, t_j)|,$$

where  $N$  represents the number of mesh points in the spatial direction. Now, the order of convergence is calculated using double mesh principle defined by

$$p_\epsilon^N = \frac{\log(E_\epsilon^{N,\Delta t}/E_\epsilon^{2N,\Delta t/2})}{\log 2}.$$

In Fig. 5.2, grid validation of the code has been tested for different values of singular perturbation parameter  $\epsilon = 2^{-11}, 2^{-14}$  at time level  $t = 1$ . From solution plots, it can be seen that a grid of 64 elements is sufficient enough to capture the boundary layers for very small values of  $\epsilon$  like  $\epsilon = 2^{-14}$ . For further numerical results to follow, grid of 128 elements has been considered. In Fig. 5.3, the behavior of singular perturba-

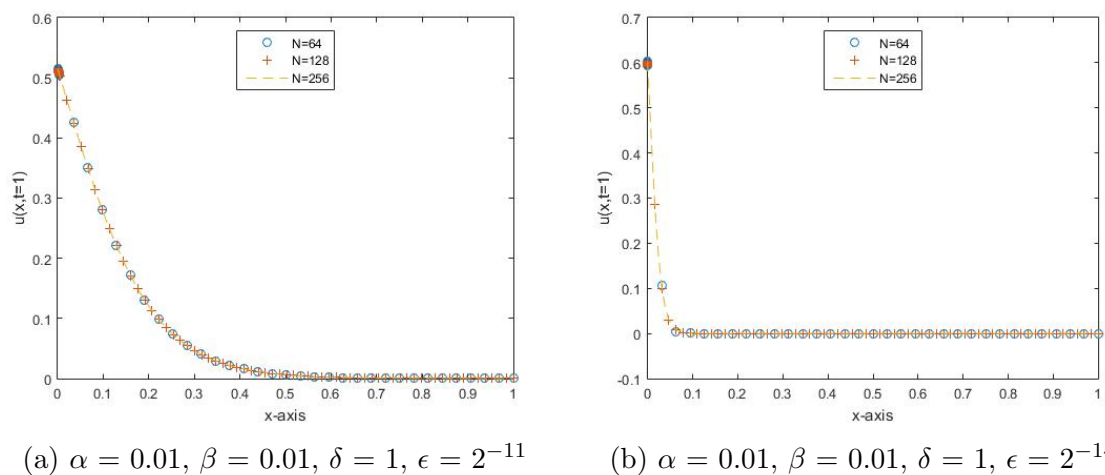
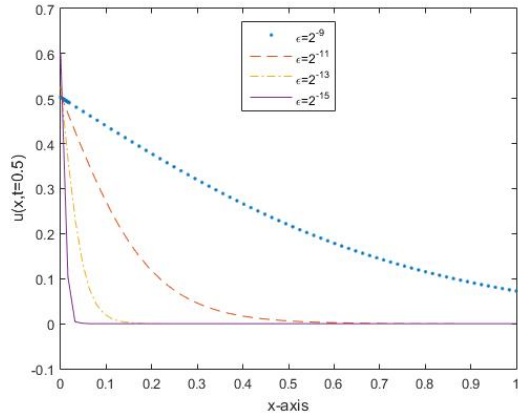
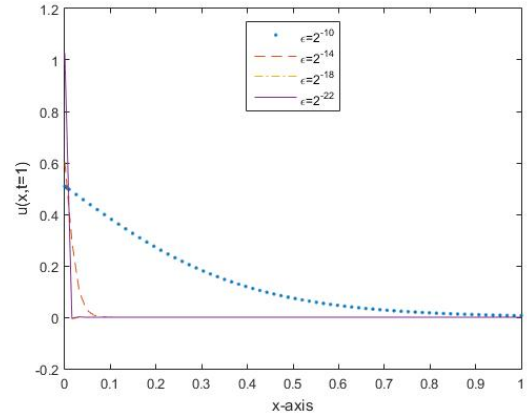


Figure 5.2: Grid validation test for  $\epsilon = 2^{-11}, 2^{-14}$

tion parameter  $\epsilon$  has been depicted as  $\epsilon \rightarrow 0$ . The solutions have been plotted for various values of  $\epsilon$  at time levels  $t = 0.5$  and  $t = 1$ . In both the plots, it is very clear that as singular perturbation parameter gets smaller and smaller, sharper boundary layers appear in the solution and the proposed numerical scheme is efficient enough to capture these boundary layers. In Fig. 5.4(a), finite element solution of singularly perturbed Burgers-Fisher equation has been plotted for  $\epsilon = 2^{-12}$  at different time levels  $t = 0.2, 0.4, 0.6, 0.8$  and  $1$ . Further, the solution has been plotted for  $\epsilon =$



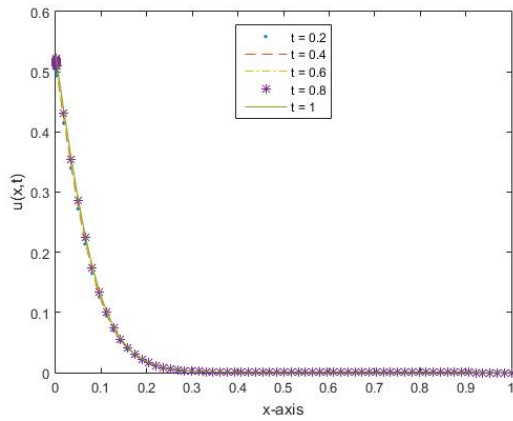
(a)  $\alpha = 0.01, \beta = 0.01, \delta = 1, t = 0.5$



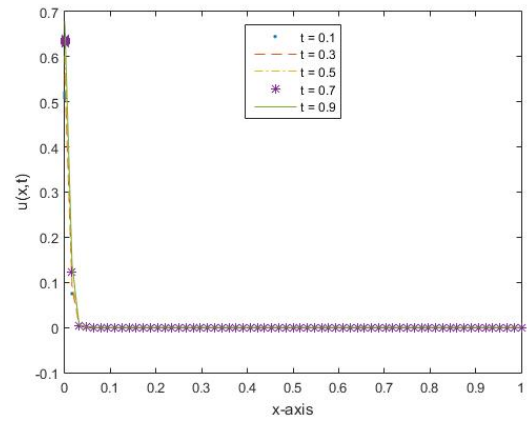
(b)  $\alpha = 0.01, \beta = 0.01, \delta = 1, t = 1.0$

Figure 5.3:  $\epsilon$  - effect at different time levels  $t = 0.5, 1.0$

$2^{-15}$  at various time levels  $t = 0.1, 0.3, 0.5, 0.7$  and  $0.9$  in Fig. 5.4(b). Both the plots depict the efficiency and robustness of the proposed method in capturing very sharp boundary layers. In Fig. 5.5, numerical solution profile for the Burgers-Fisher



(a)  $\alpha = 0.01, \beta = 0.01, \delta = 1, \epsilon = 2^{-12}$



(b)  $\alpha = 0.01, \beta = 0.01, \delta = 1, \epsilon = 2^{-15}$

Figure 5.4: Time-effect at different values of  $\epsilon = 2^{-12}, 2^{-15}$

problem has been shown for  $\epsilon = 2^{-12}$ .

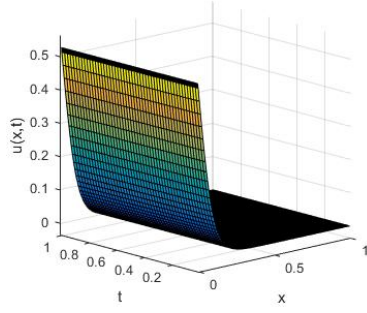


Figure 5.5: The numerical solution profile for  $\alpha = 0.01$ ,  $\beta = 0.01$ ,  $\delta = 1$ ,  $\epsilon = 2^{-12}$

## 5.4 Singularly perturbed generalized Burgers-Huxley equation

The time dependent singularly perturbed generalized Burgers-Huxley (SPGBH) problem is defined as

$$\frac{\partial v}{\partial t} + \alpha v \frac{\partial v}{\partial x} - \epsilon \frac{\partial^2 v}{\partial x^2} = \beta v(1-v)(v-\gamma), \quad 0 < x < 1, t > 0, \quad (5.4.1)$$

with initial condition

$$v(x, 0) = \phi(x), \quad x \in \Omega = (0, 1), \quad (5.4.2)$$

and boundary conditions as

$$\begin{aligned} v(0, t) &= f(t), & t > 0, \\ v(1, t) &= g(t), & t > 0, \end{aligned}$$

over a domain  $D = \Omega \times T = (0, 1) \times (0, \infty)$ , where  $\alpha, \beta \geq 0$ ,  $\gamma \in (0, 1)$  and  $\epsilon$  is the singular perturbation parameter satisfying  $0 < \epsilon \ll 1$ . The Burgers-Huxley equation is widely used to model nerve pulse propagation in nerve fibres and wall motion in liquid crystals.

Carrying out the temporal discretization and quasilinearization as discussed in Chapter 2, the linearized approximate system of Eq.(5.4.1) can be written as

$$v_{r+1}^0 = v_0(x), \quad (5.4.3)$$

$$\begin{aligned}
\frac{v_{r+1}^{j+1} - v_{r+1}^j}{\Delta t} &= \epsilon(v_{xx})_{r+1}^{j+1} - \alpha(v_x)_r^{j+1}v_{r+1}^{j+1} + (-\beta - \beta\gamma)(v_r^{j+1})^2 + 2\beta(v_r^{j+1})^3 \\
&\quad + (2\beta + 2\beta\gamma)v_r^{j+1}v_{r+1}^{j+1} - 3\beta(v_r^{j+1})^2v_{r+1}^{j+1} - \beta\gamma v_{r+1}^{j+1}.
\end{aligned} \tag{5.4.4}$$

The boundary conditions for the sys.(5.4.4) are given by

$$v_{r+1}^{j+1}(0) = f((j+1)\Delta t), \quad v_{r+1}^{j+1}(1) = g((j+1)\Delta t), \quad j \geq 0. \tag{5.4.5}$$

Here  $r = 0, 1, 2, \dots$  denotes the iteration index and  $v_0^{j+1}(x)$  is the initial approximation.

The exponentially fitted finite element weak formulation of Eq.(5.4.4) seeks  $v \in S_h = \{\psi_1(x), \psi_2(x), \dots, \psi_N(x)\}$  such that

$$\begin{aligned}
\int_{\Omega} [v_{r+1}^{j+1} - v^j] w dx &= (\Delta t) \int_{\Omega} [-\epsilon(v_x)_{r+1}^{j+1}w_x - \alpha(v_x)_r^{j+1}v_{r+1}^{j+1}w + 2\beta(v_r^{j+1})^3w \\
&\quad + (-\beta - \beta\gamma)(v_r^{j+1})^2w + (2\beta + 2\beta\gamma)v_r^{j+1}v_{r+1}^{j+1}w - 3\beta(v_r^{j+1})^2v_{r+1}^{j+1}w \\
&\quad - \beta\gamma v_{r+1}^{j+1}w] dx,
\end{aligned} \tag{5.4.6}$$

where  $V_h = \{\phi_1(x), \dots, \phi_N(x)\}$ . Stability analysis can be carried out in a similar manner as discussed in Section (2.7) of Chapter 2.

## 5.5 Numerical results

In this Section, effectivity and robustness of the proposed numerical scheme has been tested using different numerical experiments.

**Example 2.** Consider Eq.(5.4.1) for the parameter values of  $\alpha = 3$ ,  $\beta = 9.8$  and  $\gamma = 0.7$ , the initial condition

$$v(x, 0) = 1 - \cos(x), \quad 0 < x < 1,$$

and boundary conditions

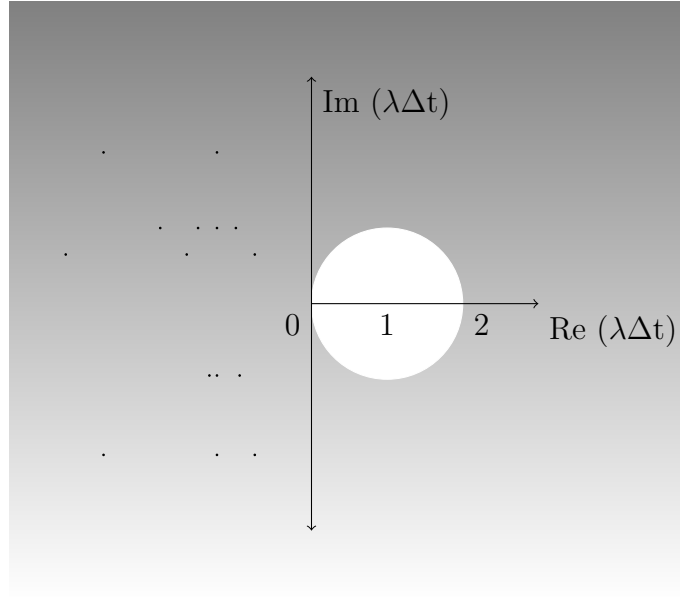


Figure 5.6: Stability region for singularly perturbed Burgers-Huxley equation

$$\begin{aligned}
 v(0, t) &= 0, & t > 0, \\
 v(1, t) &= 0, & t > 0.
 \end{aligned}$$

The region of absolute stability has been plotted in Fig. 5.6. It can be seen that all the eigen values are lying outside the unit circle which shows that the proposed scheme is stable. In Fig. 5.7, grid validation of the code has been tested for different values of singular perturbation parameter  $\epsilon = 2^{-12}$  and  $2^{-14}$  at time level  $t = 1$ . From grid validation tests, we analyze that as we move from grid of 64 elements to grid of 256 elements, the boundary layers are captured very nicely. Grid of 128 elements has been considered for further numerical results to follow. In Fig. 5.8, the behavior of parameter  $\epsilon$  has been depicted as  $\epsilon$  becomes small. The solution plots have been drawn for various values of  $\epsilon$  at time levels  $t = 0.5$  and  $t = 1.0$ . These solution plots clearly depict that the proposed scheme is very efficient in capturing sharp boundary layers. In Fig. 5.9(a) and (b), the solution of singularly perturbed Burgers-Huxley equation has been plotted for  $\epsilon = 2^{-14}$  and  $2^{-18}$  at various time levels. It can be easily seen that very sharp boundary layers appear near the boundary  $x = 1$ . Both the

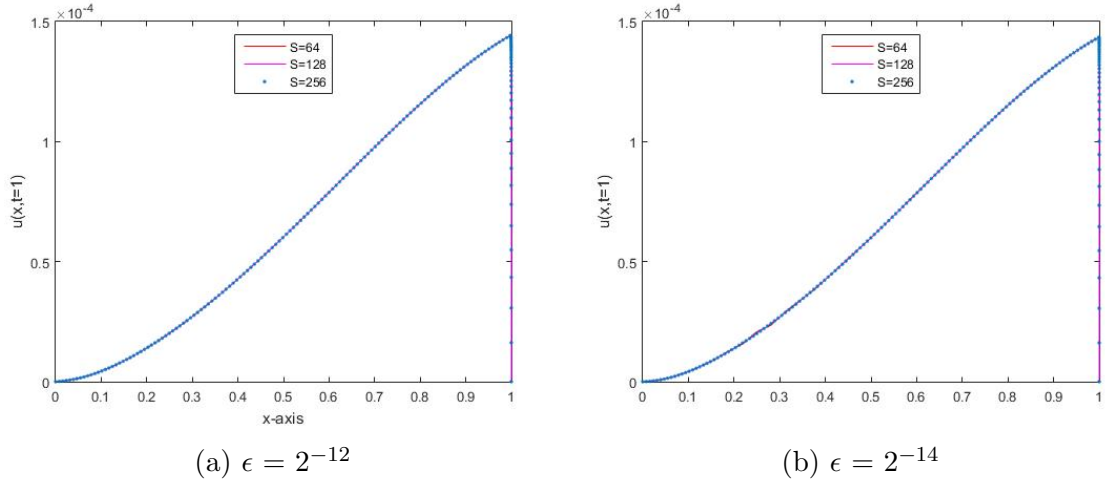


Figure 5.7: Grid validation test for  $\epsilon = 2^{-12}, 2^{-14}$

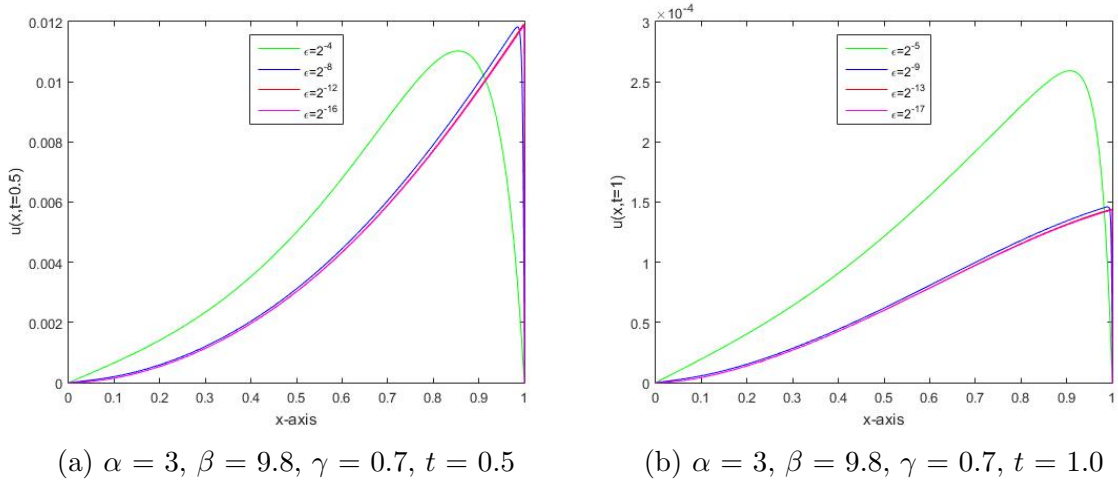


Figure 5.8:  $\epsilon$ - effect at different time levels = 0.5,1.0

plots depict the efficiency of method in capturing sharp boundary layers. Numerical solution of Example 2 has been plotted for the time-domain  $[0,1]$  for  $\epsilon = 2^{-15}$  in Fig. 5.10. From the plot, one can see how the solution evolves with the passage of time.

**Example 3.** Consider singularly perturbed Burgers-Huxley equation for the parameter values  $\alpha = 1, \beta = 0, \gamma = 0$  together with the initial condition

$$v(x, 0) = x(1 - x^2), \quad 0 \leq x \leq 1,$$

and boundary conditions

$$v(0, t) = 0, \quad t > 0,$$

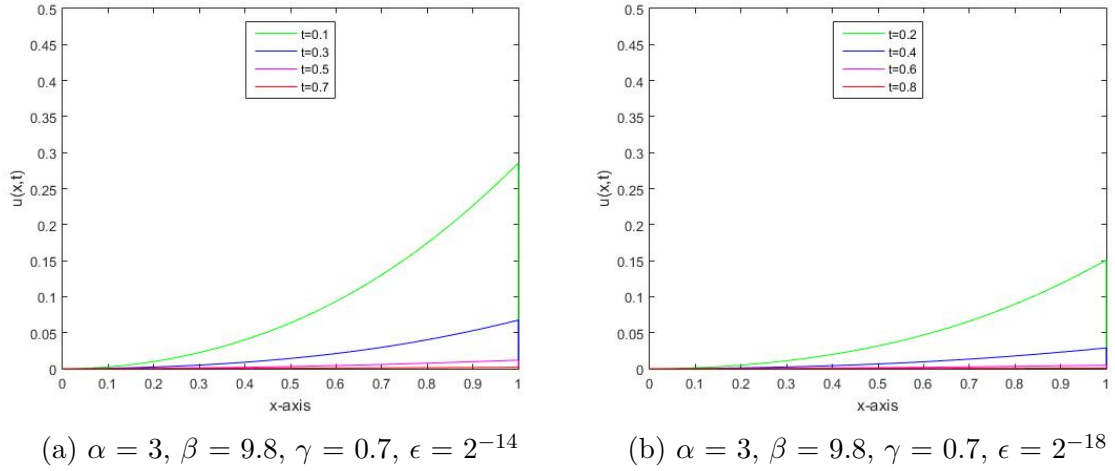


Figure 5.9: Time-effect on the sol. at  $\epsilon = 2^{-14}$  and  $2^{-18}$

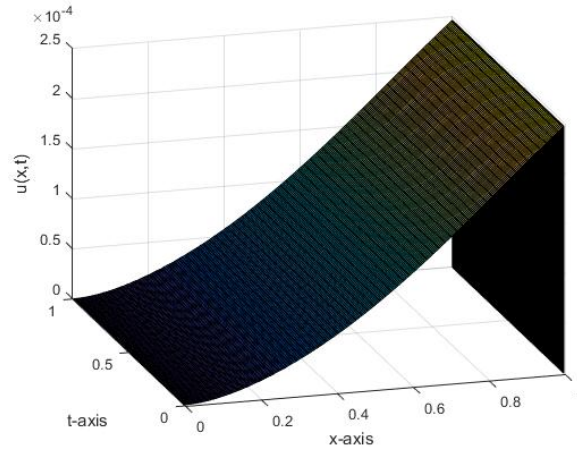
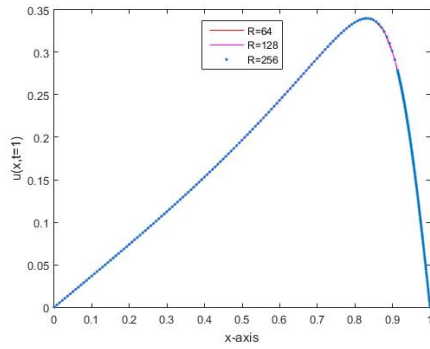


Figure 5.10: Numerical solution profile for  $\alpha = 3, \beta = 9.8, \gamma = 0.7, \epsilon = 2^{-15}$ .

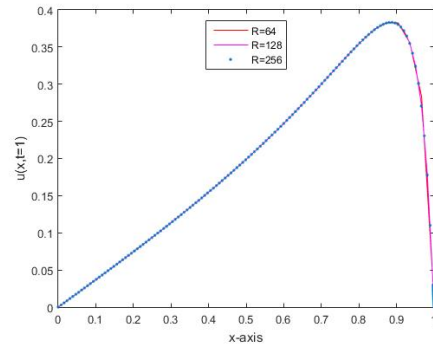
$$v(1, t) = 0, \quad t > 0.$$

In Fig. 5.11, grid validation of the code has been done for  $\epsilon = 2^{-7}$  and  $2^{-12}$  at time  $t = 1$ . Further, in Fig. 5.12  $\epsilon$ -effect has been shown on the numerical solution at  $t = 0.5$  and  $t = 1$ . It can be easily observed from the solution plots that the developed strategy is very much effective in capturing sharp changes in the solution.

In Fig. 5.13, numerical solution for the Example 3 has been plotted for  $\epsilon = 2^{-15}$  and  $2^{-17}$  at different time levels. From the solution plots, it can be verified that the proposed scheme is very much efficient in capturing sharp boundary layers near the

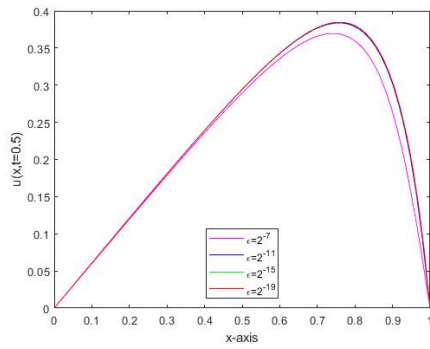


(a)  $\alpha = 1, \beta = 0, \gamma = 0, \epsilon = 2^{-7}$

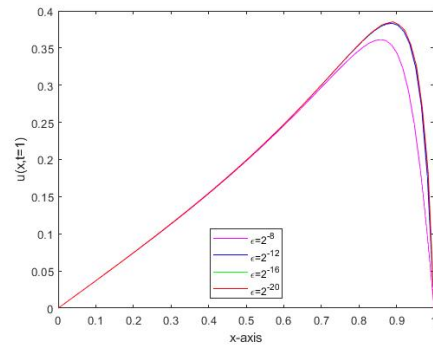


(b)  $\alpha = 1, \beta = 0, \gamma = 0, \epsilon = 2^{-12}$

Figure 5.11: Grid validation test for  $\epsilon = 2^{-7}, 2^{-12}$



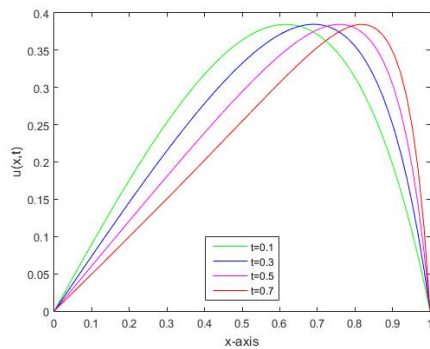
(a)  $\alpha = 1, \beta = 0, \gamma = 0, t = 0.5$



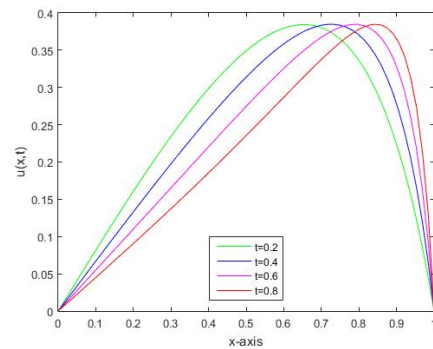
(b)  $\alpha = 1, \beta = 0, \gamma = 0, t = 1$

Figure 5.12:  $\epsilon$ -effect at  $t = 0.5$  and  $t = 1$

boundary  $x = 1$  as  $\epsilon \rightarrow 0$ .



(a)  $\alpha = 1, \beta = 0, \gamma = 0, \epsilon = 2^{-15}$



(b)  $\alpha = 1, \beta = 0, \gamma = 0, \epsilon = 2^{-17}$

Figure 5.13: Time-effect on the sol. at  $\epsilon = 2^{-15}$  and  $2^{-17}$

## 5.6 Conclusion

In this Chapter, two realistic model phenomenon arising during the analysis of biological systems and governed by singularly perturbed problems have been considered. An exponentially fitted finite element technique has been presented for solving the singularly perturbed model problems, i.e. Burgers-Fisher problem and Burgers-Huxley model problem, on a layer adapted mesh. Both the model problems are non-linear in nature. Therefore, quasilinearization process has been invoked to tackle the non-linearity occurring in the problems. Temporal semi-discretization has been carried out prior to spatial discretization using implicit Euler method. Exponentially fitted splines have been used as test functions. Further, the proposed numerical scheme has been shown to be absolute stable. It has been depicted through numerous numerical experiments that the proposed scheme approximates the solutions of both the models very nicely. The proposed scheme is very efficient in capturing the abrupt changes in the solution as  $\epsilon$  becomes small.

Table 5.2: Maximum pointwise errors and order of convergence in Example 1 with  $\alpha = 0.01$ ,  $\beta = 0.01$

| $\epsilon$ | N=16                             | N=32                             | N=64                             | N=128                   |
|------------|----------------------------------|----------------------------------|----------------------------------|-------------------------|
| $2^{-6}$   | $3.3290 \times 10^{-6}$<br>0.131 | $3.0380 \times 10^{-6}$<br>0.032 | $2.9700 \times 10^{-6}$<br>0.068 | $2.8330 \times 10^{-6}$ |
| $2^{-7}$   | $3.5180 \times 10^{-6}$<br>0.328 | $2.8020 \times 10^{-6}$<br>0.165 | $2.4990 \times 10^{-6}$<br>0.005 | $2.4890 \times 10^{-6}$ |
| $2^{-8}$   | $4.6500 \times 10^{-6}$<br>1.145 | $2.1020 \times 10^{-6}$<br>0.463 | $1.5250 \times 10^{-6}$<br>0.039 | $1.4840 \times 10^{-6}$ |
| $2^{-9}$   | $1.3840 \times 10^{-5}$<br>1.389 | $5.2850 \times 10^{-6}$<br>0.993 | $2.6550 \times 10^{-6}$<br>0.073 | $2.5240 \times 10^{-6}$ |
| $2^{-10}$  | $8.0090 \times 10^{-5}$<br>2.185 | $1.7610 \times 10^{-5}$<br>0.054 | $1.6960 \times 10^{-5}$<br>0.034 | $1.6590 \times 10^{-5}$ |
| $2^{-11}$  | $5.1070 \times 10^{-4}$<br>3.079 | $6.0410 \times 10^{-5}$<br>0.190 | $5.2950 \times 10^{-5}$<br>0.010 | $5.2560 \times 10^{-5}$ |
| $2^{-12}$  | $1.4000 \times 10^{-3}$<br>0.952 | $7.2340 \times 10^{-4}$<br>1.403 | $2.7380 \times 10^{-4}$<br>0.042 | $2.6590 \times 10^{-4}$ |
| $2^{-13}$  | $3.6000 \times 10^{-3}$<br>0.585 | $2.4000 \times 10^{-3}$<br>1.728 | $7.2420 \times 10^{-4}$<br>0.010 | $7.1900 \times 10^{-4}$ |
| $2^{-14}$  | $1.8600 \times 10^{-2}$<br>1.706 | $5.7000 \times 10^{-3}$<br>0.475 | $4.1000 \times 10^{-3}$<br>0.187 | $3.6000 \times 10^{-3}$ |
| $2^{-15}$  | $3.7900 \times 10^{-2}$<br>0.431 | $2.8100 \times 10^{-2}$<br>2.580 | $4.7000 \times 10^{-3}$<br>1.910 | $1.2500 \times 10^{-3}$ |
| $2^{-16}$  | $7.2700 \times 10^{-2}$<br>0.150 | $6.5500 \times 10^{-2}$<br>0.797 | $3.7700 \times 10^{-2}$<br>0.951 | $1.9500 \times 10^{-2}$ |
| $2^{-17}$  | $1.0730 \times 10^{-1}$<br>0.108 | $9.9500 \times 10^{-2}$<br>0.482 | $7.1200 \times 10^{-2}$<br>2.876 | $9.7000 \times 10^{-3}$ |
| $2^{-18}$  | $1.2090 \times 10^{-1}$<br>0.136 | $1.1000 \times 10^{-1}$<br>0.475 | $7.9100 \times 10^{-2}$<br>2.168 | $1.7600 \times 10^{-2}$ |
| $2^{-19}$  | $1.2220 \times 10^{-1}$<br>0.163 | $1.0910 \times 10^{-1}$<br>0.504 | $7.6900 \times 10^{-2}$<br>1.914 | $2.0400 \times 10^{-2}$ |
| $2^{-20}$  | $1.2220 \times 10^{-1}$<br>0.178 | $1.0800 \times 10^{-1}$<br>0.531 | $7.4700 \times 10^{-2}$<br>1.776 | $2.1800 \times 10^{-2}$ |
| $2^{-21}$  | $1.2210 \times 10^{-1}$<br>0.179 | $1.0780 \times 10^{-1}$<br>0.536 | $7.4300 \times 10^{-2}$<br>1.736 | $2.2300 \times 10^{-2}$ |
| $2^{-22}$  | $1.2210 \times 10^{-1}$<br>0.182 | $1.0760 \times 10^{-1}$<br>0.545 | $7.3700 \times 10^{-2}$<br>1.705 | $2.2600 \times 10^{-2}$ |
| $2^{-23}$  | $1.2220 \times 10^{-1}$<br>0.183 | $1.0760 \times 10^{-1}$<br>0.547 | $7.3600 \times 10^{-2}$<br>1.692 | $2.2800 \times 10^{-2}$ |
| $2^{-24}$  | $1.2220 \times 10^{-1}$<br>0.182 | $1.0770 \times 10^{-1}$<br>0.547 | $7.3700 \times 10^{-2}$<br>1.686 | $2.2900 \times 10^{-2}$ |

---

## Future work

---

In the presented work, some robust and efficient adaptive finite element strategies have been proposed for approximating the solutions of singularly perturbed problems in one-, two- and three-dimensions. A posteriori error estimates in energy norm have been developed for the proposed scheme for two- and three-dimensional singularly perturbed convection-diffusion problems. An adaptive mesh refinement strategy has been proposed for the proposed method. Efficiency index and the  $L_\infty$ -error vs degrees of freedom plots clearly validate the proposed adaptive refinement strategy. The proposed method provides good approximate results for singularly perturbed problems. For the future work, some other error estimates and adaptive mesh refinement strategies based on finite element estimates can be investigated for higher dimensional singularly perturbed problems.

---

# Bibliography

---

- [1] A. Abas and R.A. Rahman, Adaptive FEM with domain decomposition method for partitioned-based fluid-structure interaction, Arab. J. Sci. Eng. 41:611-622, 2016.
- [2] J.V. Aguiar and J.M. Ferrándiz, A general procedure for the adaptation of multi-step algorithms to the integration of oscillatory problems, SIAM J. Numer. Anal. 35(4):1684-1708, 1998.
- [3] J.V. Aguiar and S. Natesan, An efficient numerical method for singular perturbation problems, J. Comput. Appl. Math. 192(1):132-141, 2006.
- [4] M. Ainsworth and J.T. Oden, A unified approach to a posteriori error estimation using element residual methods, Numer. Math. 65:23-50, 1993.
- [5] M. Ainsworth and J.T. Oden, A posteriori error estimation in finite element analysis, Wiley-Interscience, 2000.
- [6] J. Aramberri, D. Padro, M. Paszynski, N. Collier, L. Dalcin and V.M. Calo, On round-off error for adaptive finite element method, Procedia Comput. Sci. 9:1474-1483, 2012.
- [7] J.H. Argyris and S. Kelsey, Energy theorems and Structural Analysis, Butterworth Scientific Publications, London, 1954.

- [8] M.G. Armentano, C. Padra, R. Rodríguez and M. Scheble, An *hp* finite element adaptive scheme to solve the Laplace model for fluid-solid vibrations, *Comput. Methods Appl. Mech. Engrg.* 200:178-188, 2011.
- [9] I. Babuška and W.C. Rheinboldt, A-posteriori error estimates for the finite element method, *Int. J. Numer. Meth. Eng.* 12:1597-1615, 1978.
- [10] I. Babuška and W.C. Rheinboldt, Error estimates for adaptive finite element computations, *SIAM J. Numer. Anal.* 15:736-754, 1978.
- [11] I. Babuška, J. Chandra and J.E. Flaherty, Adaptive computational methods for partial differential equations, 1983.
- [12] I. Babuška, O.C. Zienkiewicz and E. Oliveira, Accuracy estimates and adaptive refinements in finite element computations, John Wiley and Sons, 1986.
- [13] I. Babuska and T. Strouboulis, The finite element method and its reliability, Oxford Univeristy Press, 2001.
- [14] W. Bangerth and R. Rannacher, Adaptive finite element methods for differential equations, Springer, 2003.
- [15] R.E. Bank and J. Xu, Asymptotically exact a posteriori error estimators, part I: Grids with Superconvergence, *SIAM J. Numer. Anal.* 41:2294-2312, 2003.
- [16] R.E. Bank, J. Xu and B. Zheng, Superconvergent derivative recovery for Lagrange triangular elements of degree  $p$  on unstructured grids, *SIAM J. Numer. Anal.* 45(5):2032-2046, 2007.
- [17] G. Bao, G. Hu and D. Liu, An  $h$ -adaptive finite element solver for the calculations of the electronic structures, *J. Comput. Phys.* 231:4967-4979, 2012.

- [18] G. Bao, G. Hu and D. Liu, Numerical solution of the Kohn-Sham Equation by finite element methods with an adaptive mesh redistribution technique, *J. Sci. Comput.* 55:372-391, 2013.
- [19] R. Beck and R. Hiptmair, Multilevel solution of the time-harmonic Maxwell's equations based on edge elements, *Int. J. Numer. Meth. Eng.* 45:901-920, 1999.
- [20] R. Becker and R. Rannacher, An optimal control approach to a posteriori error estimation in finite element methods, *Acta. Numer.* 10:1-102, 2001.
- [21] L. Belenki, L. Diening and C. Kreuzer, Optimality of an adaptive finite element method for the  $p$ -Laplacian equation, *IMA. J. Numer. Anal.* 32:484-510, 2012.
- [22] R.E. Bellman and R.E. Kalaba, Quasilinearization and nonlinear boundary-value problems, American Elsevier Publishing, New York, 1965.
- [23] A. Bergam, C. Bernardi and Z. Mghazli, A posteriori analysis of the finite element discretization of some parabolic equations, *Math. Comput.* 74:1117-1138, 2005.
- [24] P. Binev, W. Dahman and R. DeVore, Adaptive finite element methods with convergence rates, *Numer. Math.* 97:219-268, 2004.
- [25] R. Branco and F.V. Antunes, Finite element modelling and analysis of crack shape evolution in mode-I fatigue Middle Cracked Tension specimens, *Eng. Fract. Mech.* 75:3020-3037, 2008.
- [26] R. Branco, F.V. Antunes and J.D. Costa, A review on 3D-FE adaptive remeshing techniques for crack growth modelling, *Eng. Fract. Mech.* 141:170-195, 2015.
- [27] A.N. Brooks and T.J.R. Hughes, Streamline upwind/Petrov-Galerkin formulations for convection dominated flows with particular emphasis on the incompressible Navier-Stokes equations, *Comput. Methods Appl. Mech. Engrg.* 32:199-259, 1982.

- [28] M. Bürg, Convergence of an automatic *hp*-adaptive finite element strategy for Maxwell's equations, *Appl. Numer. Math.* 72:188-204, 2013.
- [29] C. Canuto, R. Nochetto and M. Verani, Adaptive Fourier-Galerkin methods, *Math. Comput.* 83(288):1645-1687, 2014.
- [30] C. Canuto, R. Nochetto and M. Verani, Contraction and optimality properties of adaptive Legendre-Galerkin methods: The one-dimensional case, *Comput. Math. Appl.* 67:752-770, 2014.
- [31] C. Carstensen, R. Lazarov and S. Tomov, Explicit and averaging a posteriori error estimates for adaptive finite volume methods, *SIAM J. Numer. Anal.* 42(6):2496-2521, 2006.
- [32] C. Carstensen and H. Rabus, An optimal adaptive mixed finite element method, *Math. Comput.* 80:649-667, 2011.
- [33] C. Carstensen and J. Hu, An optimal adaptive finite element method for an obstacle problem, *Comput. Methods Appl. Math.* 15:259-277, 2015.
- [34] C. Carstensen and G. Dolzmann, Convergence of adaptive finite element methods for a nonconvex double-well minimization problems, *Math. Comput.* 84:2111-2135, 2015.
- [35] C. Carstensen and E-J. Park, Convergence and optimality of adaptive least squares finite element methods, *SIAM J. Numer. Anal.* 53:43-62, 2015.
- [36] C. Carstensen, A. Schröder and S. Wiedemann, An optimal adaptive finite element method for elastoplasticity, *Numer. Math.* 132:131-154, 2016.
- [37] C. Carstensen and J. Gedicke, Robust residual-based a posteriori Arnold-Winther finite element analysis in elasticity, *Comput. Methods Appl. Mech. Engrg.* 300:245-264, 2016.

- [38] V. Chandraker, A. Awasthi and S. Jayaraj, A numerical treatment of Fisher equation, *Procedia Engineering*. 127:1256-1262, 2015.
- [39] S.P. Chang and T.F. Chen, Optimal adaptive grids of least-squares finite element methods in two spatial dimensions, *J. Comput. Appl. Math.* 235:3817-3824, 2011.
- [40] T.F.Chen and H.D. Yang, Numerical construction of optimal grids in two spatial dimensions, *Comput. Math. Appl.* 39:101-120, 2000.
- [41] J. Chen, Z. Chen, T. Cui and L.B. Zhang, An adaptive finite element method for the eddy current model with circuit/field couplings, *SIAM J. Sci. Comput.* 32:1020-1042, 2010.
- [42] P.G. Ciarlet, *The Finite element method for elliptic problems, Studies in Mathematics and its Applications*, North Holland Publishing Company, 1978.
- [43] C. Clavero, J.C. Jorge and F. Lisbona, A uniformly convergent scheme on a nonuniform mesh for convection-diffusion parabolic problems, *J. Comput. Appl. Math.* 154:415-429, 2003.
- [44] P. Clément, Approximation by finite element functions using local regularization, *RAIRO Anal. Numer.* 2:77-84, 1975.
- [45] K.A. Cliffe, E. Hall and P. Houston, Adaptive discontinuous Galerkin methods for eigenvalue problems arising in incompressible fluid flows, *SIAM J. Sci. Comput.* 31:4607-4632, 2010.
- [46] K.A. Cliffe, E. Hall, P. Houston, E.T. Phipps and A.G. Salinger, Adaptivity and a posteriori error control for bifurcation problems II: Incompressible fluid flow in open systems with  $Z_2$  symmetry, *J. Sci. Comput.* 47:389-418, 2011.

- [47] K.A. Cliffe, E.J.C. Hall and P. Houston, *hp*-adaptive discontinuous Galerkin methods for bifurcation phenomena in open flows, *Comput. Math. Appl.* 67:796-806, 2014.
- [48] R.W. Clough, *The Finite Element Method in Plane Stress Analysis*, Proceedings, 2nd ASCE Conference on Electronic Computations, Pittsburgh Sep, 1960.
- [49] S.L. Cotter, T. Vejchodský and R. Erban, Adaptive finite element method assisted by stochastic simulation of chemical systems, *SIAM J. Sci. Comput.* 35:B107-B131, 2013.
- [50] T. Coupez and E. Hachem, Solution of high-Reynolds incompressible flow with stabilized finite element and adaptive anisotropic meshing, *Comput. Methods Appl. Mech. Engrg.* 267:65-85, 2013.
- [51] R. Courant, Variational methods for the solution of problems of equilibrium and Vibrations, *Bulletin of the American Nathemtical Society*, 49:1-23, 1943.
- [52] X. Dai, J. Xu and A. Zhou, Convergence and optimal complexity of adaptive finite element eigenvalue computations, *Numer. Math.* 110:313-355, 2008.
- [53] L. Demkowicz, Ph. Devloo and J.T. Oden, On an *h*-type mesh refinement strategy based on minimization of interpolation errors. *Comput. Methods Appl. Mech. Engrg.* 53:67-89, 1985.
- [54] L. Demkowicz, J.T. Oden, W. Rachowicz and O. Hardy, Towards a universal *h* – *p* adaptive finite element strategy, Part 1. Constrained approximation and data structure, *Comput. Methods Appl. Mech. Engrg.* 77:79-112, 1989.
- [55] L. Demkowicz and A. Buffa,  $H^1$ ,  $H(\text{curl})$  and  $H(\text{div})$ -conforming projection-based interpolation in three dimensions: Quasi optimal *p*-interpolation estimates, *Comput. Methods Appl. Mech. Engrg.* 195:267-296, 2005.

- [56] L. Demkowicz and J. Gopalakrishnan, A class of discontinuous Petrov-Galerkin methods. Part II: optimal test functions, *Numer. Meth. Part. Differ. Equat.* 27:70-105, 2011.
- [57] G. Deolmi and F. Marcuzzi, A parabolic inverse convection-diffusion-reaction problem solved using space-time localization and adaptivity, *Appl. Math. Comput* 219:8435-8454, 2013.
- [58] V. Dolejší, *hp*-DGFEM for nonlinear convection-diffusion problems, *Math. Comput. Simulat.* 87:87-118, 2013.
- [59] J. Donea, A Taylor-Galerkin method for convective transport problems, *Internat. J. Numer. Methods Engrg.* 20:101-119, 1984.
- [60] W. Dörfler, A convergent adaptive algorithm for poisson's equation, *SIAM J. Numer. Anal.* 33:1106-1124, 1996.
- [61] P. Dörsek and J.M. Melenk, Adaptive *hp*-FEM for the contact problem with Tresca friction in linear elasticity: The primal-dual formulation and a posteriori error estimation, *Appl. Numer. Math.* 60:689-704, 2010.
- [62] K. Eriksson, D. Estep, P. Hansbo and C. Johnson, Introduction to adaptive methods for differential equations, *Acta. Numer.* 4:105-158, 1995.
- [63] A. Ern, A.F. Stephansen and M. Vohralík, Guaranteed and robust discontinuous Galerkin a posteriori error estimates for convection-diffusion-reaction problems, *J. Comput. Appl. Math.* 234:114-130, 2010.
- [64] T. Fankhauser, T.P. Wihler and M. Wirz, The *hp*-adaptive FEM based on continuous Sobolev embeddings: Isotropic refinements, *Comput. Math. Appl.* 67:854-868, 2014.

- [65] M. Feischl, M. Page and D. Praetorius, Convergence and quasi-optimality of adaptive FEM with inhomogeneous Dirichlet data, *J. Comput. Appl. Math.* 255:481-501, 2014.
- [66] K. Feng, Finite difference schemes based on variational principles, *Appl. Math. Comput. Math.* 2:238-262, 1965.
- [67] L.P. Franca and F. Valentin, On an improved unusual stabilized finite element method for the advection-reactive-diffusive equation, *Comput. Methods Appl. Mech. Egrg.* 190:1785-1800, 2000.
- [68] S. Franz and G. Matthies, Local projection stabilisation on S-type meshes for convection-diffusion problems with characteristic layers, *Computing.* 87:135-167, 2010.
- [69] S. Franz, Superconvergence using pointwise interpolation in convection-diffusion problems, *Appl. Numer. Math.* 76:132-144, 2014.
- [70] S. Franz and H.G. Roos, Superconvergence of a Galerkin finite element method for higher-order elements in convection-diffusion problems, *Numer. Math. Theory. Me.* 7:356-373, 2014.
- [71] J.D. Frutos, B.G. Archilla and J. Novo, An adaptive finite element method for evolutionary convection dominated problems, *Comput. Methods Appl. Mech. Egrg.* 200:3601-3612, 2011.
- [72] R.H. Gallagher, R. Glowinski, P.M. Gresho, J.T. Oden and O.C. Zienkiewicz, *Finite elements in fluids*, Wiley-Interscience, 1988.
- [73] E.M. Garau, P. Morin and C. Zuppa, Convergence of an adaptive Kačanov FEM for quasi-linear problems, *Appl. Numer. Math.* 61:512-529, 2011.

- [74] S. Giani, An a posteriori error estimator for  $hp$ -adaptive discontinuous Galerkin methods for computing band gaps in photonic crystals, *J. Comput. Appl. Math.* 236:4810-4826, 2012.
- [75] S. Giani, L. Grubišić and J.S. Owall, Benchmark results for testing adaptive finite element eigenvalue procedures, *Appl. Numer. Math.* 62:121-140, 2012.
- [76] S. Giani, D. Schötzau and L. Zhu, An a-posteriori error estimate for  $hp$ -adaptive DG methods for convection-diffusion problems on anisotropically refined meshes, *Comput. Math. Appl.* 67:869-887, 2014.
- [77] M. Giles and E. Süli, Adjoint methods for PDEs: A posteriori error analysis and postprocessing by duality, *Acta Numer.* 11:145-236, 2002.
- [78] C.J. Gittelsohn, R. Andreev and C. Schwab, Optimality of adaptive Galerkin methods for random parabolic partial differential equations, *J. Comput. Appl. Math.* 263:189-201, 2014.
- [79] M. González and M. Strugaru, Stabilization and a posteriori error analysis of a mixed FEM for convection-diffusion problems with mixed boundary conditions, *J. Comput. Appl. Math.* 381, 2021.
- [80] S. Gowrisankar and S. Natesan, An efficient robust numerical method for singularly perturbed Burgers' equation, *Appl. Math. Comput.* 346:385-394, 2019.
- [81] A. Guaily and A. Megahed, An adaptive finite element method for planar and axisymmetric compressible flows, *Finite. Elem. Anal. Des.* 46:613-624, 2010.
- [82] H. Hakula, N. Hyvönen and T. Tuominen, On the  $hp$ -adaptive solution of complete electrode model forward problems of electrical impedance tomography, *J. Comput. Appl. Math.* 236:4645-4659, 2012.

- [83] E. Hanert, E. Deleersnijder and V. Legat, An adaptive finite element water column model using the Mellor-Yamada level 2.5 turbulence closure scheme, *Ocean. Model.* 12:205-223, 2006.
- [84] F. Hecht and R. Kuate, An approximation of anisotropic metrics from higher order interpolation error for triangular mesh adaptation, *J. Comput. Appl. Math.* 258:99-115, 2014.
- [85] J. Hoffman, J. Jansson and R.V.D. Abreu, Adaptive modeling of turbulent flow with residual based turbulent kinetic energy dissipation, *Comput. Method. Appl. M.* 200:2758-2767, 2011.
- [86] J. Hoffman, J. Jansson, R.V.D. Abreu, N.C. Degirmenci, N. Jansson, K. Müller, M. Nazarov and J.H. Spühler, Unicorn: Parallel adaptive finite element simulation of turbulent flow and fluid-structure interaction for deforming domains and complex geometry, *Comput. Fluids.* 80:310-319, 2013.
- [87] M. Holst, J.A. McCammon, Z. Yu, Y.C. Zhou and Y. Zhu, Adaptive finite element modeling techniques for the Poisson-Boltzmann equation, *Commun. Comput. Phys.* 11:179-214, 2012.
- [88] A. Hrennikoff, Solution of problems of elasticity by the framework method, *Journal of Applied Mechanics*, 8(4):169-175.
- [89] J. Hu, L. Jiang and Z. Shi, New a posteriori error estimate and quasi-optimal convergence of the adaptive nonconforming Wilson element, *J. Comput. Appl. Math.* 265:173-186, 2014.
- [90] T.J.R. Hughes, M. Mallet, Akira and Mizukami, A new finite element formulation for computational fluid dynamics: II. Beyond SUPG, *Comput. Methods Appl. Mech. Engrg.* 54:341-355, 1986.

- [91] H. Ismail, K. Raslan and A. Rabboh, Adomian decomposition method for Burger's-Huxley and Burger's-Fisher equations, *Appl. Math. Comput.* 159:291-301, 2004.
- [92] M. Jasinski and G. Zboinski, On some  $hp$ -adaptive finite element method for natural vibrations, *Comput. Math. Appl.* 66:2376-2399, 2013.
- [93] M. Javidi, Spectral collocation method for the solution of the generalized Burger-Fisher equation, *Appl. Math. Comput.* 174:345-352, 2006.
- [94] R. Jiwari, S. Pandit and M.E. Koksai, A class of numerical algorithms based on cubic trigonometric B-splines functions for numerical simulation of nonlinear parabolic problems, *Comput. Appl. Math.* 38(3):1-22, 2019.
- [95] V. John, A numerical study of a posteriori error estimators for convection-diffusion equations, *Comput. Methods Appl. Mech. Engrg.* 190:757-781, 2000.
- [96] V. John and K. Knobloch, On spurious oscillations at layers diminishing (SOLD) methods for convection-diffusion equations: Part I-A review, *Comput. Methods Appl. Mech. Engrg.* 196:2197-2215, 2007.
- [97] M.K. Kadalbajoo, K.K. Sharma and A. Awasthi, A parameter-uniform implicit difference scheme for solving time-dependent Burgers' equation, *Appl. Math. Comput.* 170:1365-1393, 2005.
- [98] M. Kardani, M. Nazem, D. Sheng and J.P. Carter, Large deformation analysis of geomechanics problems by a combined  $rh$ -adaptive finite element method, *Comput. Geotech.* 49:90-99, 2013.
- [99] B. Kaur and V. Sangwan, A Posteriori Error Estimates for Hughes Stabilized SUPG Technique and Adaptive Refinement for a Convection-Diffusion Problem, *Adv. Math. Phys.* 2020.

- [100] A. Kaushik, Pointwise uniformly convergent numerical treatment for the non-stationary Burger-Huxley equation using grid equidistribution, *Int. J. Comput. Math.* 84:1527-1546, 2007.
- [101] A. Kaushik, A.K. Vashishth, V. Kumar and M. Sharma, A modified graded mesh and higher order finite element approximation for singular perturbation problems, *J. Comput. Phy.* 395:275-285, 2019.
- [102] A. Kaushik, V. Kumar, M. Sharma and A.K. Vashishth, A higher order finite element method with modified graded mesh for singularly perturbed two-parameter problems, *Math. Mod. Meth. Appl. S.* 2020.
- [103] K. Key and C. Weiss, Adaptive finite-element modeling using unstructured grids: The 2D magnetotelluric example, *Geophysics.* 71:G291-G299, 2006.
- [104] K. Key and J. Owall, A parallel goal-oriented adaptive finite element method for 2.5-D electromagnetic modelling, *Geophys. J. Int.* 186:137-154, 2011.
- [105] M. Kimura, H. Komura, M. Mimura, H. Miyoshi, T. Takaishi and D. Ueyama, Adaptive mesh finite element method for pattern dynamics in reaction-diffusion systems, *Proceedings of the Czech-Japanese Seminar in Applied Mathematics.* 56-68, 2005.
- [106] M. Klimczak and W. Cecot, Application of local numerical homogenization and *hp*-adaptive FEM for modeling of heterogeneous viscoelastic materials, *Engng. Trans.* 63:317-327, 2015.
- [107] N. Kopteva, Maximum norm a posteriori error estimate for a 2D singularly perturbed semilinear reaction-diffusion problem, *SIAM J. Numer. Anal.* 46:1602-1618, 2008.

- [108] J. Kou and S. Sun, An adaptive finite element method for simulating surface tension with the gradient theory of fluid interfaces, *J. Comput. Appl. Math.* 255:593-604, 2014.
- [109] C. Kreuzer and A. Veese, Convergence of adaptive finite element methods with error-dominated oscillation, *European Conference on Numerical Mathematics and applied applications.* 126:471-479, 2019.
- [110] B.V.R. Kumar, V. Sangwan, S.V.S.S.N.V.G.K. Murthy and M. Nigam, A numerical study of singularly perturbed generalized Burgers-Huxley equation using three-step Taylor-Galerkin method, *Comput. Math. Appl.* 62:776-786, 2011.
- [111] G. Kunert, An a posteriori residual error estimator for the finite element method on anisotropic tetrahedral meshes, *Numer. Math.* 86:471-490, 2000.
- [112] G. Kunert, Robust a posteriori error estimation for a singularly perturbed reaction-diffusion equation on anisotropic tetrahedral meshes, *Adv. Comp. Math.* 15:237-259, 2001.
- [113] G. Kunert, A posteriori error estimation for convection dominated problems on anisotropic meshes, *Math. Methods Appl. Sci.* 26(7):589-617, 2003.
- [114] J. Lang, An adaptive finite element method for convection-diffusion problems by interpolation techniques, 1991.
- [115] J. Lang, W. Cao, W. Huang and R.D. Russell, A two-dimensional moving finite element method with local refinement based on a posteriori error estimates, *Appl. Numer. Math.* 46:75-94, 2003.
- [116] R. Lazarov and S. Tomov, A posteriori error estimates for finite volume element approximations of convection-diffusion-reaction equations, *Computat Geosci.* 6(3):483-503, 2002.

- [117] C.K. Lee and Y.Y. Shuai, An automatic adaptive refining procedure for the reproducing kernel particle method. Part II: Adaptive refinement, *Comput. Mech.* 40:415-427, 2007.
- [118] H. Li and Y. Yang, The adaptive finite element method based on multi-scale discretizations for eigenvalue problems, *Comput. Math. Appl.* 65:1086-1102, 2013.
- [119] Q. Lin, F. Luo and H. Xie, A posterior error estimator and lower bound of a nonconforming finite element method, *J. Comput. Appl. Math.* 265:243-254, 2014.
- [120] R. Lin, X. Ye, S. Zhang and P. Zhu, A weak galerkin finite element method for singularly perturbed convection-diffusion-reaction problems, *SIAM J. Numer. Anal.* 56:1482-1497, 2018.
- App. Math. Mech.* 37:151-168, 2016.
- [121] X. Liu and J. Zhang, Galerkin finite element methods for convection-diffusion problems with exponential layers on Shishkin triangular meshes and hybrid meshes, *Appl. Math. Comput.* 307:244-256, 2017.
- [122] C.S. MacDonald, J.A. Mackenzie, A. Ramage and C.J.P. Newton, Robust adaptive computation of a one-dimensional Q-tensor model of nematic liquid crystals, *Comput. Math. Appl.* 64:3627-3640, 2012.
- [123] S. Mao, X. Zhao and Z. Shi, Convergence of a standard adaptive nonconforming finite element method with optimal complexity, *Appl. Numer. Math.* 60:673-688, 2010.
- [124] P.J. Matuszyk, M. Sieniek and M. Paszyński, Fully automatic 2D hp-adaptive finite element method for non-stationary heat transfer, *Procedia Comput. Sci.* 51:2883-2887, 2015.

- [125] K. Mekchay and R.H. Nochetto, Convergence of adaptive finite element methods for general second order linear elliptic PDEs, *SIAM J. Numer. Anal.* 43:1803-1827, 2005.
- [126] J.M. Melenk and B.I. Wohlmuth, On residual-based a posteriori error estimation in  $hp$ -FEM, *Adv. Comput. Math.* 15:311-331, 2001.
- [127] J.J.H. Miller, E.O. Riordan and G.I. Shishkin, *Fitted Numerical Methods for Singular Perturbation Problems: error estimates in the maximum norm for linear problems in one and two dimensions*, World Scientific, Singapore, 1996.
- [128] W.F. Mitchell, A comparison of adaptive refinement techniques for elliptic problems, *ACM. Trans. Math. Softw.* 15:326-347, 1989.
- [129] W.F. Mitchell, A collection of 2D elliptic problems for testing adaptive grid refinement algorithms, *Appl. Math. Comput.* 220:350-364, 2013.
- [130] R.C. Mittal and R. Jiwari, A high order numerical scheme for some nonlinear differential equations: models in biology, *Int. J. Comput. Meth. Eng. Sci. Mech.* 12:134-140, 2011.
- [131] R.C. Mittal, R. Jiwari and K.K. Sharma, A numerical scheme based on differential quadrature method to solve time dependent Burger's equation, *Eng. Comput.* 30(1):117-131, 2013.
- [132] R.C. Mittal and A. Tripathi, Numerical solutions of generalized Burgers-Fisher and generalized Burgers-Huxley equations using collocation of cubic B-splines, *Int. J. Comput. Math.* 92:1053-1077, 2015.
- [133] R.K. Mohanty and N. Setia, A new high order compact off-step discretization for the system of 3D quasi-linear elliptic partial differential equations, *Appl. Math. Model.* 37:6870-6883, 2013.

- [134] R.K. Mohanty, W. Dai and F. Han, Compact operator method of accuracy two in time and four in space for the numerical solution of coupled viscous Burger's equations, *Appl. Math. Comput.* 256:381-393, 2015.
- [135] P.M. Mohite and C.S. Upadhyay, A generalized adaptive finite element analysis of laminated plates, *Comput. Struct.* 112-113:217-234, 2012.
- [136] A. Mola, L. Heltai and A.D. Simone, A stable and adaptive semi-Lagrangian potential model for unsteady and nonlinear ship-wave interactions, *Eng. Anal. Bound. Elem.* 37:128-143, 2013.
- [137] P.K. Moore, Solving regularly and singularly perturbed reaction-diffusion equations in three space dimensions, *J. Comput. Phys.* 224:601-615, 2007.
- [138] P. Mostaghimi, B.S. Tollit, S.J. Neethling, G.J. Gorman and C.C. Pain, A control volume finite element method for adaptive mesh simulation of flow in heap leaching, *J. Eng. Math.* 87:111-121, 2014.
- [139] S.S. Motsa, P. Sibanda and S. Shateyi, On a new quasi-linearization method for systems of nonlinear boundary value problems, *Math. Methods Appl. Sci.* 34(11):1406-1413, 2011.
- [140] S.S. Motsa, A new spectral local linearization method for nonlinear boundary layer flow problems, *J. Appl. Math.* 2013.
- [141] K. Murotani, G. Yagawa and J.B. Choi, Adaptive finite elements using hierarchical mesh and its application to crack propagation analysis, *Comput. Methods Appl. Mech. Engrg.* 253:1-14, 2013.
- [142] S. Natesan, J. Jayakumar and J.V. Aguiar, Parameter uniform numerical method for singularly perturbed turning point problems exhibiting boundary layers, *J. Comput. Appl. Math.* 158:121-134, 2003.

- [143] M. Nazarov and J. Hoffman, Residual-based artificial viscosity for simulation of turbulent compressible flow using adaptive finite element methods. *Inter. J. Numer. Methods. Fluids.* 1-23, 2012.
- [144] H.T. Nguyen,  $p$ -adaptive and automatic  $hp$ -adaptive finite element methods for elliptic partial differential equations, PhD Thesis, 2010.
- [145] S. Nicaise, A posteriori error estimations of some cell-centered finite volume methods for diffusion-convection-reaction problems, *SIAM J. Numer. Anal.* 43:1481-1503, 2005.
- [146] S. Nicaise and S.I. Repin, Functional a posteriori error estimates for the reaction-convection-diffusion problem, *Zapiski Nauchnykh Seminarov POMI.* 348:127-146, 2007.
- [147] G. Nicolas and T. Fouquet, Adaptive mesh refinement for conformal hexahedral meshes, *Finite. Elem. Anal. Des.* 67:1-12, 2013.
- [148] J.T. Oden, L. Demkowicz, W. Rachowicz and T.A. Westermann, Towards a universal  $h-p$  adaptive finite element strategy, Part 2. A posteriori error estimation, *Comput. Methods Appl. Mech. Engrg.* 77:113-180, 1989.
- [149] J. Oden and A. Patra, A parallel adaptive strategy for  $hp$  finite element computations, *Comput. Methods Appl. Mech. Engrg.* 121:449-470, 1995.
- [150] T.K. Ohsumi, J.E. Flaherty, V.H. Barocas, S. Adjerid and M. Aiffa, Adaptive finite element analysis of the anisotropic biphasic theory of tissue-equivalent mechanics, *Comput. Methods. Biomech. Biomed. Eng.* 3:215-229, 2000.
- [151] M. Oleksy and W. Cecot, Application of  $hp$ -adaptive finite element method to two-scale computation, *Arch. Comput. Methods. Eng.* 22:105-134, 2015.

- [152] M. Paszyński, D. Padro, C.T. Verdín, L. Demkowicz and V. Calo, A parallel direct solver for the self-adaptive *hp* finite element method, *J. Parallel Distrib. Comput.* 70:270-281, 2010.
- [153] A. Paszyńska and E. Grabska, A graph grammar model of the *hp* adaptive three dimensional finite element method. Part I, *Fundam. Inform.* 114:149-182, 2012.
- [154] M. Paszynski, D. Padro and V.M. Calo, A direct solver with reutilization of LU factorizations for *h*-adaptive finite element grids with point singularities. *Comput. Math. Appl.* 65:1140-1151, 2013.
- [155] D.W. Pepper, Y.T. Chen and L. Li, Subsurface transport modeling using adaptive finite elements, *Transactions on Ecology and the environment.* 33, 1999.
- [156] J. Peraire, M. Vahdati, K. Morgan and O.C. Zienkiewicz, Adaptive remeshing for compressible flow computations, *J. Comput. Phys.* 72:449-466, 1987.
- [157] M. Picasso, Adaptive finite elements for a linear parabolic problem, *Comput. Methods Appl. Mech. Engrg.* 167:223-237, 1998.
- [158] G.M. Porta, S. Perotto and F. Ballio, A space-time adaptation scheme for unsteady shallow water problems, *Math. Comput. Simul.* 82:2929-2950, 2013.
- [159] E.B. Postnikov, Evaluation of a continuous wavelet transform by solving the Cauchy problem for a system of partial differential equations, *Comput. Math. Math. Phys.* 46:73-78, 2006.
- [160] E.B. Postnikov and O.V. Titkova, A correspondence between the models of Hodgkin-Huxley and FitzHugh-Nagumo revisited, *Eur. Phys. J. Plus.* 131:1-9, 2016.
- [161] D.L. Quan, T. Toulorge, E. Marchandise, J.F. Remacle and G. Bricteux, Anisotropic mesh adaptation with optimal convergence for finite elements using embedded geometries, *Comput. Methods Appl. Mech. Engrg.* 268:65-81, 2014.

- [162] J.I. Ramos, An exponentially-fitted method for singularly perturbed, one-dimensional, parabolic problems, *Appl. Math. Comput.* 161:513-523, 2005.
- [163] H. Ramos, J.V. Aguiar, S. Natesan, R.G. Rubio and M.A. Queiruga, Numerical solution of nonlinear singularly perturbed problems on nonuniform meshes by using a non-standard algorithm, *J. Math. Chem.* 48(1):38-54, 2010.
- [164] Z. Ren and J. Tang, 3D direct current resistivity modeling with unstructured mesh by adaptive finite-element method, *Geophysics.* 75:H7-H17, 2010.
- [165] I.G. Revuelto, L.E. Castillo, S.L. Romano and D. Pardo, A three-dimensional self-adaptive *hp* finite element method for the characterization of waveguide discontinuities, *Comput. Methods Appl. Mech. Engrg.* 249:62-74, 2012.
- [166] M.C. Rivara, Design and data structures of fully adaptive, multigrid, finite-element software, *ACM. Trans. Math. Softw.* 10:242-264, 1984.
- [167] M.C. Rivara, Mesh refinement processes based on the generalized bisection of simplices, *SIAM J. Numer. Anal.* 21:604-613, 1984.
- [168] N.V. Roberts, L. Demkowicz and R. Moser, A discontinuous Petrov-Galerkin methodology for adaptive solutions to the incompressible Navier-Stokes equations, *J. Comput. Phys.* 301:456-483, 2015.
- [169] H.G. Roos, M. Stynes and L. Tobiska, *Numerical methods for Singularly Perturbed Differential Equations*, Springer, Berlin, 1996.
- [170] H.G. Roos, M. Stynes and L. Tobiska, *Robust Numerical Methods for Singularly Perturbed Differential Equations*, Springer, 2008.
- [171] R. Rossi, J. Cotella, N.M. Lafontaine, P. Dadvand and S.R. Idelsohn, Parallel adaptive mesh refinement for incompressible flow problems, *Comput. Fluids.* 80:342-355, 2013.

- [172] V. Sangwan, B.V.R. Kumar, S.V.S.S.N.V.G.K. Murthy and M. Nigam, Three-step Taylor Galerkin method for singularly perturbed generalized Hodgkin-Huxley equation, *Int. J. Model. Simul. Sci. Comput.* 1:257-276, 2010.
- [173] V. Sangwan and B.V.R. Kumar, Finite element analysis for mass-lumped three-step Taylor Galerkin method for time dependent singularly perturbed problems with exponentially fitted splines, *Numer. Func. Anal. Opt.* 33(6):638-660, 2012.
- [174] V. Sangwan and B. Kaur, An exponentially fitted numerical technique for singularly perturbed Burgers-Fisher equation on a layer adapted mesh, *Int. J. Comput. Math.* 96(7):1502-1513, 2019.
- [175] M. Sari, G. Gürarlan and I. Dağ, A compact finite difference method for the solution of the generalized Burgers-Fisher equation, *Numer. Methods. Partial. Differ. Equ.* 26:125-134, 2010.
- [176] D. Schillinger and E. Rank, An unfitted  $hp$ -adaptive finite element method based on hierarchical B-splines for interface problems of complex geometry, *Comput. Methods Appl. M.* 200:3358-3380, 2011.
- [177] C. Schwab and R. Stevenson, Space-time adaptive wavelet methods for parabolic evolution problems, *Math. Comp.* 78:1293-1318, 2009.
- [178] C. Schwarzbach, R.U. Börner and K. Spitzer, Three-dimensional adaptive higher order finite element simulation for geo-electromagnetics-a marine CSEM example. *Geophys. J. Int.* 187:63-74, 2011.
- [179] K. Selim, A. Logg and M.G. Larson, An adaptive finite element splitting method for the incompressible Navier-Stokes equations, *Comput. Methods Appl. Mech. Engrg.* 209:54-65, 2012.

- [180] K.K. Sharma, P. Rai and K.C. Patidar, A review on singularly perturbed differential equations with turning points and interior layers, *Appl. Math. Comput.* 219(22):10575-10609, 2013.
- [181] Z. Shi and M. Wang, *Finite Element Methods*, Science Publishers, Beijing, 2010.
- [182] Y. Shi, K. Bao and X.P. Wang, 3D adaptive finite element method for a phase field model for the moving contact line problems, *Inverse. Probl. Imag.* 7, 2013.
- [183] P. Solin, L. Dubcova and J. Kruis, Adaptive *hp*-FEM with dynamical meshes for transient heat and moisture transfer problems, *J. Comput. Appl. Math.* 233:3103-3112, 2010.
- [184] P. Solin and M. Kuraz, Solving the nonstationary Richards equation with adaptive *hp*-FEM, *Adv. Water Resour.* 34:1062-1081, 2011.
- [185] P. Solin, O. Certik and L. Korous, Three anisotropic benchmark problems for adaptive finite element methods, *Appl. Math. Comput.* 219:7286-7295, 2013.
- [186] T. Tang, Moving mesh methods for computational fluid dynamics, *Contemp. Math.* 383:141-173, 2005.
- [187] A. Tavakoli and F. Zarmehi, Adaptive finite element methods for solving Saint-Venant equations, *Sci. Iran.* 18:1321-1326, 2011.
- [188] V. Thomee and B. Wendroff, Convergence estimates for Galerkin methods for variable coefficient initial value problems, *SIAM J. Numer. Anal.* 11:1059-1068, 1974.
- [189] L. Tian, F. Chen and Q. Du, Adaptive finite element methods for elliptic equations over hierarchical T-meshes, Li Tian, Falai Chen, Qiang Du, *J. Comput. Appl. Math.* 236:878-891, 2011.

- [190] L. Tobiska and R. Verfürth, Robust a posteriori error estimates for stabilized finite element methods, *IMA Journal of Numerical Analysis*. 35:1652-1671, 2015.
- [191] E. Tsuchida, Y.K. Choe and T. Ohkubo, An adaptive finite-element method for large-scale ab initio molecular dynamics simulations, *Phy. Chem. Chem. Phys.* 17:31444-31452, 2015.
- [192] R. Verfürth, A posteriori error estimators for the Stokes equations, *Numer. Math.* 55:309-325, 1989.
- [193] R. Verfürth, A review of a posteriori error estimation and adaptive mesh-refinement techniques, Wiley-Teubner, New York, 1996.
- [194] R. Verfürth, Robust a posteriori error estimates for stationary convection-diffusion equations, *SIAM J. Numer. Anal.* 43:1766-1782, 2005.
- [195] A.V. Vuong, C. Giannelli, B. Jüttler and B. Simeon, A hierarchical approach to adaptive local refinement in isogeometric analysis, *Comput Methods Appl. Mech. Engrg.* 200:3554-3567, 2011.
- [196] X.Y. Wang, Z.S. Zhu and Y.K. Lu, Solitary wave solutions of the generalised Burgers-Huxley equation, *Journal of Physics A- Mathematical and General*. 23:271-274, 2004.
- [197] T.P. Wihler, An  $hp$ -adaptive strategy based on continuous Sobolev embeddings, *J. Comput. Appl. Math.* 235:2731-2739, 2011.
- [198] J. Wu, J.Z. Zhu, J. Szmelter and O.C. Zienkiewicz, Error estimation and adaptivity in Navier-Stokes incompressible flows, *Comput. Mech.* 6:259-270, 1990.
- [199] A. Yakar and M.E. Koksal, Quasilinearization method for nonlinear differential equations with casual operators, *J. Nonlinear. Sci. Appl.* 9(3):1356-1364, 2016.

- [200] Y. Yang and H. Bi, Two-grid finite element discretization schemes based on shifted-inverse power method for elliptic eigenvalue problems, *SIAM J. Numer. Anal.* 49:1602-1624, 2011.
- [201] G. Zboinski, Adaptive *hpq* finite element methods for the analysis of 3D-based models of complex structures. Part 1. Hierarchical modeling and approximations, *Comput. Methods Appl. Mech. Enrg.* 199:2913-2940, 2010.
- [202] G. Zboinski, Adaptive *hpq* finite element methods for the analysis of 3D-based models of complex structures. Part 2. A posteriori error estimation, *Comput. Methods Appl. Mech. Engrg.* 267:531-565, 2013.
- [203] S. Zhai, X. Feng and Y. He, An unconditionally stable compact ADI method for three-dimensional time-fractional convection-difusion equation. *J. Comput. Phys.* 269:138-155, 2014.
- [204] C.S. Zhang, Adaptive finite element methods for variational inequalities: Theory and Applications in Finance, PhD Thesis, 2007.
- [205] Y. Zhang, Y. Hou and H. Zuo, A posteriori error estimation and adaptive computation of conduction convection problems, *Appl. Math. Model.* 35:2336-2347, 2011.
- [206] R.P. Zhang and L.W. Zhang, Direct discontinuous Galerkin method for the generalized Burgers-Fisher equation, *Chin. Phys. B.* 21:1-4, 2012.
- [207] R.P. Zhang, X.J. Yu and G.Z. Zhao, The local discontinuous Galerkin method for Burger's-Huxley and Burger's-Fisher equations, *Appl. Math. Comput.* 218:8773-8778, 2012.

- [208] J. Zhao, S. Chen and B. Zhang, A posteriori error estimates for nonconforming streamline-diffusion finite element methods for convection-diffusion problems, *Calcolo*. 52:407-424, 2015.
- [209] X. Zhao, X. Hu, W. Cai and G. EM. Karniadakis, Adaptive finite element method for fractional differential equations using hierarchical matrices, *Comput. Method. Appl. M.* 325:56-76, 2017.
- [210] C.G. Zhu and W.S. Kang, Numerical solution of Burgers-Fisher equation by cubic B-spline quasi-interpolation, *Appl. Math. Comput.* 216:2679-2686, 2010.
- [211] O.C. Zienkiewicz and R.L. Taylor, *The Finite Element Method for Solid and Structural Mechanics*, McGraw-Hill, 1967.
- [212] O.C. Zienkiewicz, R.L. Taylor and J.Z. Zhu, *The Finite Element method: Its Basis and Fundamentals*, McGrawHill, 1967.
- [213] O.C. Zienkiewicz and J.Z. Zhu, A simple error estimator and adaptive procedure for practical engineering analysis, *Inter. J. Numer. Meth. Eng.* 24:337-357, 1987.
- [214] J. Zitelli, I. Muga, L. Demkowicz, J. Gopalakrishnan, D. Pardo and V.M. Calo, A class of discontinuous Petrov-Galerkin methods. Part IV: The optimal test norm and time-harmonic wave propagation in 1D, *J. Comput. Phys.* 230:2406-2432, 2011.